creative commons
COMMONS DEED

저작자표시-비영리-변경금지 2.0 대한민국

이용자는 아래의 조건을 따르는 경우에 한하여 자유롭게

- 이 저작물을 복제, 배포, 전송, 전시, 공연 및 방송할 수 있습니다.

다음과 같은 조건을 따라야 합니다:

저작자표시. 귀하는 원저작자를 표시하여야 합니다.

비영리. 귀하는 이 저작물을 영리 목적으로 이용할 수 없습니다.

변경금지. 귀하는 이 저작물을 개작, 변형 또는 가공할 수 없습니다.

- 귀하는, 이 저작물의 재이용이나 배포의 경우, 이 저작물에 적용된 이용허락조건을 명확하게 나타내어야 합니다.
- 저작권자로부터 별도의 허가를 받으면 이러한 조건들은 적용되지 않습니다.

저작권법에 따른 이용자의 권리는 위의 내용에 의하여 영향을 받지 않습니다.

이것은 이용허락규약(Legal Code)을 이해하기 쉽게 요약한 것입니다.

Disclaimer

dCollection

ULSAN NATIONAL INSTITUTE OF SCIENCE AND TECHNOLOGY

Doctoral Thesis

Synthesis of Multifunctional Polyethers: Anionic Ring-Opening Polymerization of Functional Epoxide Monomers

Joonhee Lee

Department of Chemistry

Graduate School of UNIST

2020

ULSAN NATIONAL INSTITUTE OF
SCIENCE AND TECHNOLOGY

Synthesis of Multifunctional Polyethers: Anionic Ring-Opening Polymerization of Functional Epoxide Monomers

Joonhee Lee

Department of Chemistry

Graduate School of UNIST

ULSAN NATIONAL INSTITUTE OF
SCIENCE AND TECHNOLOGY

Synthesis of Multifunctional Polyethers: Anionic Ring-Opening Polymerization of Functional Epoxide Monomers

A thesis/dissertation
submitted to the Graduate School of UNIST
in partial fulfillment of the
requirements for the degree of
Doctor of Philosophy

Joonhee Lee

December/13/2019

Approved by

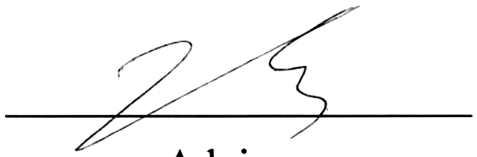

Advisor
Tae-Hyuk Kwon

ULSAN NATIONAL INSTITUTE OF SCIENCE AND TECHNOLOGY

Synthesis of Multifunctional Polyethers: Anionic Ring-Opening Polymerization of Functional Epoxide Monomers

Joonhee Lee

This certifies that the thesis/dissertation of Joonhee Lee is approved.

December/13/2019

Advisor: Tae-Hyuk Kwon

Byeong-Su Kim: Thesis Committee Member #1

Dong Woog Lee: Thesis Committee Member #2

Young S. Park: Thesis Committee Member #3

Jeung Gon Kim: Thesis Committee Member #4

ULSAN NATIONAL INSTITUTE OF
SCIENCE AND TECHNOLOGY

Abstract

Polyethers, such as poly(ethylene glycol) (PEG), have been widely used for a variety of applications, owing to their high water solubility, superior biocompatibility, low toxicity, and flexible backbone. However, PEG possesses only two hydroxyl groups at both ends of the polymer chain, and this limits its functionalization. In this regard, the design and synthesis of functional epoxide monomers must be investigated for the preparation of various multifunctional polyethers, which have the potential for broad applications. This thesis describes the design and synthesis of functional epoxide monomers, followed by the synthesis of multifunctional polyethers using these monomers.

Chapter 1 covers the general introduction and background of PEG and its derivatives, as well as the methods for further modification of polymers. The synthesis of thermoresponsive PEG-based functional polymers containing pendant amine groups is described in Chapter 2. Chapter 3 presents a one-pot synthesis of primary amine-containing hyperbranched polyglycerols (PGs) using a newly designed amino glycidyl ether monomer. Chapter 4 describes a series of novel azidoalkyl glycidyl ethers as universal monomers for the synthesis of azide-functional polyethers. Post-polymerization modification of the polymer through Cu-catalyzed azide-alkyne cycloaddition (CuAAC) and Staudinger reduction is demonstrated to propose the versatility of azide-functional polymers. Thus, this method acts as a new platform for the preparation of functional polyethers.

ULSAN NATIONAL INSTITUTE OF SCIENCE AND TECHNOLOGY

Contents

ULSAN NATIONAL INSTITUTE OF SCIENCE AND TECHNOLOGY

ULSAN NATIONAL INSTITUTE OF SCIENCE AND TECHNOLOGY

List of Figures

Chapter 1.

ULSAN NATIONAL INSTITUTE OF SCIENCE AND TECHNOLOGY

Chapter 2.

ULSAN NATIONAL INSTITUTE OF SCIENCE AND TECHNOLOGY

Chapter 3.

ULSAN NATIONAL INSTITUTE OF SCIENCE AND TECHNOLOGY

ULSAN NATIONAL INSTITUTE OF SCIENCE AND TECHNOLOGY

ULSAN NATIONAL INSTITUTE OF SCIENCE AND TECHNOLOGY

ULSAN NATIONAL INSTITUTE OF SCIENCE AND TECHNOLOGY

List of Tables

ULSAN NATIONAL INSTITUTE OF SCIENCE AND TECHNOLOGY

Chapter 1

General Introduction

1.1 Poly(ethylene glycol) (PEG): The most famous class of polyethers

Poly(ethylene glycol) (PEG), also known as poly(ethylene oxide) (PEO), is the most famous class of aliphatic polyethers and has ethylene glycol or ethylene oxide as the repeating unit. Compared with other synthetic polymers, PEG has unusual solubility in both water and organic solvents. It shows higher water solubility than other aliphatic polyethers such as poly(butylene oxide), which has only one more repeating methylene group in the polymer backbone.[1] PEG has been widely used in pharmaceutical, cosmetic, and various biomedical applications because of its superior biocompatibility and water solubility and low toxicity.[2] In particular, PEGs are commonly used in our daily lives as ingredients in cosmetics such as shampoos, toothpastes, and hair wax (Figure 1.1). In addition, the US Food and Drug Administration (FDA) has approved the use of PEG for nontoxic and immunogenic pharmaceutical formulations.[3] In this respect, for therapeutics, the conjugation of PEG with protein or small molecules, known as PEGylation, is one of the most successful techniques for utilization of the biocompatible nature of PEG.

PEG is a relatively soft material at room temperature, existing in the form of viscous liquid or solid, and its melting point depends on its molecular weight. The melting point of PEG can be manipulated by mixing and co-crystallizing with other PEG polymers having different molecular weights. This co-crystallization is an important process to manufacture cosmetics such as ointments and skin creams.[4]

Despite the exceptional advantages of PEG, there are several drawbacks that need to be considered. First, PEG has a maximum of only two hydroxyl groups at both ends of the polymer chain; this limits its multifunctionalization. The repeating ether linkages along the PEG backbone are chemically inert and, thus, limit further chemical modification. Second, ethylene oxide, the monomer for the synthesis of PEG, is gaseous and exhibits acute toxicity and is, therefore, difficult to handle. In order to overcome these limitations, direct access to the multifunctional PEG is required, accompanied by proper design of novel epoxide monomers. This thesis describes the entire process of the synthesis of multifunctional polyethers from the design of functional monomers to the controlled anionic ring-opening polymerization (AROP).

ULSAN NATIONAL INSTITUTE OF SCIENCE AND TECHNOLOGY

Figure 1.1. PEG-containing products ((1) Hair wax, (2) shower gel, (3) shaving foam, (4) liquid soap, and (5) toothpaste) in everyday use. On the right side of the figure are the commercial names of the contained PEG derivatives listed on the respective packages. Nonionic PEG surfactants, in particular, play an important role. Reprinted with permission from ref. 2. Copyright © 2011 WILEY-VCH Verlag GmbH & Co. KGaA, Weinheim.

ULSAN NATIONAL INSTITUTE OF SCIENCE AND TECHNOLOGY

1.2 Synthesis of Multifunctional PEG

As mentioned in Chapter 1.1, PEG lacks functionality, which limits its applications. Therefore, it is essential to impart multiple functionalities to the PEG backbone for enhancing the versatility of the polymer. In order to meet the increasing demand for multifunctional PEG-based polymers, the design and synthesis of the functional epoxide monomers need to be considered first. Thereafter, the monomers could be utilized to yield multifunctional PEG via anionic ring-opening polymerization. Synthetic strategies for the multifunctional PEG are discussed in detail as follows.

1.2.1 Synthesis of Functional Epoxide Monomers

Aliphatic polyethers including PEG, poly(propylene oxide) (PPO), poly(tetrahydrofuran) (polyTHF), and polyoxymethylene (POM) are commercially available, versatile polymers. The monomers for the synthesis of the aforementioned polymers have simple chemical structures and are also commercially available. To tailor the structure and properties of polymers while maintaining the intrinsic properties derived from the backbone, the design and synthesis of a proper functional monomer is a prerequisite. Williamson ether synthesis is a simple and facile method for preparation of glycidyl ether-type monomers, which would be used for multifunctional PEGs. Functional glycidyl ethers can be synthesized by the reaction of epichlorohydrin and alcohol under basic conditions (Figure 1.2a) using NaOH, KOH, and sometimes *t*-BuOK.[5–7] Epichlorohydrin is a commercially available and economical precursor. Despite the direct epoxidation on the terminal olefins being a possible option (Figure 1.2b),[8] compared to the scope of alcohols, the scope of functional terminal olefins is limited. In a particular case, acid-catalyzed addition of alcohol is conducted for the formation of acetal to prepare novel pH-responsive monomers (Figure 1.3).[9]

In the case of designing functional monomers for AROP, the functional groups need to endure harsh conditions, such as high temperatures and strong bases, which limit the utilization of the monomer. Many novel monomers bearing functional groups that are stable under AROP conditions have been reported to date (Figure 1.4).[10–21] Hawker and Lynd *et al*. conducted intensive studies on the allyl glycidyl ether as a versatile epoxide monomer for imparting multiple functionalities to PEG. Allyl groups are stable under highly basic AROP conditions, and they can further react with functional thiols via thiol-ene reaction, thereby tailoring the polyethers with a multitude of pendant functional groups.[10,22–26] Frey group has introduced a novel epoxide monomer containing 3,3-dimethoxypropanyl moiety to afford PEG possessing multiple aldehyde functionalities.[7] Numerous efforts have gone into the development of novel functional epoxide monomers, and our research group has successfully developed several novel functional monomers that are compatible with AROP (Figure 1.5).[5,9,27–29]

ULSAN NATIONAL INSTITUTE OF SCIENCE AND TECHNOLOGY

a) Williamson ether synthesis

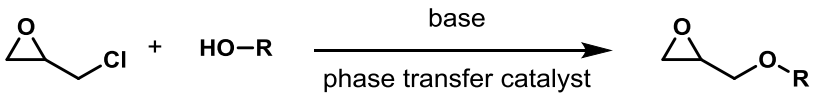

b) Direct epoxidation of olefin

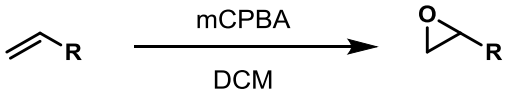

Figure 1.2. (a)Williamson ether synthesis using epichlorohydrin and alcohols. (b) Direct epoxidation of functional olefins using *meta*-chloroperoxybenzoic acid.

ULSAN NATIONAL INSTITUTE OF SCIENCE AND TECHNOLOGY

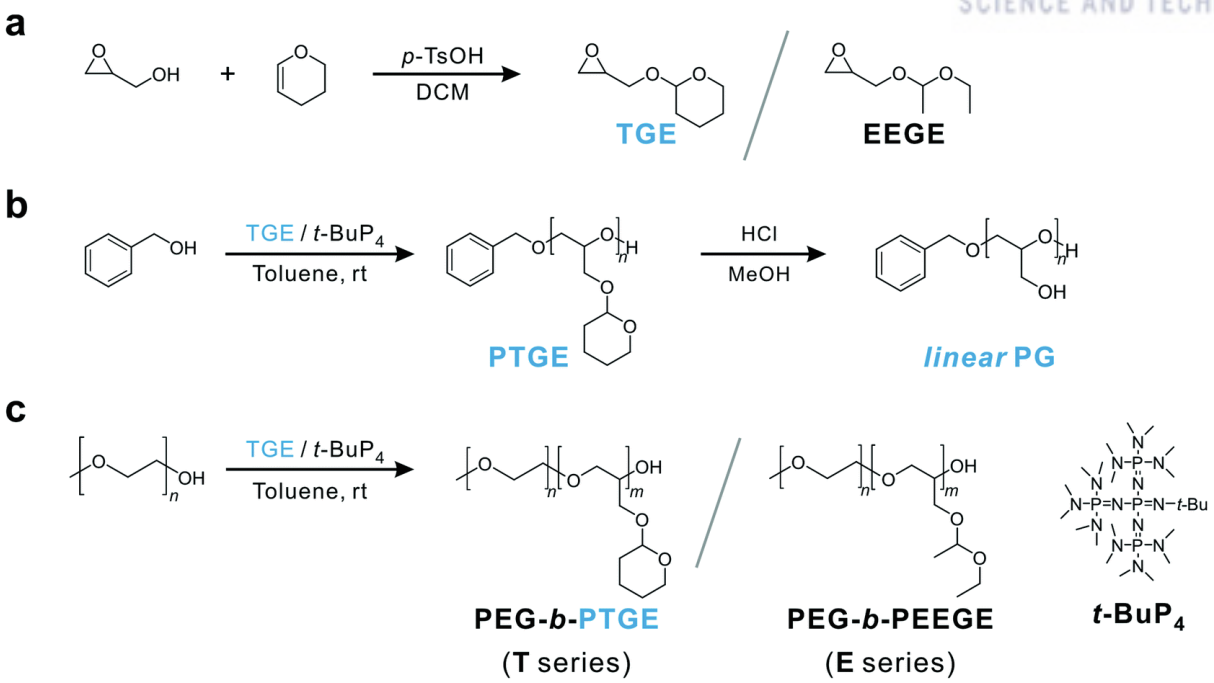

Figure 1.3. Synthetic scheme for the (a) TGE monomer, (b) PTGE homopolymer and linear PG, and (c) PEG-b-PTGE block copolymer. Structures of the EEGE monomer and the PEG-*b*-PEEGE block copolymer are presented for comparison. *t*-BuP$_4$ was employed as a metal-free organic base for polymerization. Reproduced from Ref. 9 with permission from The Royal Society of Chemistry.

ULSAN NATIONAL INSTITUTE OF SCIENCE AND TECHNOLOGY

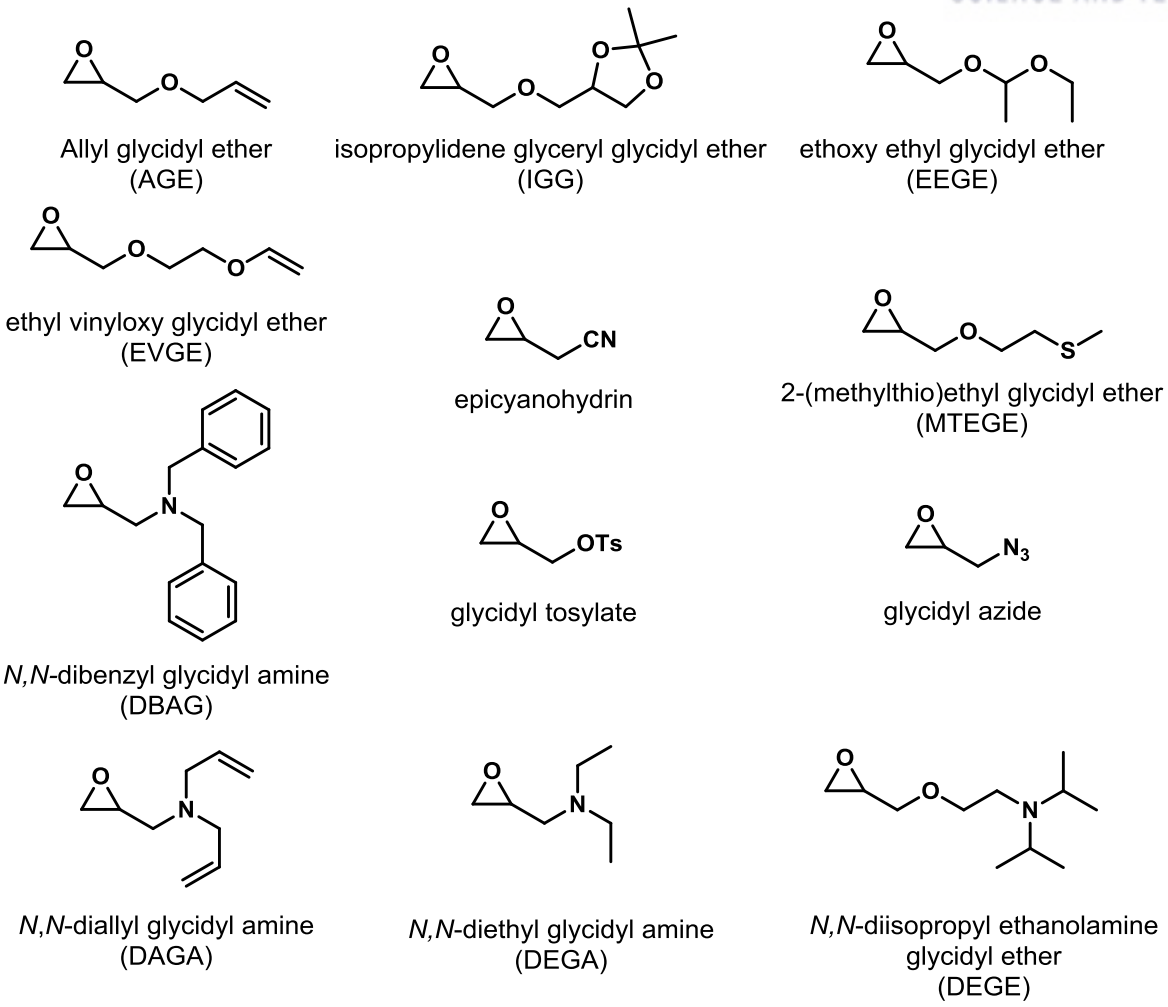

Figure 1.4. Overview of functional epoxide monomers.[10-21]

ULSAN NATIONAL INSTITUTE OF SCIENCE AND TECHNOLOGY

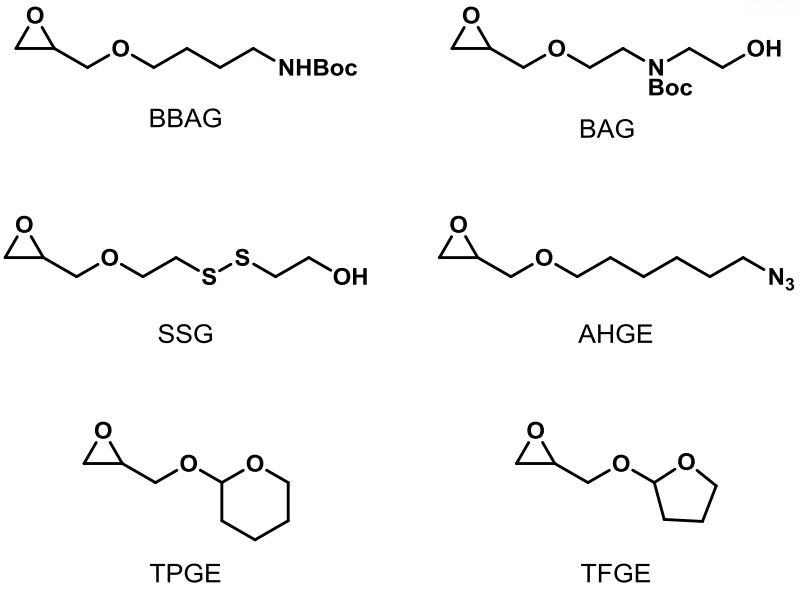

Figure 1.5. Overview of functional epoxide monomers developed by Kim group.[5,9,27–29]

ULSAN NATIONAL INSTITUTE OF SCIENCE AND TECHNOLOGY

1.2.2 Anionic Ring-Opening Polymerization (AROP)

Anionic ring-opening polymerization (AROP) of epoxide monomers was first explained by Staudinger and Flory in early 1990s.[30,31] It is a reliable polymerization method for epoxide monomers because of the fast polymerization kinetics and well-controlled molecular weight and dispersity. Initiation is carried out by using alcohol with alkali metal salts such as alkoxides of potassium, sodium, and cesium.[32,33] The potassium base is frequently used because of the more efficient polymerization and better cost-effectiveness than the corresponding cesium base. However, the cesium base performs faster polymerization and suppresses chain transfer reactions in the case of monosubstituted epoxide such as propylene oxide (Figure 1.6).[34,35] The difference in the polymerization rates is derived from the size of the metal cation and the hard and soft acids and bases (HSAB) theory.[36] In general, small and hard metal cations tend to aggregate with the growing polymer chains, leading to low polymerization rates. In contrast, bulky and soft metal cations being distant from the propagating chains, exist as free ions, and therefore exhibit high polymerization rates.[4] Sometimes, it is not suitable for certain monomers containing sensitive functionalities because of the relatively high operating temperature of alkali metal-based AROP. Lynd *et al.* demonstrated AROP of allyl glycidyl ether using potassium naphthalenide at various temperatures; they observed unexpected isomerization of allyl group (Figures 1.7, 1.8).[10] In this regard, finding an appropriate polymerization system that could be operated at room temperature is necessary.

Non-ionic organic superbase is an alternative candidate for successful AROP. Phosphazene base *t*-BuP_4 is a commercially available and well-known organic superbase used for both organic reactions and AROP.[37] This base can readily deprotonate alcohols in organic solvents to generate alkoxide ion pairs (Figure 1.9). The phosphazene base exhibits high basicity and the corresponding cation possesses relatively larger volume than other cations. Therefore, polymerization using *t*-BuP_4 exhibits higher propagation rate at room temperature than that using conventional alkali metal bases. To date, Satoh *et al.* have reported several examples of AROP using phosphazene base. Satoh and coworkers demonstrated *t*-BuP_4-catalyzed AROP of dibenzyl-protected epoxide monomer for the synthesis of primary-amine-functionalized polyether, followed by deprotection of dibenzyl group.[38] They also investigated the AROP of styrene oxide using phosphazene base with various initiators at room temperature.[39]

ULSAN NATIONAL INSTITUTE OF SCIENCE AND TECHNOLOGY

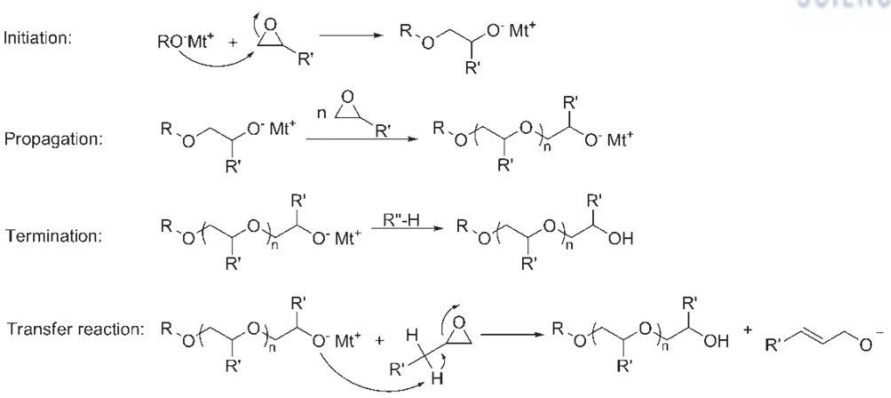

Figure 1.6. Mechanism of the anionic ring-opening polymerization (AROP) of functional epoxide monomers. Copyright © 2015 WILEY-VCH Verlag GmbH & Co. KGaA, Weinheim.[35]

ULSAN NATIONAL INSTITUTE OF SCIENCE AND TECHNOLOGY

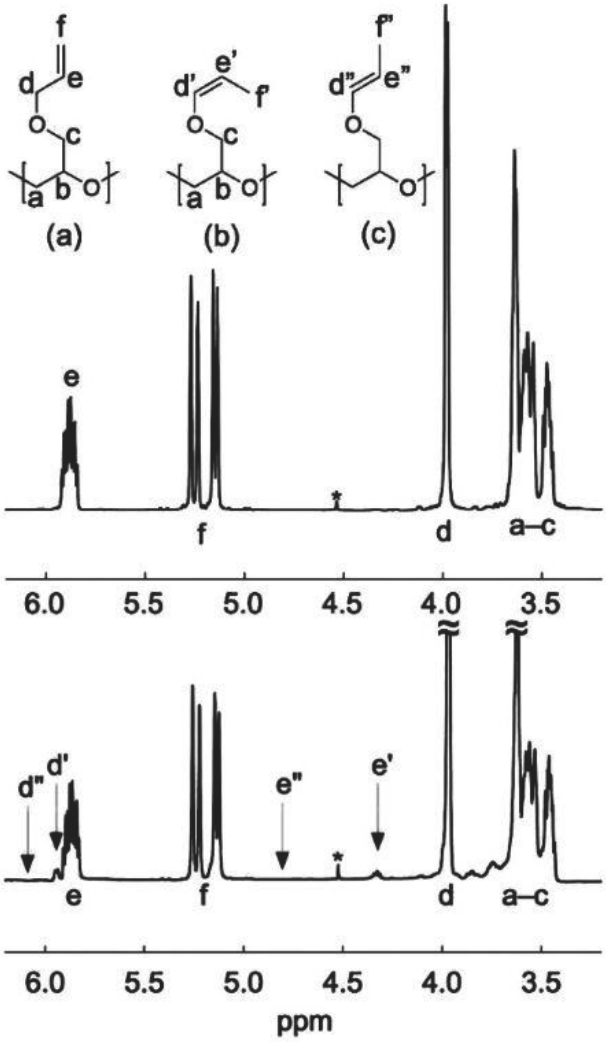

Figure 1.7. (Top) ^{1}H NMR spectrum of poly(allyl glycidyl ether) polymerized neat at 30 °C. Peak assignments are shown in the inset. The resonance near 4.5 ppm marked with an asterisk is due to the benzyl (2H) end group protons used for determination of molar mass. (Bottom) ^{1}H NMR spectrum of PAGE polymerized neat at 120 °C with inset peak assignments showing the presence of extra resonances due to the presence of *cis*-propenyl isomers. Three possible isomers exist: (a) allyl, (b) *cis*-prop-1-enyl, (c) *trans*-prop-1-enyl. Resonances are observed for the monomer-derived allyl, and *cis*-prop-1-enyl isomers only. No evidence of trans isomerization is present. Copyright © 2011 Wiley Periodicals, Inc.[10]

ULSAN NATIONAL INSTITUTE OF SCIENCE AND TECHNOLOGY

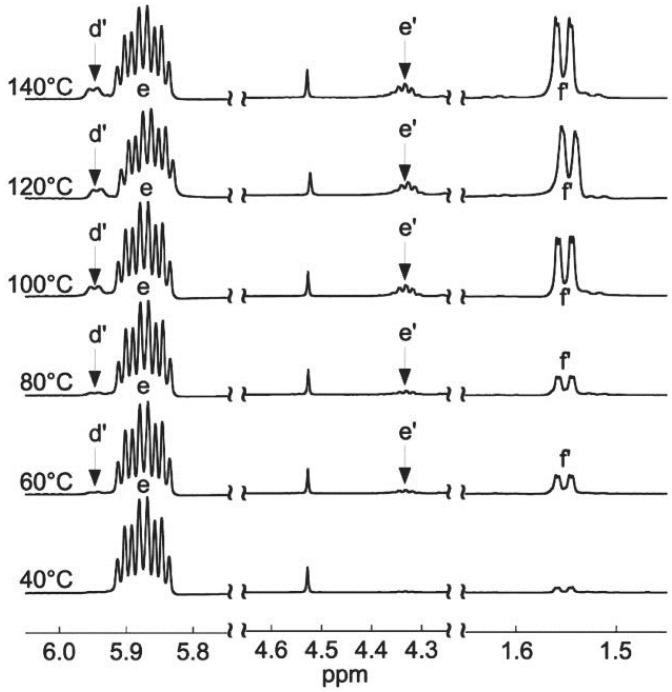

Figure 1.8. ^{1}H NMR spectra resulting from polymerizations carried out at various temperatures (40–140 °C). All spectra are normalized to the intensity of the benzyl resonance near 4.5 ppm (2H), and peak assignments are shown in Figure 1.7. The mole percent incorporation of cis-prop-1-enyl isomers increases with polymerization temperature for polymerizations of equivalent duration as evidenced by the increase in intensity of the peaks due to the d′ (1H), e′ (1H), and f′ (3H) protons. Copyright © 2011 Wiley Periodicals, Inc.[10]

ULSAN NATIONAL INSTITUTE OF SCIENCE AND TECHNOLOGY

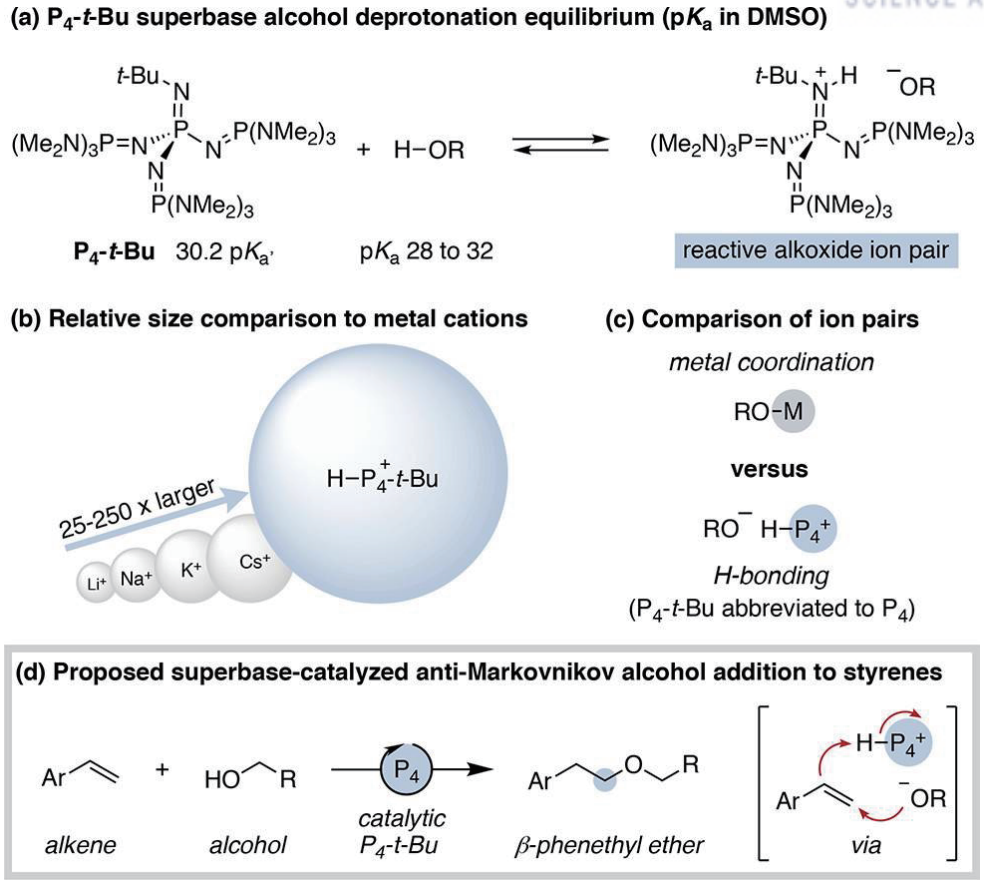

Figure 1.9. *t*-BuP$_4$ (a) alcohol deprotonation, (b, c) ion pair properties and (d) proposed addition reaction. Reprinted with permission from *J. Am Chem. Soc.* **2018**, *140*, 3547-3550. Copyright 2018 American Chemical Society.[37]

ULSAN NATIONAL INSTITUTE OF SCIENCE AND TECHNOLOGY

1.2.3 Post-polymerization Modification

Not all monomers are directly polymerizable. For example, allyl alcohol is not suitable for radical polymerization because it can undergo chain transfer by hydrogen abstraction (Figure 1.10a). To bypass the undesired side reaction, post-polymerization modification (PPM) is a promising alternative approach to obtain the desired polymer.[40,41] Hillmyer group recently introduced bis(*tert*-butyloxycarbonyl) twisted acrylamide monomer to synthesize poly(allyl alcohol) as a compatible precursor for the free or controlled radical polymerization (Figure 1.10b).[42] Klausen *et al*. developed BN 2-vinylnaphthalene to prepare poly(vinyl alcohol) derivatives via organoborane oxidation.[43] PPM of functional polymers has been demonstrated through myriad chemical reactions, such as transesterification,[44] Diels-Alder reaction,[45] azide-alkyne cycloaddition,[46] and Suzuki–Miyaura coupling.[47]

Several monomers containing functional groups that are not only stable under AROP conditions but also chemically modifiable have been reported to date.[48] Allyl glycidyl ether (AGE) is a representative functional epoxide monomer, which is widely used for decorating PEG-based polymers. Allyl group can undergo thiol-ene reaction to yield diverse pendant functionalities.[10,22–26] The development of epoxide monomers bearing tolerable functional groups is still necessary to broaden the scope of monomers, thereby providing an efficient PPM strategy for polyethers.

ULSAN NATIONAL INSTITUTE OF SCIENCE AND TECHNOLOGY

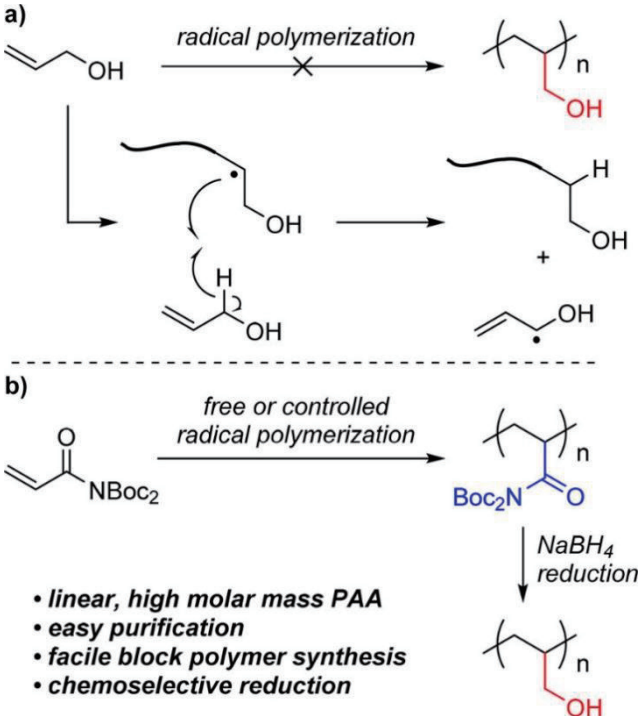

Figure 1.10. (a) Radical polymerization of allyl alcohol results in degradative chain transfer to monomer, limiting molar mass; (b) synthesis of linear, high molar mass PAA by postpolymerization reduction of PDBAm. Reprinted with permission from *J. Am. Chem. Soc.* **2018**, *140*, 11911-11915. Copyright 2018 American Chemical Society.[42]

ULSAN NATIONAL INSTITUTE OF SCIENCE AND TECHNOLOGY

1.3 Hyperbranched Polyglycerols: The Promising PEG Alternatives

The major disadvantage of PEG is the limited functionalization capacity, which restricts further modifications to introducing extra utilities. Recently, polyglycerol (PG) has emerged as an analogue of conventional PEG because of its multiple hydroxyl functionalities as well as its structural similarity with the latter. Both polyethers have several common properties such as superior biocompatibility and excellent solubility in polar solvents.[49] Hyperbranched PG (hbPG) possesses a compact, three-dimensional structure exhibiting lower hydrodynamic volume than that exhibited by PEG. A large number of hydroxyl groups of hbPG results in lower intrinsic viscosity and crystallinity than those of PEG.[50] The architecture of PG is divided into linear and hyperbranched structures, which can be obtained by different approaches (Figure 1.11). In this part, the synthetic procedure for the linear and hyperbranched polyglycerols is described. Furthermore, the strategy to functionalize hyperbranched polyglycerol is discussed.

1.3.1 Synthesis of Hyperbranched and Linear Polyglycerols

PG is a representative analogue of PEG, which is of significant interest in various fields. PG can be tailored from a linear to hyperbranched structure by several synthetic approaches. hbPG can be obtained by anionic ring-opening multibranching polymerization (ROMBP) of glycidol.[51] Glycidol is a reactive epoxide monomer possessing AB_2 monomer structure. The activated alkoxide initiator opens the epoxide ring of glycidol and the resultant new alkoxide can undergo fast proton exchange during the propagation step. The fast proton exchange at this stage results in a branched structure (Figure 1.12). The degree of branching, molecular weight, and dispersity can be controlled by the rate of monomer addition to a solution of partially deprotonated trihydroxyl functional initiator.[50]

To synthesize the linear PG, the hydroxyl group of glycidol should be protected in order to prevent the proton exchange (which generates the hyperbranched structure). Several protected glycidol monomers have been introduced to date (Figure 1.13a).[52] Ethoxyethyl glycidyl ether is one of the most common protected glycidol monomers containing acetal linkage, which can be deprotected by acid treatment (Figure 1.13b). Trimethylsilyl glycidyl ether, *tert*-butyl glycidyl ether, and allyl glycidyl ether are additional choices for the synthesis of linear PG. Recently, our group developed a cyclic acetal-containing epoxide monomer, tetrahydropyranyl glycidyl ether (Figure 1.3). This new monomer allowed the synthesis of a linear protected polyglycerol with a controllable deprotection rate.

The functionalization of hyperbranched polyglycerol is achieved by copolymerization of glycidol and functional epoxide monomer. Glycidol provides branching, and the functional epoxide monomer is copolymerized into the hyperbranched backbone to introduce certain functional groups in

ULSAN NATIONAL INSTITUTE OF
SCIENCE AND TECHNOLOGY

a single step. The introduction of allyl, phenyl, and catechol moieties was accomplished by this approach. In this thesis, we present amine-functional hyperbranched polyglycerol by ROMBP using glycidol and a newly designed Boc-protected butanolamine glycidyl ether (BBAG) monomer.

ULSAN NATIONAL INSTITUTE OF SCIENCE AND TECHNOLOGY

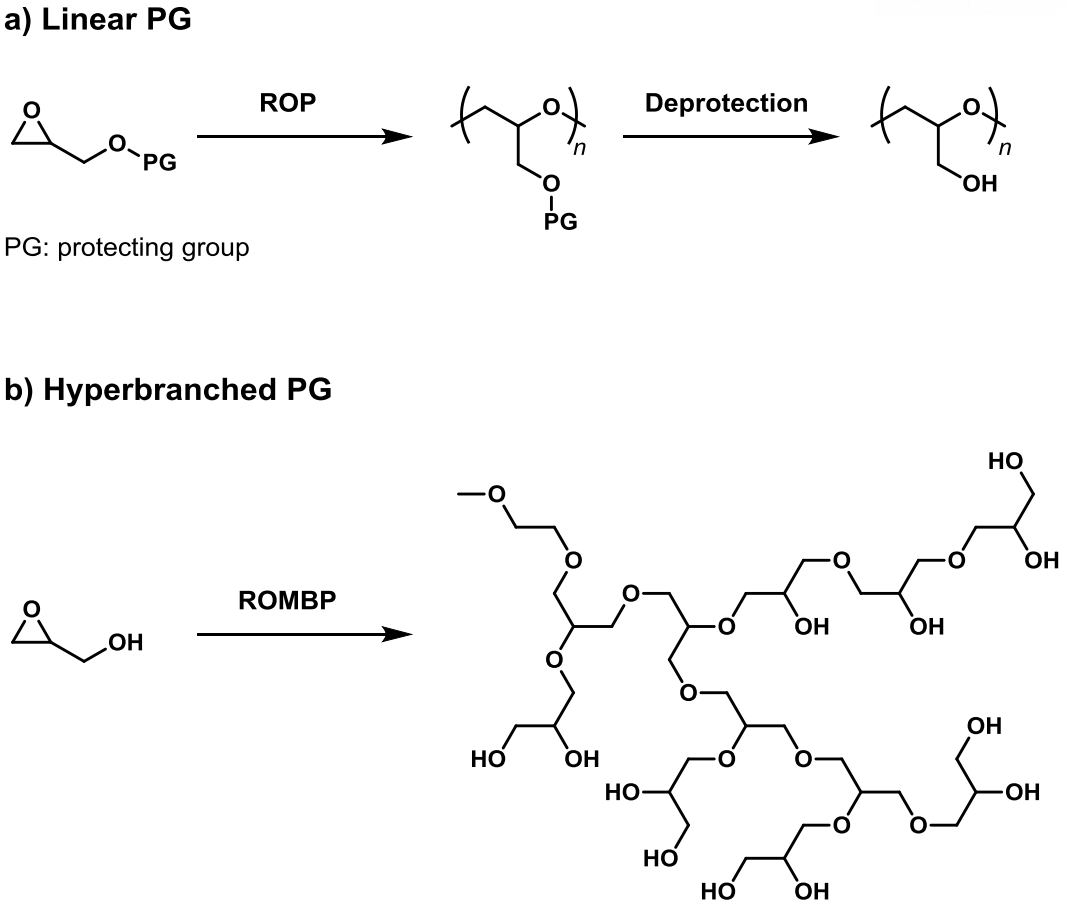

Figure 1.11. Synthetic approaches for (a) linear PG and (b) hyperbranched PG.

ULSAN NATIONAL INSTITUTE OF SCIENCE AND TECHNOLOGY

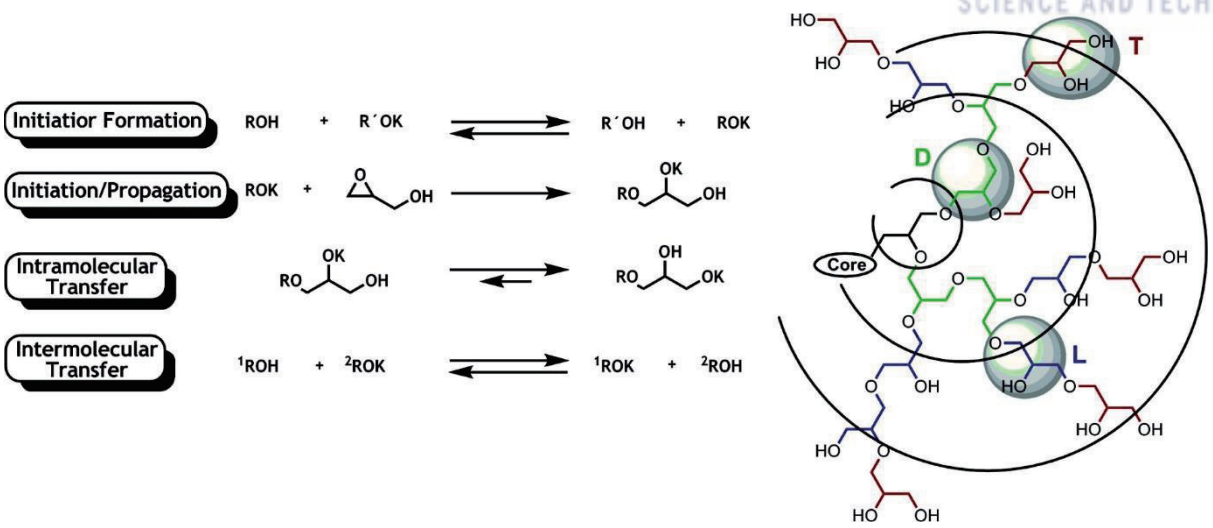

Figure 1.12. Mechanistic pathway of the base-catalyzed ring-opening polymerization of glycidol and structure of the resulting hyperbranched PG (small fragment of the actual polymer structure).[51]

ULSAN NATIONAL INSTITUTE OF SCIENCE AND TECHNOLOGY

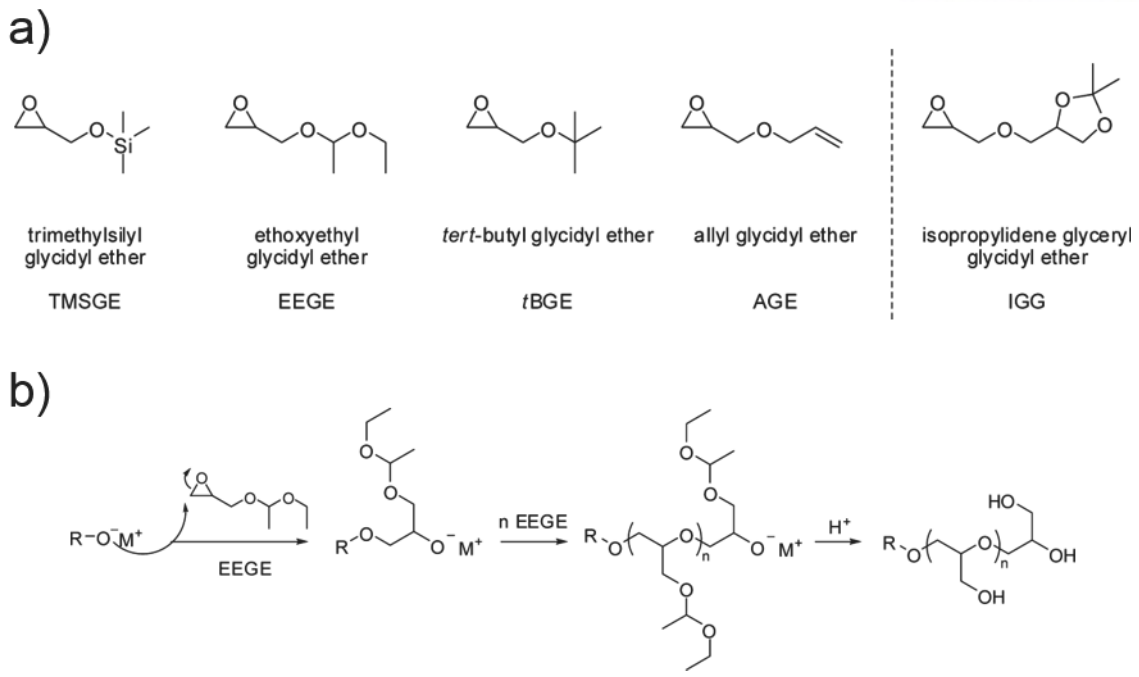

Figure 1.13. (a) Typical monomers for the synthesis of linear polyglycerol (*lin*PG) structures. (b) Anionic ring-opening polymerization of EEGE followed by acidic deprotection of the acetal protecting group.[52]

ULSAN NATIONAL INSTITUTE OF SCIENCE AND TECHNOLOGY

1.4 Overview of The Thesis

With the background described in General Introduction, the work reported in this thesis has been directed towards the anionic ring-opening polymerization (AROP) of functional epoxide monomers to synthesize multifunctional polyethers (Figure 1.14). First, commercially available allyl glycidyl ether (AGE) is utilized to synthesize well-defined allyl-functionalized polyether while aiming for the modular thiol-ene reaction with several aminothiols. The thermoresponsive behavior of the aqueous polymer solution was investigated. After establishing successful AROP with commercial monomer, we have developed a new Boc-protected butanolamine glycidyl ether (BBAG) monomer. The monomer was copolymerized with glycidol to obtain amine-functional hyperbranched polyglycerol. Lastly, we developed a series of azidoalkyl glycidyl ethers and polymerized the monomers. The PPM of azide-functional polyethers was demonstrated to decorate the polymer with various functional groups. We anticipate that this thesis can provide a comprehensive understanding of the development of functional polyethers, accompanied by the careful design of novel monomers.

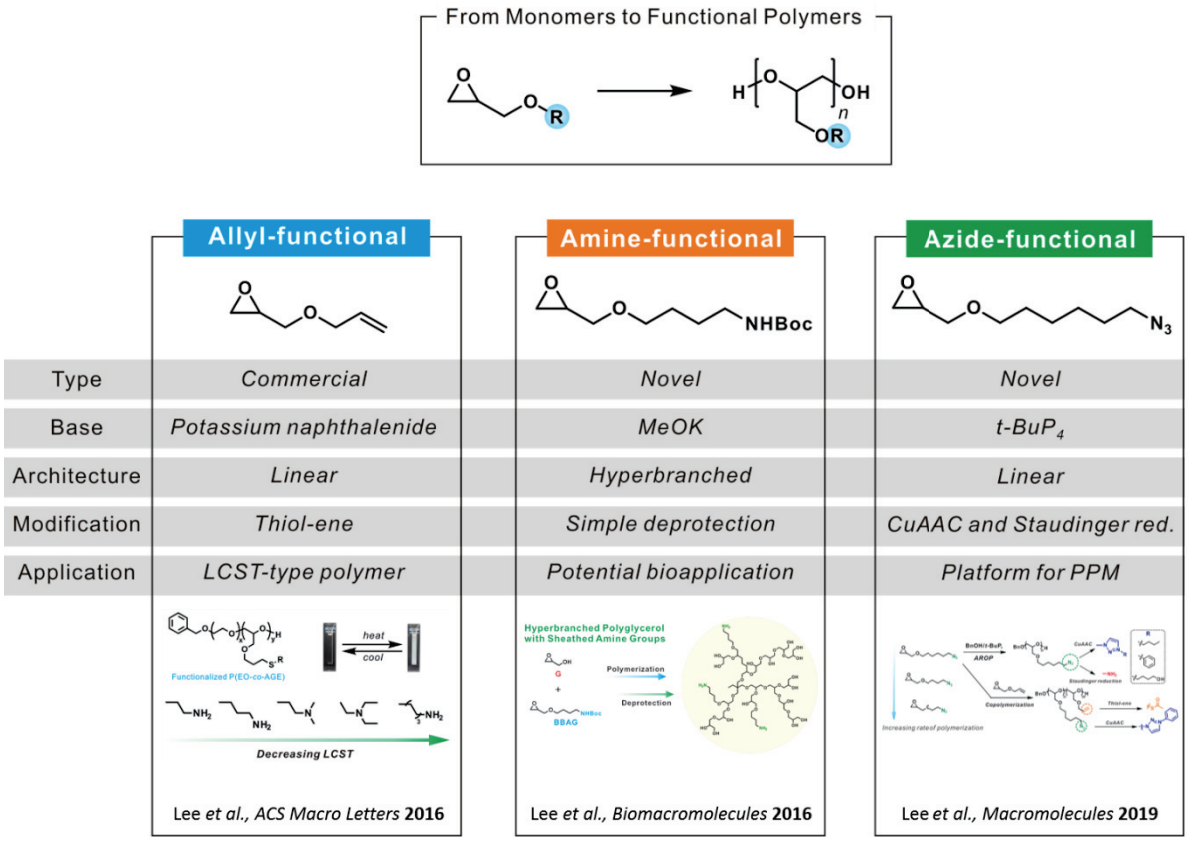

Figure 1.14. Overview of the thesis.

ULSAN NATIONAL INSTITUTE OF SCIENCE AND TECHNOLOGY

1.5 References

(1) Israelachvili, J. The Different Faces of Poly(ethylene glycol). *Proc. Natl. Acad. Sci.* **1997**, *94*, 8378–8379.

(2) Dingels, C.; Schömer, M.; Frey, H. Die Vielen Gesichter Des Poly(ethylenglykol)s. *Chemie unserer Zeit* **2011**, *45*, 338–349.

(3) Veronese, F. M.; Pasut, G. PEGylation, Successful Approach to Drug Delivery. *Drug Discov. Today* **2005**, *10*, 1451–1458.

(4) Herzberger, J.; Niederer, K.; Pohlit, H.; Seiwert, J.; Worm, M.; Wurm, F. R.; Frey, H. Polymerization of Ethylene Oxide, Propylene Oxide, and Other Alkylene Oxides: Synthesis, Novel Polymer Architectures, and Bioconjugation. *Chem. Rev.* **2016**, *116*, 2170–2243.

(5) Ahn, G.; Kweon, S.; Yang, C.; Hwang, J. E.; Kim, K.; Kim, B.-S. One-Pot Synthesis of Hyperbranched Polyamines Based on Novel Amino Glycidyl Ether. *J. Polym. Sci. Part A Polym. Chem.* **2017**, *55*, 4013–4019.

(6) Niederer, K.; Schüll, C.; Leibig, D.; Johann, T.; Frey, H. Catechol Acetonide Glycidyl Ether (CAGE): A Functional Epoxide Monomer for Linear and Hyperbranched Multi-Catechol Functional Polyether Architectures. *Macromolecules* **2016**, *49*, 1655–1665.

(7) Blankenburg, J.; Maciol, K.; Hahn, C.; Frey, H. Poly(ethylene glycol) with Multiple Aldehyde Functionalities Opens up a Rich and Versatile Post-Polymerization Chemistry. *Macromolecules* **2019**, *52*, 1785–1793.

(8) Elter, J. K.; Biehl, P.; Gottschaldt, M.; Schacher, F. H. Core-Crosslinked Worm-like Micelles from Polyether-Based Diblock Terpolymers. *Polym. Chem.* **2019**, *10*, 5425–5439.

(9) Song, S.; Lee, J.; Kweon, S.; Song, J.; Kim, K.; Kim, B.-S. Hyperbranched Copolymers Based on Glycidol and Amino Glycidyl Ether: Highly Biocompatible Polyamines Sheathed in Polyglycerols. *Biomacromolecules* **2016**, *17*, 3632–3639.

(10) Lee, B. F.; Kade, M. J.; Chute, J. A.; Gupta, N.; Campos, L. M.; Fredrickson, G. H.; Kramer, E. J.; Lynd, N. A.; Hawker, C. J. Poly(allyl glycidyl ether)-A Versatile and Functional Polyether Platform. *J. Polym. Sci. Part A Polym. Chem.* **2011**, *49*, 4498–4504.

(11) Mangold, C.; Wurm, F.; Obermeier, B.; Frey, H. "Functional Poly(ethylene glycol)": PEG-Based Random Copolymers with 1,2-Diol Side Chains and Terminal Amino Functionality. *Macromolecules* **2010**, *43*, 8511–8518.

(12) Jung, P.; Ziegler, A. D.; Blankenburg, J.; Frey, H. Glycidyl Tosylate: Polymerization of a "Non-

ULSAN NATIONAL INSTITUTE OF SCIENCE AND TECHNOLOGY

Polymerizable" Monomer Permits Universal Post-Functionalization of Polyethers. *Angew. Chemie Int. Ed.* **2019**, *58*, 12883–12886.

(13) Boopathi, S. K.; Hadjichristidis, N.; Gnanou, Y.; Feng, X. Direct Access to Poly(glycidyl azide) and Its Copolymers through Anionic (Co-)Polymerization of Glycidyl Azide. *Nat. Commun.* **2019**, *10*, 293.

(14) Mangold, C.; Dingels, C.; Obermeier, B.; Frey, H.; Wurm, F. PEG-Based Multifunctional Polyethers with Highly Reactive Vinyl-Ether Side Chains for Click-Type Functionalization. *Macromolecules* **2011**, *44*, 6326–6334.

(15) Herzberger, J.; Fischer, K.; Leibig, D.; Bros, M.; Thiermann, R.; Frey, H. Oxidation-Responsive and "Clickable" Poly(ethylene glycol) via Copolymerization of 2-(Methylthio)Ethyl Glycidyl Ether. *J. Am. Chem. Soc.* **2016**, *138*, 9212–9223.

(16) Herzberger, J.; Frey, H. Epicyanohydrin: Polymerization by Monomer Activation Gives Access to Nitrile-, Amino-, and Carboxyl-Functional Poly(ethylene glycol). *Macromolecules* **2015**, *48*, 8144–8153.

(17) Lee, A.; Lundberg, P.; Klinger, D.; Lee, B. F.; Hawker, C. J.; Lynd, N. A. Physiologically Relevant, pH-Responsive PEG-Based Block and Statistical Copolymers with N,N-Diisopropylamine Units. *Polym. Chem.* **2013**, *4*, 5735–5742.

(18) Reuss, V. S.; Werre, M.; Frey, H. Thermoresponsive Copolymers of Ethylene Oxide and N,N-Diethyl Glycidyl Amine: Polyether Polyelectrolytes and PEGylated Gold Nanoparticle Formation. *Macromol. Rapid Commun.* **2012**, *33*, 1556–1561.

(19) Reuss, V. S.; Obermeier, B.; Dingels, C.; Frey, H. N,N-Diallylglycidylamine: A Key Monomer for Amino-Functional Poly(ethylene glycol) Architectures. *Macromolecules* **2012**, *45*, 4581–4589.

(20) Obermeier, B.; Wurm, F.; Frey, H. Amino Functional Poly(ethylene glycol) Copolymers via Protected Amino Glycidol. *Macromolecules* **2010**, *43*, 2244–2251.

(21) Oikawa, Y.; Lee, S.; Kim, D. H.; Kang, D. H.; Kim, B.-S.; Saito, K.; Sasaki, S.; Oishi, Y.; Shibasaki, Y. One-Pot Synthesis of Linear-Hyperbranched Amphiphilic Block Copolymers Based on Polyglycerol Derivatives and Their Micelles. *Biomacromolecules* **2013**, *14*, 2171–2178.

(22) Le Devedec, F.; Won, A.; Oake, J.; Houdaihed, L.; Bohne, C.; Yip, C. M.; Allen, C. Postalkylation of a Common MPEG-*b*-PAGE Precursor to Produce Tunable Morphologies of Spheres, Filomicelles, Disks, and Polymersomes. *ACS Macro Lett.* **2016**, *5*, 128–133.

ULSAN NATIONAL INSTITUTE OF SCIENCE AND TECHNOLOGY

(23) Obermeier, B.; Frey, H. Poly(ethylene glycol-*co*-allyl glycidyl ether)s: A PEG-Based Modular Synthetic Platform for Multiple Bioconjugation. *Bioconjugate Chem.* **2011**, *22*, 436–444.

(24) Lee, J.; McGrath, A. J.; Hawker, C. J.; Kim, B.-S. PH-Tunable Thermoresponsive PEO-Based Functional Polymers with Pendant Amine Groups. *ACS Macro Lett.* **2016**, *5*, 1391–1396.

(25) Fleischmann, C.; Gopez, J.; Lundberg, P.; Ritter, H.; Killops, K. L.; Hawker, C. J.; Klinger, D. A Robust Platform for Functional Microgels via Thiol–Ene Chemistry with Reactive Polyether-Based Nanoparticles. *Polym. Chem.* **2015**, *6*, 2029–2037.

(26) Oleske, K. W.; Barteau, K. P.; Turker, M. Z.; Beaucage, P. A.; Estroff, L. A.; Wiesner, U. Block Copolymer Directed Nanostructured Surfaces as Templates for Confined Surface Reactions. *Macromolecules* **2017**, *50*, 542–549.

(27) Song, S.; Lee, J.; Kweon, S.; Song, J.; Kim, K.; Kim, B.-S. Hyperbranched Copolymers Based on Glycidol and Amino Glycidyl Ether: Highly Biocompatible Polyamines Sheathed in Polyglycerols. *Biomacromolecules* **2016**, *17*, 3632–3639.

(28) Hwang, E.; Kim, K.; Lee, C. G.; Kwon, T.-H.; Lee, S.-H.; Min, S. K.; Kim, B.-S. Tailorable Degradation of PH-Responsive All-Polyether Micelles: Unveiling the Role of Monomer Structure and Hydrophilic–Hydrophobic Balance. *Macromolecules* **2019**, *52*, 5884–5893.

(29) Ahn, G.; Kweon, S.; Yang, C.; Hwang, J. E.; Kim, K.; Kim, B.-S. One-Pot Synthesis of Hyperbranched Polyamines Based on Novel Amino Glycidyl Ether. *J. Polym. Sci. Part A Polym. Chem.* **2017**, *55*, 4013–4019.

(30) Staudinger, H.; Lohmann, H. Über Hochpolymere Verbindungen. 81. Mitteilung. Über Eukolloides Polyäthylenoxyd. *Justus Liebig's Ann. der Chemie* **1933**, *505*, 41–51.

(31) Flory, P. J. Molecular Size Distribution in Ethylene Oxide Polymers. *J. Am. Chem. Soc.* **1940**, *62*, 1561–1565.

(32) Penczek, S.; Cypryk, M.; Duda, A.; Kubisa, P.; Slomkowski, S. Living Ring-Opening Polymerizations of Heterocyclic Monomers. *Prog. Polym. Sci.* **2007**, *32*, 247–282.

(33) Brocas, A.-L.; Mantzaridis, C.; Tunc, D.; Carlotti, S. Polyether Synthesis: From Activated or Metal-Free Anionic Ring-Opening Polymerization of Epoxides to Functionalization. *Prog. Polym. Sci.* **2013**, *38*, 845–873.

(34) de Lucas, A.; Rodríguez, L.; Pérez-Collado, M.; Sánchez, P.; Rodríguez, J. F. Synthesis of Polyols by Anionic Polymerization: Determination of Kinetic Parameters of Propylene Oxide Polymerization Using Caesium and Potassium Alcoholates. *Polym. Int.* **2002**, *51*, 1066–1071.

ULSAN NATIONAL INSTITUTE OF SCIENCE AND TECHNOLOGY

(35) Klein, R.; Wurm, F. R. Aliphatic Polyethers: Classical Polymers for the 21st Century. *Macromol. Rapid Commun.* **2015**, *36*, 1147–1165.

(36) Pearson, R. G. Hard and Soft Acids and Bases. *J. Am. Chem. Soc.* **1963**, *85*, 3533–3539.

(37) Luo, C.; Bandar, J. S. Superbase-Catalyzed Anti-Markovnikov Alcohol Addition Reactions to Aryl Alkenes. *J. Am. Chem. Soc.* **2018**, *140*, 3547–3550.

(38) Isono, T.; Asai, S.; Satoh, Y.; Takaoka, T.; Tajima, K.; Kakuchi, T.; Satoh, T. Controlled/Living Ring-Opening Polymerization of Glycidylamine Derivatives Using *t*-Bu-P_4 /Alcohol Initiating System Leading to Polyethers with Pendant Primary, Secondary, and Tertiary Amino Groups. *Macromolecules* **2015**, *48*, 3217–3229.

(39) Misaka, H.; Sakai, R.; Satoh, T.; Kakuchi, T. Synthesis of High Molecular Weight and End-Functionalized Poly(styrene oxide) by Living Ring-Opening Polymerization of Styrene Oxide Using the Alcohol/Phosphazene Base Initiating System. *Macromolecules* **2011**, *44*, 9099–9107.

(40) Blasco, E.; Sims, M. B.; Goldmann, A. S.; Sumerlin, B. S.; Barner-Kowollik, C. 50th Anniversary Perspective : Polymer Functionalization. *Macromolecules* **2017**, *50*, 5215–5252.

(41) Hawker, C. J. The Convergence of Synthetic Organic and Polymer Chemistries. *Science.* **2005**, *309*, 1200–1205.

(42) Larsen, M. B.; Wang, S.-J.; Hillmyer, M. A. Poly(allyl alcohol) Homo- and Block Polymers by Postpolymerization Reduction of an Activated Polyacrylamide. *J. Am. Chem. Soc.* **2018**, *140*, 11911–11915.

(43) van de Wouw, H. L.; Lee, J. Y.; Awuyah, E. C.; Klausen, R. S. A BN Aromatic Ring Strategy for Tunable Hydroxy Content in Polystyrene. *Angew. Chemie Int. Ed.* **2018**, 1–6.

(44) Ito, D.; Ogura, Y.; Sawamoto, M.; Terashima, T. Acrylate-Selective Transesterification of Methacrylate/Acrylate Copolymers: Postfunctionalization with Common Acrylates and Alcohols. *ACS Macro Lett.* **2018**, *7*, 997–1002.

(45) Yuksekdag, Y. N.; Gevrek, T. N.; Sanyal, A. Diels-Alder “Clickable” Polymer Brushes: A Versatile Catalyst-Free Conjugation Platform. *ACS Macro Lett.* **2017**, *6*, 415–420.

(46) Doran, S.; Yilmaz, G.; Yagci, Y. Tandem Photoinduced Cationic Polymerization and CuAAC for Macromolecular Synthesis. *Macromolecules* **2015**, *48*, 7446–7452.

(47) Howe, D. H.; McDaniel, R. M.; Magenau, A. J. D. From Click Chemistry to Cross-Coupling: Designer Polymers from One Efficient Reaction. *Macromolecules* **2017**, *50*, 8010–8018.

ULSAN NATIONAL INSTITUTE OF SCIENCE AND TECHNOLOGY

(48) Obermeier, B.; Wurm, F.; Mangold, C.; Frey, H. Multifunctional Poly(ethylene glycol)s. *Angew. Chemie Int. Ed.* **2011**, *50*, 7988–7997.

(49) Kainthan, R. K.; Janzen, J.; Levin, E.; Devine, D. V; Brooks, D. E. Biocompatibility Testing of Branched and Linear Polyglycidol. *Biomacromolecules* **2006**, *7*, 703–709.

(50) Sunder, A.; Hanselmann, R.; Frey, H.; Mülhaupt, R. Controlled Synthesis of Hyperbranched Polyglycerols by Ring-Opening Multibranching Polymerization. *Macromolecules* **1999**, *32*, 4240–4246.

(51) Wilms, D.; Stiriba, S.-E.; Frey, H. Hyperbranched Polyglycerols: From the Controlled Synthesis of Biocompatible Polyether Polyols to Multipurpose Applications. *Acc. Chem. Res.* **2010**, *43*, 129–141.

(52) Thomas, A.; Müller, S. S.; Frey, H. Beyond Poly(ethylene glycol): Linear Polyglycerol as a Multifunctional Polyether for Biomedical and Pharmaceutical Applications. *Biomacromolecules* **2014**, *15*, 1935–1954.

ULSAN NATIONAL INSTITUTE OF SCIENCE AND TECHNOLOGY

Chapter 2

pH-Tunable Thermoresponsive PEO-Based Functional Polymers Containing Pendant Amine Groups*

2.1. Abstract

Thermoresponsive polymers exhibiting lower critical solution temperatures (LCSTs) in aqueous solution have garnered considerable attention for the development of smart materials. Herein, we report the synthesis and properties of pH-tunable thermoresponsive poly(ethylene oxide) (PEO)-based functional polymers bearing pendant amine groups with varying cloud points. Well-defined poly(ethylene oxide-*co*-allyl glycidyl ether) (P(EO-*co*-AGE)) copolymers were prepared via controlled anionic ring-opening polymerization of ethylene oxide (EO) with 10 mol % of a functional allyl glycidyl ether (AGE) comonomer. Facile, modular thiol–ene click chemistry was then employed to introduce a library of different aminothiols as side chains to the initial P(EO-*co*-AGE) copolymer. Depending on the nature of the pendant amine groups (primary amine, dimethylamine, and diethylamine) and the hydrophobicity of the side chains (ethyl, propyl, and hexyl), the cloud points could be tuned from 44–100 °C under different pH conditions. This is the first systematic investigation into the effect of PEO copolymer side chains on cloud point, which opens up the opportunity to make new thermoresponsive polymers for a variety of smart material applications.

*Chapter 2 is reproduced in part with permission from *ACS Macro Letters* **2016**, *5*, 1391–1306 by Joonhee Lee, Alaina J. McGrath, Craig J. Hawker, and Byeong-Su Kim. Copyright 2016 American Chemical Society.

ULSAN NATIONAL INSTITUTE OF SCIENCE AND TECHNOLOGY

2.2. Introduction

Polymers capable of responding to various environmental stimuli such as temperature,[1-3] pH,[4] light,[5] and mechanical force[6] have attracted significant attention, with applications ranging from environmental materials to biomedical devices. Thermoresponsive polymers, in particular, have been investigated for the development of smart materials due to their unique phase transition properties in aqueous solution, including lower critical solution temperature (LCST) and upper critical solution temperature (UCST).[7-10] In particular, the lower critical solution temperature (LCST) is the temperature above which phase separation is observed, which coincides with decreasing polymer solubility.[11, 12] At low temperatures, LCST-type thermoresponsive polymers are soluble, owing to hydrogen bonding with the surrounding water molecules, resulting in restricted intra/intermolecular interactions between polymer chains. Upon heating, the hydrogen bonds are disrupted, and the polymer chains exhibit a phase transition, with solubility decreasing due to the disruption of the interactions between the polymer and the solvating water molecules. It has been suggested that the LCST is dependent on many external parameters, including monomer composition, the hydrophilic/hydrophobic balance, molecular weight, concentration, and the ionic species present.[13-16] The ability to develop thermoresponsive polymers with a wide range of LCSTs that can be tuned depending on external stimuli is therefore of significant interest.[17-20]

The most studied thermoresponsive polymer, poly(*N*-isopropylacrylamide) (PNIPAM), exhibits a clear phase transition at a LCST of 32 °C, close to body temperature.[13] Water-soluble, nontoxic, and nonimmunogenic poly(ethylene oxide) (PEO) is another biologically important synthetic polymer that is widely used in biomedical applications.[21-23] However, PEO's LCST (nearly 100 °C)[24] is too high for most biomedical applications, prompting studies on the LCST behavior of PEO-based polymers. These studies have tailored the LCST of PEO by introducing hydrophobic side chains to the PEO backbone or by the integration of new functional monomers.[25] As notable examples, a range of monomers containing hydrophobic side chains have been copolymerized with ethylene oxide (EO) to yield functional PEO derivatives exhibiting varying LCST values, including glycidyl methyl ether,[26] ethoxyl vinyl glycidyl ether,[27, 28] *N*,*N*-diisopropyl ethanol amine glycidyl ether,[4] allyl glycidyl ether (AGE),[28] and *N*,*N*-dibenzyl amino glycidyl.[28, 29] Although the aforementioned functional monomers lead to modulation of the LCST, a major drawback of their use is the requirement of separate syntheses for each functional copolymer with varying comonomer contents. As a result, there is a significant time and materials investment for the preparation of a library of materials with a range of LCST values.

As an alternative strategy, postpolymerization functionalization of a single PEO-based starting copolymer with a defined molecular weight, architecture, and polydispersity can be used to furnish a library of copolymers with varying LCSTs. In particular, PEO-based copolymers with functional allyl

ULSAN NATIONAL INSTITUTE OF SCIENCE AND TECHNOLOGY

side chains offer a unique handle that is amenable to quantitative thiol–ene click chemistry, with prior work showing the successfully controlled copolymerization of EO and AGE, followed by conjugation with multifunctional peptide units.[30] In addition to lowering the LCST, controlling the LCST behavior of PEO-based polymers with external stimuli such as pH can offer new application opportunities.

Herein, we describe the synthesis of a series of thermoresponsive, functional PEO-based polymers bearing pendant amine groups via postpolymerization modification of P(EO-*co*-AGE) copolymers through thiol–ene coupling chemistry using five different aminothiols (R-SH, see Figure 2.1), including cysteamine (R_1), *N*,*N*-dimethylaminoethanethiol (R_2), *N*,*N*-diethylaminoethanethiol (R_3), 3-amino-1-propanethiol (R_4), and 6-amino-1-hexanethiol (R_5). This allowed a systematic investigation into the effect of PEO copolymer side chains on LCST behavior through varying the nature of the amine groups (primary R_1 vs tertiary R_2 and R_3), the length of the side chains (R_1, R_4, and R_5), and the pH. Generally, LCST behavior is determined qualitatively by measuring the cloud point temperature; this is the temperature that corresponds to the polymer solution optically changing from transparent to turbid.[31] The modified functional copolymers, **P1**–**P5**, were successfully characterized by ^{1}H NMR and GPC analysis, with the resulting copolymers exhibiting significantly different, yet tunable LCST behavior under varying pH conditions. Lee and co-workers previously reported that the LCST of amine-functionalized poly(2-hydroxyethyl methacrylate) (PHEMA) was significantly affected by the pH of the solution.[32] However, to the best of our knowledge, there have been no reports on thermoresponsive PEO-based polymers that have cloud points that can be tuned by varying the nature of the amino group or side-chain length.

ULSAN NATIONAL INSTITUTE OF SCIENCE AND TECHNOLOGY

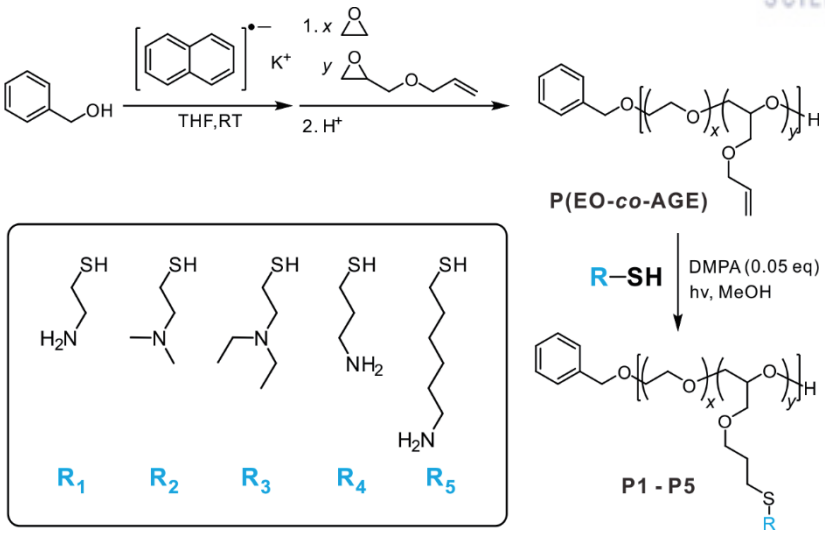

Figure 2.1. Synthesis of amine-functionalized PEO-based polymers, **P1** – **P5** with different pendant amine groups (R1–R5)

ULSAN NATIONAL INSTITUTE OF SCIENCE AND TECHNOLOGY

2.3. Experimental Section

Materials

All chemicals were used as received from Sigma-Aldrich unless otherwise specified. THF was collected from a dry solvent system and used immediately thereafter. Allyl glycidyl ether was degassed via several freeze-pump-thaw cycles and was distilled from butyl magnesium chloride to a flask for storage. Ethylene oxide (EO) was condensed into a Schlenk flask and degassed via several freeze-pump-thaw cycles, then distilled to a flame-dried burette immediately before use. Potassium naphthalenide was prepared from potassium metal and recrystallized naphthalene in dry THF and stirred with a glass-coated stirrer bar for 24 h at room temperature before use.

Characterization

^{1}H NMR spectra were recorded on a Varian VNMRS 600 MHz spectrometer at room temperature using $CDCl_3$ as a solvent. Gel permeation chromatography (GPC) analysis was carried out using a Waters 2695 separation module with a Waters 2414 refractive index (RI) detector and a Waters Alliance HPLC system (2695 separation module) using chloroform containing 0.25 wt% triethylamine as a mobile phase. Linear poly(ethylene oxide) (PEO) standards were applied as calibration samples. Thiol-ene reactions were irradiated with a UVP Black ray UV Bench Lamp XX-15L, which emits 365 nm light at 15 W. The transmittances of the aqueous polymer solutions were measured using a Shimadzu UV3600 UV-vis spectrometer equipped with a temperature controller. A 500 nm wavelength was used to determine the LCST, which was defined as a temperature at which the transmittance had decreased by 10%. [33, 34]

Synthesis of P(EO-co-AGE)

This procedure is based upon the synthesis of P(EO-*co*-AGE) described by Lee et al.[4] Polymerizations were performed in a custom-made five-armed thick-walled glass reactor fitted with ACE-threads under an inert argon atmosphere. The reactors were fitted with Teflon stoppers, a burette containing anhydrous tetrahydrofuran (THF), a flexible connector attached to a burette containing ethylene oxide (EO) (stored in an ice bath), and a glass arm connector sealed with a 6 mm Puresep septum and attached to a Schlenk line via a flexible connector. The reactor was flame-dried under vacuum and refilled with argon five times. Under a positive pressure of argon, anhydrous THF was added by opening the threaded stopcock on the attached burette. Benzyl alcohol initiator was added via a gastight syringe through a 6 mm Puresep septum. Potassium naphthalenide (0.30 M in THF) was added dropwise via gastight syringe until a light green color persisted in the solution, indicating complete deprotonation of the benzyl alcohol initiator. Condensed EO was added by lifting the cold burette and allowing the EO to drain into THF solution while AGE was simultaneously added via

ULSAN NATIONAL INSTITUTE OF SCIENCE AND TECHNOLOGY

gastight syringe. The addition of the monomers immediately quenched the green color, and the polymerization was carried out at room temperature for 2 days. The reaction was quenched with degassed acidic methanol and precipitated from hexane. The resulting polymer was purified using a short pad of silica gel (10% MeOH/dichloromethane as eluent). M_n and $Đ$ (M_w/M_n) were determined by ^{1}H NMR and GPC analysis, respectively.

General procedure for thiol-ene coupling

This procedure is based upon the synthesis of P(EO-*co*-AGE) described by Kang et al.[35] The thiol-ene reactions between P(EO-*co*-AGE) and the aminoethanethiol hydrochlorides (3.0 equivalents for each "ene" moiety) were carried out using 2,2-dimethoxy-2-phenylacetophenone (0.05 equivalents for each "ene" moiety) as a photoinitiator in methanol. The reaction mixture was degassed via three freeze-pump-thaw cycles, backfilled with argon, and irradiated with UV light (λ = 365 nm) for 2 h until complete disappearance of the alkene peaks as indicated by ^{1}H NMR analysis. Triethylamine and water were then added to the reaction mixtures to neutralize the hydrochloride salt and obtain the free amines. Methanol and excess triethylamine were then removed under reduced pressure. The aqueous layers were extracted with dichloromethane three times and washed with brine. The organic fractions were dried over anhydrous Na_2SO_4, filtered, and concentrated under reduced pressure. The concentrated mixtures were precipitated twice into hexane. The resulting viscous polymers were obtained and dried under high vacuum for one day (typical isolated yield of 80–90%).

ULSAN NATIONAL INSTITUTE OF SCIENCE AND TECHNOLOGY

2.4 Results and Discussion

As illustrated in Figure 2.1, the copolymer precursor used for thiol–ene addition was synthesized via anionic ring-opening copolymerization of EO and AGE, following the procedure reported by Lynd and co-workers.[36] Polymerization was initiated with benzyl alkoxide, which was generated by treatment of benzyl alcohol with a dilute solution of potassium naphthalenide. This method is known to be a convenient and effective method for initiating anionic ring-opening polymerization of glycidyl ethers.[37] The molecular weight and $Đ$ of P(EO-*co*-AGE) were characterized by ^{1}H NMR spectroscopy and GPC (Figure 2.2 – 2.4). The number average molecular weight (M_n) was found to be ~6400 g·mol^{-1} by ^{1}H NMR using the methylene protons of the terminal benzyl group as an internal reference (4.55 ppm). In addition, the ratio of the comonomers in the polymer backbone was determined using the characteristic allyl peaks at 5.13 and 5.22 ppm (peak *f* in Figure 2.2a) and 5.85 ppm (peak *e* in Figure 2.2a), with the results being in good agreement with the targeted value (10 mol % AGE units). The GPC of P(EO-*co*-AGE) showed a similar molecular weight to that obtained via ^{1}H NMR and a narrow molecular weight distribution for P(EO-*co*-AGE) ($Đ$ = 1.10, Figure 2.4).

After successful polymerization of P(EO-*co*-AGE), we performed photochemical-mediated thiol–ene additions with five different aminothiols (R_1–R_5) to give the copolymers **P1**–**P5**, as shown in Figure 2.1. ^{1}H NMR spectroscopy clearly confirmed the successful functionalization of P(EO-*co*-AGE) with different pendant amine groups that are sensitive to external pH (Figure 2.2). The quantitative addition of aminothiols to the P(EO-*co*-AGE) allyl groups was indicated by the disappearance of the allylic peaks from the functional AGE comonomer. The concomitant appearance of peaks corresponding to aminoalkyl groups also supported the successful conversion. GPC analyses showed narrow single peaks for **P2** and **P3**, verifying the purity of the resulting polymers and the lack of interchain coupling (Figure 2.4). It should be noted that **P1**, **P4**, and **P5** could not be analyzed by GPC due to the strong interactions between the pendant primary amine groups and the GPC column. Table 2.1 summarizes the characterization data for the PEO-based copolymers with pendant amine groups prepared through anionic ring-opening polymerization and thiol–ene addition.

The resulting polymers formed transparent aqueous solutions at room temperature due to the high aqueous solubility of the PEO backbone. Significantly, raising the temperature induced an abrupt increase in turbidity, demonstrating thermally induced phase transition behavior. This allowed the thermoresponsive phase transition behaviors of the polymers to be investigated by UV–vis spectroscopy. Transmittance changes in 0.10 wt % aqueous polymer solutions as a function of temperature were measured by UV–vis spectroscopy at 500 nm, with the cloud points being defined as the temperature at which a 10% decrease in transmittance was recorded (Figure 2.5).[33,34] The cloud points of **P1** were 70 and 91 °C at pH 13.0 and 12.5, respectively (Figure 2.5a). When the pH was below 12.5, no phase transitions were observed below 100 °C, suggesting that the primary amine groups on the side chains

ULSAN NATIONAL INSTITUTE OF SCIENCE AND TECHNOLOGY

were protonated under more acidic conditions. Consequently, **P1** consists of both a hydrophilic PEO backbone and protonated amine groups below pH 12, resulting in increased solubility in water at higher temperatures. This observation was in accordance with previous reports showing the effect of hydrophobic/hydrophilic side chains on the nature of the ionizable groups.[19,38] As shown in Figure 2.5b, the behavior of **P2** showed significant variation, with the cloud point being 91 °C at pH 9.0 and 50 °C at pH 13.0. The LCST decreased with increasing pH as the balance of hydrophilicity and hydrophobicity was changed by the protonation state of the *N*,*N*-dimethylamino group. Figure 2.5c also clearly shows that the cloud point of **P3** decreased as the pH was increased from 9.0 to 13.0. The results from these three polymers show that as the amine group is changed from primary to tertiary, the cloud point of the polymer at pH 13 decreased. Although a phase transition below 100 °C was not observed for **P1** at pH 12.0, **P2** and **P3** showed clear decreases in transmittance at pH 12.0 and 11.0, suggesting that the alkyl groups on the tertiary amines enhanced their hydrophobicity, inhibiting the hydration of the protonated amine moieties. As a result, the polymers retained a hydrophobicity/hydrophilicity balance and exhibited LCST behavior at lower pH values. These observations indicate that the LCST transition is primarily affected by the hydrophobicity of the amine groups, in accordance with previous findings for other materials.[39] As further evidence, the phase transition behavior of **P3** in Figure 2.5c shows that the cloud points of **P3** were lower than those of **P1** and **P2** at high pH, and that the transmittance dropped more drastically upon heating. This was likely due to the increased hydrophobicity of the diethylamino group in **P3**, which resulted in this polymer showing the lowest cloud points under basic conditions.

In order to investigate the effect of side chain hydrophobicity further, polymers with primary amine groups but different side chain lengths were examined. In this series, the cloud point of **P1**, **P4**, and **P5** were compared and analyzed according to the length of the pendant chains. Again, **P1**, **P4**, and **P5** showed pH-responsive LCST behavior due to the primary amine groups. By comparing the transmittance curves shown in Figure 2.5, it can be seen that the polymer with the longest side chain (**P5**) exhibited the lowest cloud point at a given pH. As the side chain length was increased from ethyl (**P1**) to propyl (**P4**) to hexyl (**P5**), the cloud point at pH 13 decreased from 70 to 66 to and 44 °C for **P1**, **P4**, and **P5**, respectively. These observations indicate that the LCST transition is significantly affected by the length of the side chain. It was observed that the phase transition of **P5** was reversible with a clear hysteresis occurring during the cooling process (Figure 2.6).

A comparison of the cloud points of the different polymers as a function of pH is shown in Figure 2.7, which clearly shows that the cloud point at a given pH decreased as the hydrophobicity of the amine group or length of the side chain was increased. To quantitatively investigate the effect of side chain hydrophobicity, the octanol/water coefficients (log *P*) of the thiols (R_1–R_5) were calculated using the software ALOGPS 2.1, based on a well-known computational model (Table 2.1).[40,41] Comparing the log *P* values of the side chain of **P1**, **P2**, and **P3**, it can be seen that the

ULSAN NATIONAL INSTITUTE OF SCIENCE AND TECHNOLOGY

hydrophobicity increased as the number of carbons on the N atom increased. Increasing the hydrophobicity of the amine moiety significantly lowered the cloud points at all pH values. As expected, the side chain length was also highly correlated with hydrophobicity, as can be seen by comparing the log *P* values of **P1**, **P4**, and **P5**.

Despite these relationships, comparing the log *P* values of **P3** and **P5** shows there was not an exact correlation between cloud point and hydrophobicity. It should be noted that **P3** and **P5** have the same number of carbons on their side chains. Nevertheless, the log *P* values of **P3** and **P5** are 2.34 and 2.07, respectively, indicating that **P3** was more hydrophobic than **P5**. However, the cloud point of **P3** was higher than **P5** between pH 11.0 and 13.0, suggesting that the primary amine group on **P5** can collapse into a globule state at lower temperatures due to intra/interchain hydrogen bonds.[42] As shown in Figure 2.6, the hysteresis is observed clearly in a heating-and-cooling cycle, attributed to the formation of additional hydrogen bonds of each primary amine groups that inhibits hydration in the cooling process. The LCST trends of **P3** and **P5** reversed below pH 11.0, as protonated primary amines can be hydrated much more easily than the protonated tertiary amines due to the hydrophobic diethyl groups that inhibit interaction with water. It can therefore be concluded that LCST-type phase transition is affected by a complicated interaction of the hydrophilicity/hydrophobicity balance with hydrogen bonding ability.

ULSAN NATIONAL INSTITUTE OF SCIENCE AND TECHNOLOGY

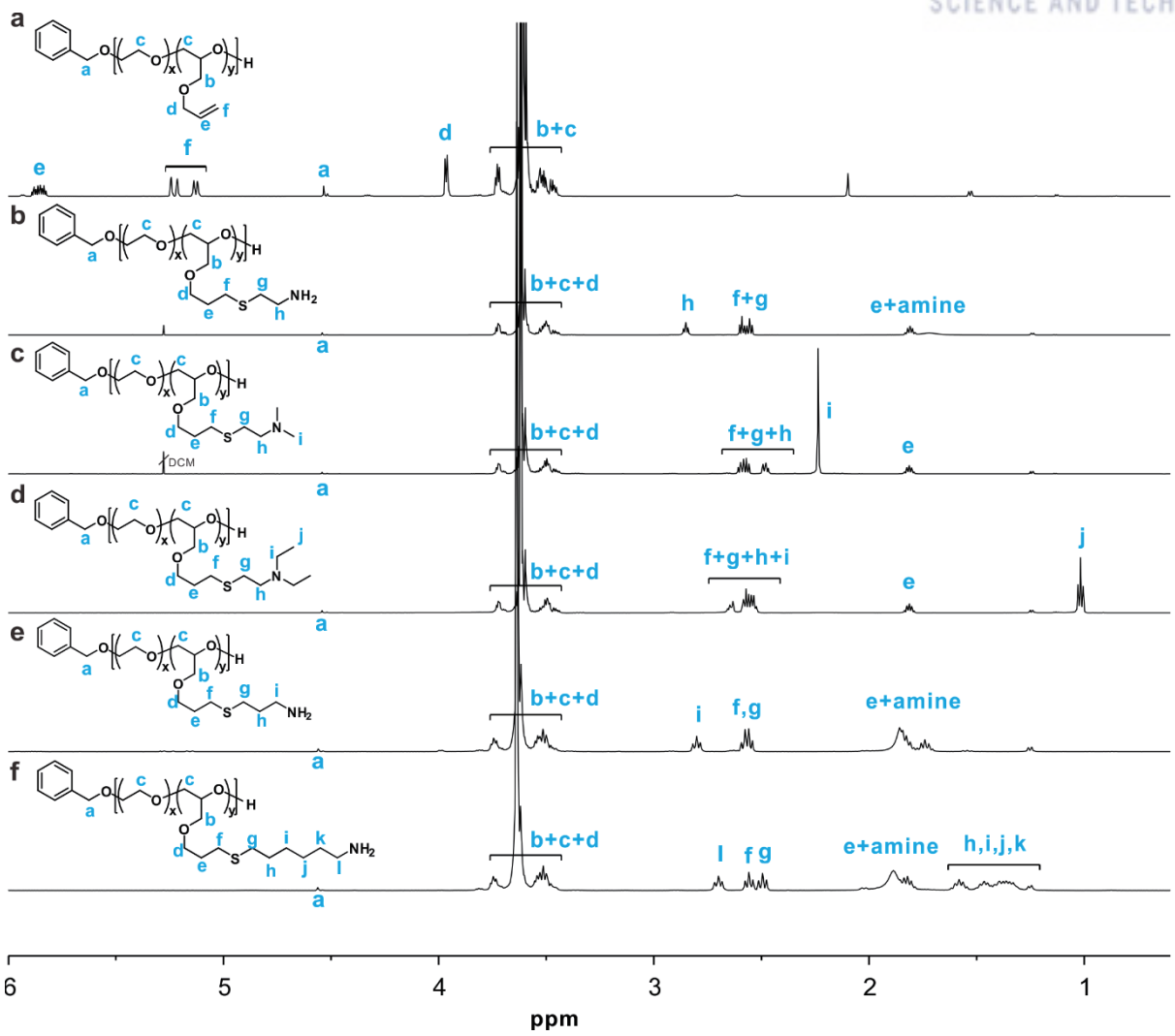

Figure 2.2. Representative ^{1}H NMR spectra of the synthesized polymers (600 MHz in $CDCl_3$). (a) P(EO-*co*-AGE), (b) **P1**, (c) **P2**, (d) **P3**, (e) **P4**, and (f) **P5**.

ULSAN NATIONAL INSTITUTE OF SCIENCE AND TECHNOLOGY

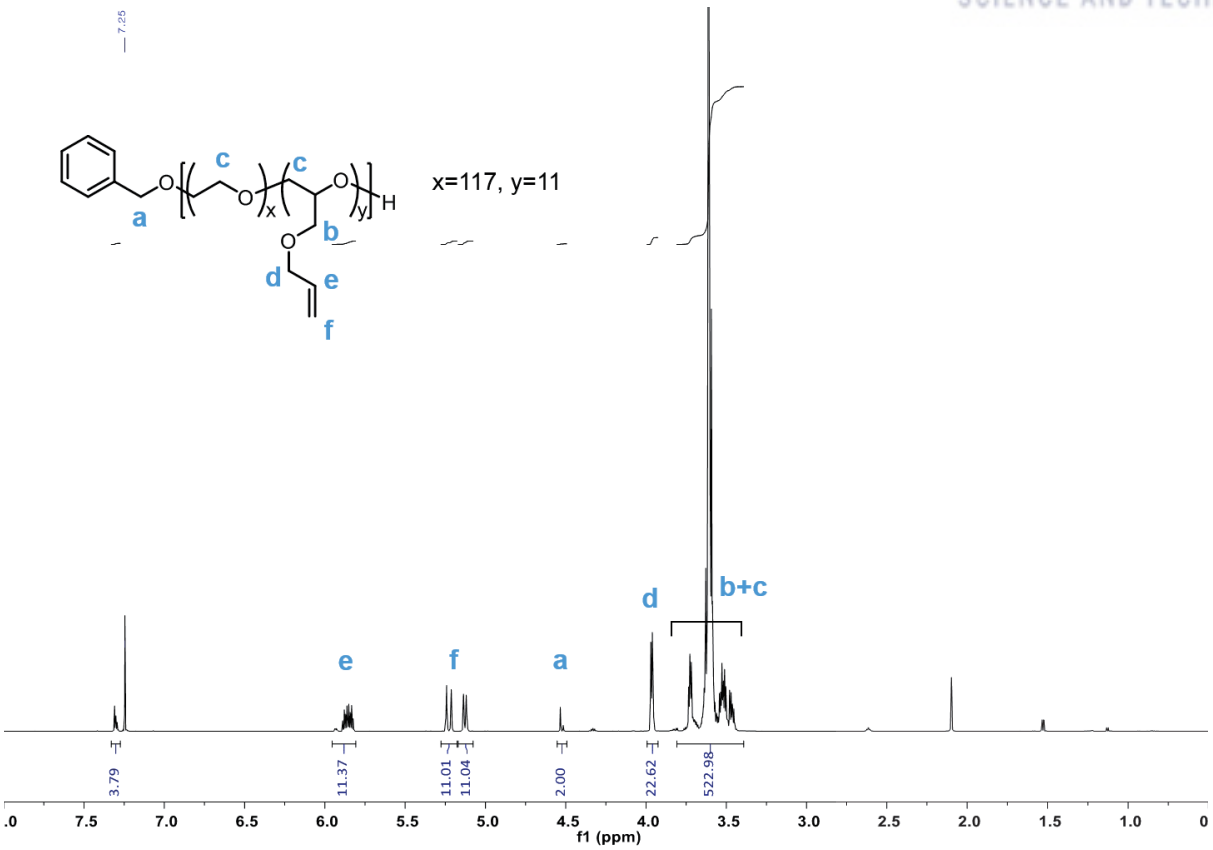

Figure 2.3. ^{1}H NMR spectrum of P(EO-*co*-AGE) polymer precursor (600 MHz, $CDCl_3$, 298 K).

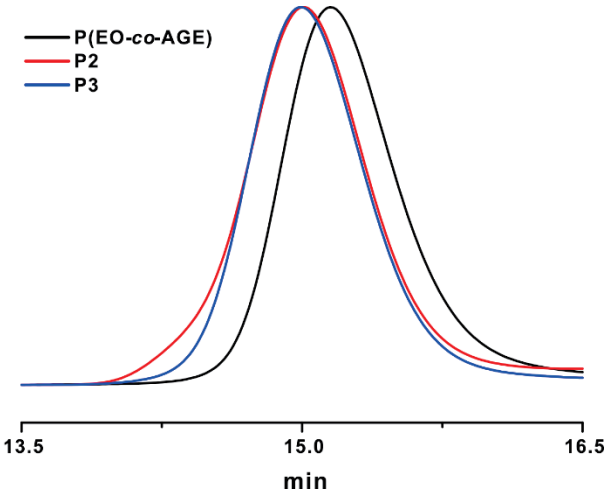

Figure 2.4. GPC traces of P(EO-*co*-AGE), **P2**, and **P3**. $CHCl_3$ was used as an eluent.

ULSAN NATIONAL INSTITUTE OF SCIENCE AND TECHNOLOGY

Table 2.1. Molecular Weight Data and Cloud Points of Polymers Prepared in This Study

Entry	Thiols	M_n (g/mol) / NMR[a]	$Đ$[b]	Cloud point (°C) pH 11	pH 12	pH 13	log P[c]
$P(EO_{117}$-*co*-$AGE_{11})$	-	6400	1.10	-	-	-	-
P1	cysteamine	6900	N/A	100	100	70	0.01
P2	*N*,*N*-dimethylaminoethanethiol	7800	1.10	72	63	50	1.19
P3	*N*,*N*-diethylaminoethanethiol	8000	1.12	65	58	45	2.34
P4	3-amino-1-propanethiol	7500	N/A	85	79	66	0.53
P5	6-amino-1-hexanethiol	7800	N/A	61	51	44	2.07

[a] Molecular weight (M_n) as determined from ^{1}H NMR spectra of resulting polymer.

[b] $Đ$ was measured by GPC using $CHCl_3$ as an eluent.

[c] log P values for thiols were obtained using ALOGPS 2.1[40,41]

ULSAN NATIONAL INSTITUTE OF SCIENCE AND TECHNOLOGY

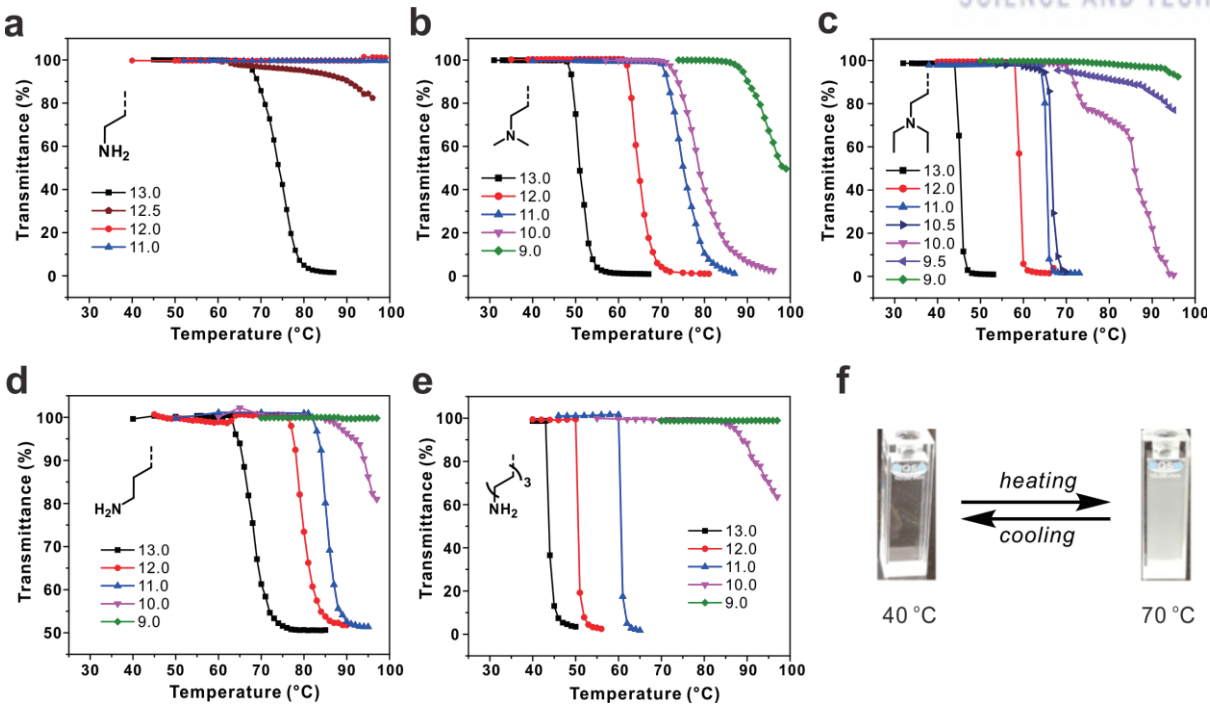

Figure 2.5. (a-e) Temperature-dependent transmittance curves for (a) **P1**, (b) **P2**, (c) **P3**, (d) **P4**, and (e) **P5** in solutions with different pH values. (f) Turbidity changes of **P2** at pH 13 when cycling the temperature. All polymers were tested at a concentration of 0.10 wt%.

ULSAN NATIONAL INSTITUTE OF SCIENCE AND TECHNOLOGY

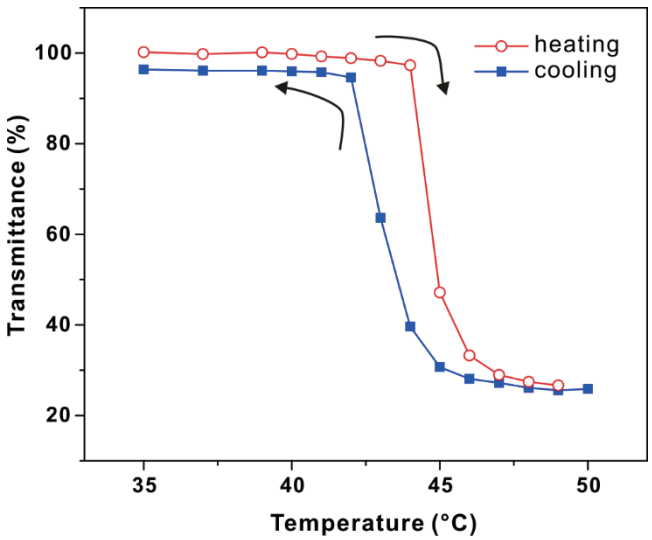

Figure 2.6. Transmittance curves of **P5** in aqueous solution at pH 13 during heating (red circle) and cooling (blue square) scans.

ULSAN NATIONAL INSTITUTE OF SCIENCE AND TECHNOLOGY

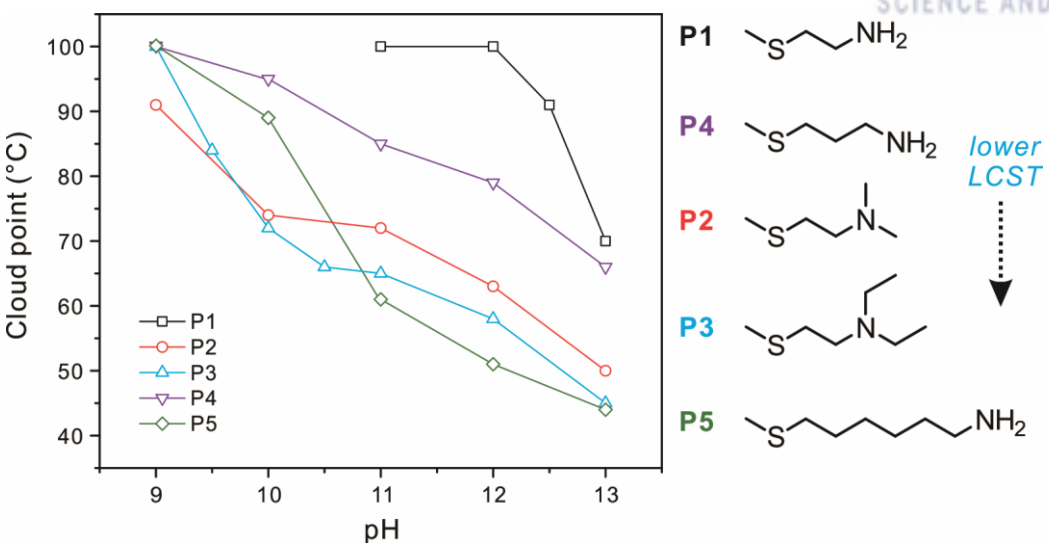

Figure 2.7. Summary of all cloud points for **P1** – **P5** as a function of pH.

ULSAN NATIONAL INSTITUTE OF
SCIENCE AND TECHNOLOGY

2.5 Conclusion

In summary, the pH-responsive LCST behavior of PEO-based functional polymers with different pendant amine groups and varying side chain lengths has been investigated. Five different aminothiols, including cysteamine, *N*,*N*-dimethylaminoethanethiol, *N*,*N*-diethyl aminoethanethiol, 3-amino-1-propanethiol, and 6-amino-1-hexanethiol could be quantitatively introduced to a single, well-defined P(EO-*co*-AGE) copolymer starting material via facile and modular thiol–ene chemistry. The transmission spectra for aqueous solutions of these copolymers revealed that cloud point was not only tuned by the pH of the solution but also by the hydrophobicity of the pendant amine moieties. The polymer library also exhibited different thermoresponsive phase transition behavior depending on the side chain length with the hydrophilicity/hydrophobicity balance being the dominant factor in controlling LCST behavior. By designing pH-tunable, thermoresponsive PEO-based polymers with multiple types of amine and different chain lengths, an effective and facile method of controlling LCST behavior has been developed. This fundamental and systematic investigation provides a platform to understand a wide range of LCST behaviors.

ULSAN NATIONAL INSTITUTE OF SCIENCE AND TECHNOLOGY

2.6 References

(1) Congdon, T.; Shaw, P.; Gibson, M. I. Thermoresponsive, Well-Defined, Poly(vinyl alcohol) Co-polymers. *Polym. Chem.* **2015**, *6*, 4749–4757.

(2) Jiang, X.; Feng, C.; Lu, G.; Huang, X. Thermoresponsive Homopolymer Tunable by pH and CO_2. *ACS Macro Lett.* **2014**, *3*, 1121–1125.

(3) Tang, Z.; Wilson, P.; Kempe, K.; Chen, H.; Haddleton, D. M. Reversible Regulation of Thermoresponsive Property of Dithiomaleimide-Containing Copolymers via Sequential Thiol Exchange Reactions. *ACS Macro Lett.* **2016**, *5*, 709–713.

(4) Lee, A.; Lundberg, P.; Klinger, D.; Lee, B. F.; Hawker, C. J.; Lynd, N. A. Physiologically Relevant pH-Responsive PEG-Based Block and Statistical Copolymers with N,N-Diisopropyl amine Units. *Polym. Chem.* **2013**, *4*, 5735.

(5) Son, S.; Shin, E.; Kim, B.-S. Light-Responsive Micelles of Spiropyran Initiated Hyperbranched Polyglycerol for Smart Drug Delivery. *Biomacromolecules* **2014**, *15*, 628–634.

(6) Davis, D. A.; Hamilton, A.; Yang, J.; Cremar, L. D.; Van Gough, D.; Potisek, S. L.; Ong, M. T.; Braun, P. V; Martinez, T. J.; White, S. R.; Moore, J. S.; Sottos, N. R. Force-Induced Activation of Covalent Bonds in Mechanoresponsive Polymeric Materials. *Nature* **2009**, *459*, 68–72.

(7) Pang, Y.; Zhu, Q.; Zhou, D.; Liu, J.; Chen, Y.; Su, Y.; Yan, D.; Zhu, X.; Zhu, B. Synthesis of Backbone Thermo and pH Dual-Responsive Hyperbranched Poly(amine-ether)s Through Proton-Transfer Polymerization. *J. Polym. Sci. Part A Polym. Chem.* **2011**, *49*, 966–975.

(8) Kojima, C.; Yoshimura, K.; Harada, A.; Sakanishi, Y.; Kono, K. Synthesis and Characterization of Hyperbranched Poly(glycidol) Modified with pH- and Temperature-Sensitive Groups. *Bioconjugate Chem.* **2009**, *20*, 1054–1057.

(9) Zhang, H.; Guo, S.; Fan, W.; Zhao, Y. Ultrasensitive pH-Induced Water Solubility Switch Using UCST Polymers. *Macromolecules* **2016**, *49*, 1424–1433.

(10) Zhu, Y.; Batchelor, R.; Lowe, A. B.; Roth, P. J. Design of Thermoresponsive Polymers with Aqueous LCST, UCST, or Both: Modification of a Reactive Poly(2-vinyl-4,4-dimethylazlactone) Scaffold. *Macromolecules* **2016**, *49*, 672–680.

(11) Smith, G. D.; Bedrov, D. Roles of Enthalpy, Entropy, and Hydrogen Bonding in the Lower Critical Solution Temperature Behavior of Poly(ethylene oxide)/Water Solutions. *J. Phys. Chem. B* **2003**, *107*, 3095–3097.

(12) Hou, L.; Wu, P. LCST Transition of PNIPAM-*b*-PVCL in Water: Cooperative Aggregation of Two Distinct Thermally Responsive Segments. *Soft Matter* **2014**, *10*, 3578–3586.

(13) Lutz, J.-F.; Akdemir, Ö.; Hoth, A. Point by Point Comparison of Two Thermosensitive Polymers Exhibiting a Similar LCST: Is the AGE of Poly(NIPAM) Over? *J. Am. Chem. Soc.* **2006**, *128*, 13046–13047.

ULSAN NATIONAL INSTITUTE OF SCIENCE AND TECHNOLOGY

(14) Lutz, J.-F.; Hoth, A. Preparation of Ideal PEG Analogues with a Tunable Thermosensitivity by Controlled Radical Copolymerization of 2-(2-Methoxyetoxy)ethyl Methacrylate and Oligo(ethylene glycol) Methacrylate. *Macromolecules* **2006**, *39*, 893–896.

(15) Lutz, J.-F.; Weichenhan, K.; Akdemir, Ö.; Hoth, A. About the Phase Transitions in Aqueous Solutions of Thermoresponsive Copolymers and Hydrogels Based on 2-(2-Methoxyethoxy)ethyl Methacrylate and Oligo(ethylene glycol) Methacrylate. *Macromolecules* **2007**, *40*, 2503–2508.

(16) Min, S. H.; Kwak, S. K.; Kim, B.-S. Atomistic Simulation for Coil-to-Globule Transition of Poly(2-dimethylaminoethyl methacrylate). *Soft Matter* **2015**, *11*, 2423–2433.

(17) Yamamoto, S.; Pietrasik, J.; Matyjaszewski, K. Temperature- and pH-Responsive Dense Copolymer Brushes Prepared by ATRP. *Macromolecules* **2008**, *41*, 7013–7020.

(18) Lei, L.; Zhang, Q.; Shi, S.; Zhu, S. Oxygen and Carbon Dioxide Dual Gas-Switchable Thermoresponsive Homopolymers. *ACS Macro Lett.* **2016**, *5*, 828–832.

(19) Jiang, X.; Feng, C.; Lu, G.; Huang, X. Thermoresponsive Homopolymer Tunable by pH and CO_2. *ACS Macro Lett.* **2014**, *3*, 1121–1125.

(20) Kohsaka, Y.; Matsumoto, Y.; Kitayama, T. α-(Aminomethyl)acrylate: Polymerization and Spontaneous Post-Polymerization Modification of β-Amino Acid Ester for a pH/Temperature-Responsive Material. *Polym. Chem.* **2015**, *6*, 5026–5029.

(21) Fruijtier-Pölloth, C. Safety Assessment on Polyethylene glycols (PEGs) and Their Derivatives as Used in Cosmetic Products. *Toxicology* **2005**, *214*, 1–38.

(22) Fuertges, F.; Abuchowski, A. The Clinical Efficacy of Poly(ethylene glycol)-Modified Proteins. *J. Control. Release* **1990**, *11*, 139–148.

(23) Pelegri-O'Day, E. M.; Lin, E.-W.; Maynard, H. D. Therapeutic Protein-Polymer Conjugates: Advancing Beyond PEGylation. *J. Am. Chem. Soc.* **2014**, *136*, 14323–14332.

(24) Saeki, S.; Kuwahara, N.; Nakata, M.; Kaneko, M. Upper and Lower Critical Solution Temperatures in Poly(ethylene glycol) Solutions. *Polymer* **1976**, *17*, 685–689.

(25) Aoki, S.; Koide, A.; Imabayashi, S.; Watanabe, M. Novel Thermosensitive Polyethers Prepared by Anionic Ring-Opening Polymerization of Glycidyl Ether Derivatives. *Chem. Lett.* **2002**, *31*, 1128–1129.

(26) Müller, S. S.; Moers, C.; Frey, H. A Challenging Comonomer Pair: Copolymerization of Ethylene Oxide and Glycidyl Methyl Ether to Thermoresponsive Polyethers. *Macromolecules* **2014**, *47*, 5492–5500.

(27) Mangold, C.; Dingels, C.; Obermeier, B.; Frey, H.; Wurm, F. PEG-Based Multifunctional Polyethers with Highly Reactive Vinyl-Ether Side Chains for Click-Type Functionalization. *Macromolecules* **2011**, *44*, 6326–6334.

ULSAN NATIONAL INSTITUTE OF SCIENCE AND TECHNOLOGY

(28) Mangold, C.; Obermeier, B.; Wurm, F.; Frey, H. From an Epoxide Monomer Toolkit to Functional PEG Copolymers With Adjustable LCST Behavior. *Macromol. Rapid Commun.* **2011**, *32*, 1930–1934.

(29) Obermeier, B.; Wurm, F.; Frey, H. Amino Functional Poly(ethylene glycol) Copolymers via Protected Amino Glycidol. *Macromolecules* **2010**, *43*, 2244–2251.

(30) Obermeier, B.; Frey, H. Poly(ethylene glycol-*co*-allyl glycidyl ether)s: A PEG-Based Modular Synthetic Platform for Multiple Bioconjugation. *Bioconjugate Chem.* **2011**, *22*, 436–444.

(31) Jain, K.; Vedarajan, R.; Watanabe, M.; Ishikiriyama, M.; Matsumi, N. Tunable LCST Behavior of Poly(N-isopropylacrylamide/ionic liquid) Copolymers. *Polym. Chem.* **2015**, *6*, 6819–6825

(32) Jung, S.-H.; Song, H.-Y.; Lee, Y.; Jeong, H. M.; Lee, H. Novel Thermoresponsive Polymers Tunable by pH. *Macromolecules* **2011**, *44*, 1628–1634.

(33) Kawaguchi, T.; Kojima, Y.; Osa, M.; Yoshizaki, T. Cloud Points in Aqueous Poly(N-isopropylacrylamide) Solutions. *Polym. J.* **2008**, *40*, 455–459.

(34) Koda, Y.; Terashima, T.; Sawamoto, M. LCST-Type Phase Separation of Poly[poly(ethylene glycol) methyl ether methacrylate]s in Hydrofluorocarbon. *ACS Macro Lett.* **2015**, *4*, 1366–1369.

(35) Kang, T.; Amir, R. J.; Khan, A.; Ohshimizu, K.; Hunt, J. N.; Sivanandan, K.; Montañez, M. I.; Malkoch, M.; Ueda, M.; Hawker, C. J. Facile Access to Internally Functionalized Dendrimers Through Efficient and Orthogonal Click Reactions. *Chem. Commun*. **2010**, *46*, 1556–1558.

(36) Lee, B. F.; Wolffs, M.; Delaney, K. T.; Sprafke, J. K.; Leibfarth, F. A.; Hawker, C. J.; Lynd, N. A. Reactivity Ratios and Mechanistic Insight for Anionic Ring-Opening Copolymerization of Epoxides. *Macromolecules* **2012**, *45*, 3722–3731.

(37) Lee, B. F.; Kade, M. J.; Chute, J. A.; Gupta, N.; Campos, L. M.; Fredrickson, G. H.; Kramer, E. J.; Lynd, N. A.; Hawker, C. J. Poly(allyl glycidyl ether)-A Versatile and Functional Polyether Platform. *J. Polym. Sci. Part A Polym. Chem.* **2011**, *49*, 4498–4504.

(38) Dimitrov, I.; Trzebicka, B.; Müller, A. H. E.; Dworak, A.; Tsvetanov, C. B. Thermosensitive Water-Soluble Copolymers with Doubly Responsive Reversibly Interacting Entities. *Prog. Polym. Sci.* **2007**, *32*, 1275–1343.

(39) Aoshima, S.; Oda, H.; Kobayashi, E. Synthesis of Thermally-Induced Phase Separating Polymer with Well-Defined Polymer Structure by Living Cationic Polymerization. I. Synthesis of Poly(vinyl ether)s with Oxyethylene Units in The Pendant and Its Phase Separation Behavior in Aqueous Solution. *J. Polym. Sci. Part A Polym. Chem.* **1992**, *30*, 2407–2413.

(40) Tetko, I. V.; Gasteiger, J.; Todeschini, R.; Mauri, A.; Livingstone, D.; Ertl, P.; Palyulin, V. A.; Radchenko, E. V.; Zefirov, N. S.; Makarenko, A. S.; Tanchuk, V. Y.; Prokopenko, V. V. Virtual Computational Chemistry Laboratory – Design and Description. *J. Comput.-Aided Mol. Des.* **2005**, *19*, 453-463.

ULSAN NATIONAL INSTITUTE OF SCIENCE AND TECHNOLOGY

(41) VCCLAB, Virtual Computational Chemistry Laboratory. *VCCLAB*, *Virtual Computational Chemistry Laboratory*; http://www.vcclab.org, 2005.

(42) Cheng, H.; Shen, L.; Wu, C. LLS and FTIR Studies on the Hysteresis in Association and Dissociation of Poly(N-isopropylacrylamide) Chains in Water. *Macromolecules* **2006**, *39*, 2325–2329.

ULSAN NATIONAL INSTITUTE OF SCIENCE AND TECHNOLOGY

Chapter 3

Hyperbranched Copolymers Based on Glycidol and Amino Glycidyl Ether: Highly Biocompatible Polyamines Sheathed in Polyglycerols*

3.1 Abstract

Functional hyperbranched polyglycerols (PGs) have recently garnered considerable interest due to their potential in biomedical applications. Here, we present a one-pot synthesis of hyperbranched PGs possessing amine functionality using a novel amino glycidyl ether monomer. A Boc-protected butanolamine glycidyl ether (BBAG) monomer was designed and polymerized with glycidol (G) through anionic ring-opening multibranching polymerization to yield a series of hyperbranched P(G-*co*-BBAG) with controlled molecular weights (4800−16700 g/mol) and relatively low molecular weight distributions (1.2−1.6). The copolymerization and subsequent deprotection chemistry allow the incorporation of an adjustable fraction of primary amine moieties (typically, 5–20% monomer ratio) within the hyperbranched PG backbones, thus providing potentials for varying charge densities and functionality in PGs. The copolymerization kinetics of G and BBAG was also evaluated using a quantitative *in situ* ^{13}C NMR spectroscopic analysis, which revealed gradient copolymerization between the comonomers. The free amine groups within the deprotected P(G-*co*-BAG) copolymer were further utilized for facile conjugation chemistry with a model molecule in a quantitative manner. Furthermore, the superior biocompatibility of the prepared P(G-*co*-BAG) polymers was demonstrated via cell viability assays, outperforming many existing polyamines possessing relatively high cytotoxicity. Taken together, the biocompatibility with facile conjugation chemistry of free amine groups sheathed within the framework of hyperbranched PGs holds the prospect of advancing biological and biomedical applications.

---

*Chapter 3 is reproduced in part with permission from *Biomacromolecules* **2016**, *17*, 3632–3639 by Suhee Song,† Joonhee Lee,† Songa Kweon, Jaeeun Song, Kyuseok Kim, and Byeong-Su Kim. Copyright 2016 American Chemical Society.

†These authors contributed equally to this work (S.S. and J.L).

ULSAN NATIONAL INSTITUTE OF SCIENCE AND TECHNOLOGY

3.2 Introduction

Poly(ethylene glycol) (PEG) represents the most important class of polyethers with a broad range of potential impact in biological fields and pharmaceutical industry, owing to its superior biocompatibility and low immunogenicity and toxicity.[1–7] A fundamental challenge with PEG, however, lies in the lack of functionality within the polymer backbone, limiting the tunability for a wider range of applications.[7–9] As an alternative to linear polyether analogues of PEG, hyperbranched polyglycerols (PGs) have recently attracted significant attention due to their unique three-dimensional architecture that comprises a polyether backbone with a large number of functional hydroxyl groups together with their facile synthetic nature.[7,10–14]

Recent synthetic advancements have allowed the development of well-defined and complex architectures of PGs with a broad range of molecular weights and functionality, typically using a ring-opening multibranching polymerization of glycidol (G) and functional epoxide monomers.[10,15–18] To date, in order to build the complex architectures of PGs and tailor their physicochemical properties, many novel functional epoxide monomers have been developed.[7,10,19,20] In particular, polyethers with amine functional groups have been actively investigated because of their high potential in surface modification and biological conjugation.[21-25] As direct polymerization of an epoxide monomer bearing primary amine groups is not feasible, two approaches are typically employed to introduce amine groups on polyethers, such as post-polymerization modification and direct copolymerization using protected monomeric building blocks. Koyama et al. first introduced primary amine moieties via copolymerization of ethylene oxide with allyl glycidyl ether (AGE) followed by thiol−ene coupling of 2-aminoethanethiol to the AGE.[26] In another approach, Frey and co-workers have reported a series of protected glycidyl amine derivatives as novel functional monomers, including *N*,*N*-dibenzyl amino glycidol,[27] *N*,*N*-diallyl glycidyl amine,[28] and epicyanohydrin.[29] Recently, Satoh and co-workers reported the use of *N*,*N*-disubstituted glycidyl amine derivatives to obtain well-defined polyethers with various pendant amine groups as well.[30] In another notable effort, Lynd and Hawker's group reported the use of *N*,*N*-diisopropyl ethanolamine glycidyl ether to investigate the pH-responsive behavior of polyethers in physiologically relevant conditions.[31] Nonetheless, many of these studies were limited to the investigation of random copolymer systems in linear polyethers such as PEG.

In a continuation of our endeavor to develop functional hyperbranched PGs for biomedical applications,[32–34] we now report on the one-pot synthesis of a series of hyperbranched PGs possessing amino functionality by using a Boc-protected butanolamine glycidyl ether monomer (BBAG) (Figure 3.1). Specifically, *t*-butyl 4-(oxiran-2-ylmethoxy)butylcarbamate (BBAG) was designed and polymerized through anionic ring-opening multibranching polymerization to yield a series of hyperbranched P(G-*co*-BBAG) with controlled molecular weights (4800−16700 g/mol) and relatively low molecular weight distributions (M_w/M_n = 1.2−1.6). The copolymerization and subsequent

ULSAN NATIONAL INSTITUTE OF SCIENCE AND TECHNOLOGY

deprotection chemistry allowed for the incorporation of an adjustable fraction of primary amine moieties (typically, 5–20% monomer ratio) within the hyperbranched PG backbones, thus, providing the potential for varying charge densities and functionality within the hyperbranched PG. We also investigated the copolymerization kinetics of G and BBAG using a quantitative *in situ* ^{13}C NMR spectroscopic analysis. The free amine groups within the deprotected P(G-*co*-BAG) copolymers were further utilized for facile conjugation chemistry with a model molecule in a quantitative manner. Furthermore, we demonstrated the superior biocompatibility of the prepared polymers via cell viability assays.

ULSAN NATIONAL INSTITUTE OF SCIENCE AND TECHNOLOGY

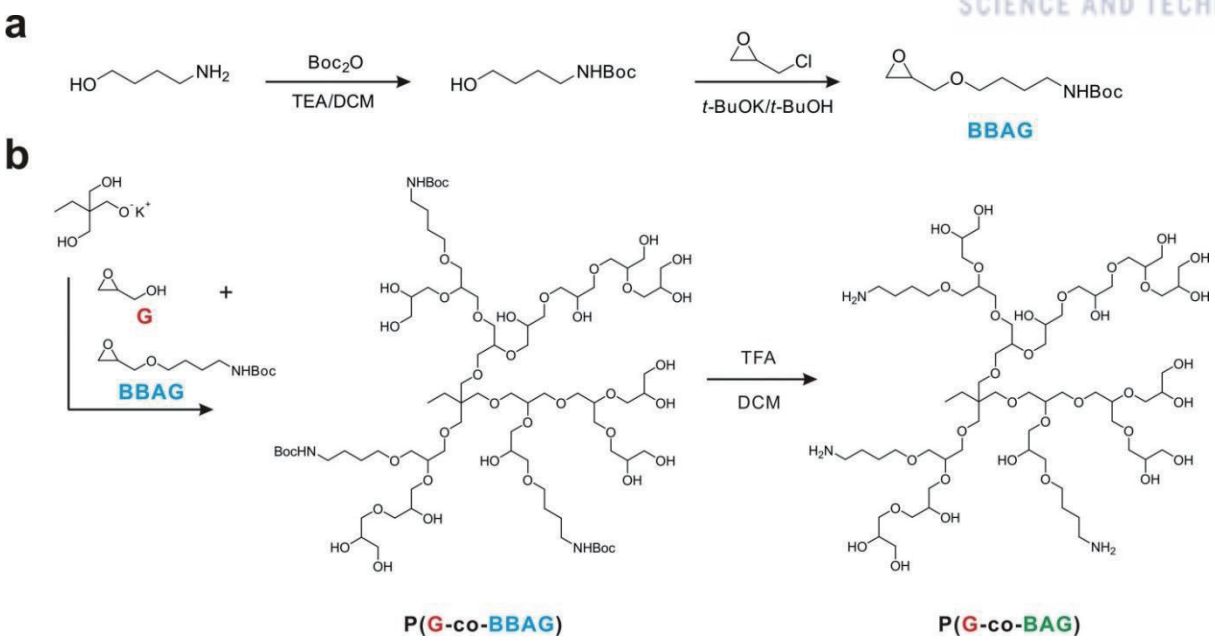

Figure 3.1. Synthetic pathways of (a) the BBAG monomer and (b) anionic ring-opening copolymerization of P(G-*co*-BBAG) and subsequent deprotection to yield P(G-*co*-BAG).

ULSAN NATIONAL INSTITUTE OF SCIENCE AND TECHNOLOGY

3.3 Experimental Section

Materials

All reagents and solvents were purchased from Sigma-Aldrich and Acros and used as received unless otherwise stated. All deuterated NMR solvents such as $CDCl_3$, D_2O, and DMSO-d_6 were purchased from Cambridge Isotope Laboratory.

Characterization

^1H and ^{13}C NMR spectra were acquired using a 400-MR DD2 (400 MHz) and VNMRS 600 (600 MHz) spectrometer using $CDCl_3$, D_2O, and DMSO-d_6 as solvents and chemical shifts were recorded in ppm units with TMS as an internal standard. The number- (M_n) and weight-averaged (M_w) molecular weights and molecular weight distribution (M_w/M_n) were measured using gel permeation chromatography (GPC, Agilent Technologies 1200 series) with a polystyrene (PS) standard and 0.010 M lithium bromide containing dimethylformamide (DMF) as an eluent at 30 °C with a flow rate of 1.00 mL/min. Matrix-assisted laser desorption and ionization time-of-flight (MALDI-ToF) mass spectrometry measurements were carried out on an Ultraflex III MALDI mass spectrometer with α-cyano-4-hydroxycinnamic acid as the matrix. Differential scanning calorimetry (DSC) was performed using a differential scanning calorimeter (Q200 model, TA Instruments) in the temperature range of -80–50 °C at a heating rate of 10 K/min under nitrogen. The zeta potential was measured using a Malvern Zetasizer Nano-ZS.

Protection of 4-Amino-1-butanol

The precursor, *t*-butyl *N*-(4-hydroxybutyl)carbamate was synthesized according to the literature procedure with slight modification.[35] To a solution of 4-amino-1-butanol (10 g, 112 mmol) and triethylamine (17.1 mL, 123 mmol) in dichloromethane (CH_2Cl_2, 35 mL), a solution of di-*tert*-butyl-dicarbonate (25.7 g, 118 mmol) in CH_2Cl_2 (100 mL) was added dropwise over 30 min at room temperature. The mixture was stirred at room temperature for 6 h and the reaction mixture was concentrated under reduced pressure. The crude mixture was dissolved in CH_2Cl_2, washed with water and then with brine. The organic phase was dried over Na_2SO_4 and concentrated under reduced pressure. The residue was purified by flash column chromatography eluting with 10% methanol in CH_2Cl_2 to give a compound as colorless oil.

Synthesis of BBAG Monomer

ULSAN NATIONAL INSTITUTE OF SCIENCE AND TECHNOLOGY

A solution of *t*-butyl *N*-(4-hydroxybutyl)carbamate (14.5 g, 76.6 mmol) in *t*-butanol (100 mL) was slowly added to a solution of potassium *t*-butoxide (8.50 g, 76.6 mmol) in *t*-butanol (100 mL) with stirring for 15 min at room temperature under argon. After stirring for an additional 15 min, excess epichlorohydrin (35.9 mL, 459 mmol) was added dropwise for 30 min. The solution was stirred at room temperature for 24 h after which additional water (100 mL) and CH_2Cl_2 (200 mL) were added. The aqueous phase was extracted with CH_2Cl_2 and combined organic layers were dried over $MgSO_4$. The organic phase was concentrated under reduced pressure and the residue was purified by flash column chromatography with CH_2Cl_2/hexane (1:100 v/v) eluent to give 11.2 g (60%) of the BBAG monomer as a colorless oil. The synthesis of the BBAG monomer was successfully confirmed through various characterizations, including ^{1}H and ^{13}C NMR, COSY, HMQC, and DEPT spectroscopy and ESI-MS (see Figure 3.2 for corresponding peak assignments and Figures 3.3–3.6). ^{1}H NMR (600 MHz, DMSO-d_6): δ ppm 3.61 (dd, 1H, J = 11.6 and 2.8 Hz, e), 3.34–3.40 (m, 2H, f), 3.18 (dd, 1H, J = 11.5 and 6.3 Hz, d), 3.03–3.05 (m, 1H, c), 2.88 (q, 2H, J = 6.7 Hz, i), 2.68 (dd, 1H, J = 4.3 and 5.1 Hz, b), 2.49 (dd, 1H, J = 5.1 and 2.6 Hz, a), 1.42–1.47 (m, 2H, g), 1.36–1.39 (m, 2H, h), 1.34 (s, 9H, j). ^{13}C NMR (150 MHz, DMSO-d_6): δ ppm 158.66, 80.38, 74.24, 73.29, 53.41, 46.46, 42.88, 31.34, 29.65, 29.34. MS(*m/z* + Na^+, ESI^+) calcd for $C_{12}H_{23}NO_2$ 268.3, found 268.3

Synthesis of P(G$_{56}$-co-BBAG$_2$) (Polymer 1)

Trimethylolpropane (TMP) (54.6 mg, 0.407 mmol) was placed in a two-neck round bottom flask. Potassium methoxide in methanol (25 wt %, 45 μL, 0.163 mmol) was diluted with 0.70 mL of methanol, and then added to the flask and stirred for 30 min at room temperature under an argon atmosphere. Excess methanol was removed using a rotary evaporator and the resulting product was dried in a vacuum oven at 90 °C for 3 h to yield a white salt of the initiator. The flask was then purged with argon and heated to 90 °C. A mixture of *t*-butyl 4-(oxiran-2-ylmethoxy)butylcarbamate (BBAG) (0.30 g, 1.22 mmol) and glycidol (G) (1.54 g, 23.23 mmol) was added dropwise over 12 h using a syringe pump. After the complete addition of the monomer, the reaction was continued for an additional 5 h. The resulting P(G$_{56}$-*co*-BBAG$_2$) copolymer was dissolved in 1.0 mL of methanol; the homogeneous polymer solution was then precipitated in excess diethyl ether, and the precipitate was washed twice using diethyl ether. The resulting polymer was dried under vacuum at 90 °C for one day. All polymers synthesized in this study were isolated in approximately 90% yield. The M_n of the P(G$_{56}$-*co*-BBAG$_2$) polymer was determined to be 4773 g/mol, as calculated from the NMR data (see Figure 3.7) using the following equation: number of repeating units (BBAG) = 17.25 (integration value)/9 (number of protons of *t*-butyl of BBAG) = 2, number of repeating units (G) = [292.13 (integration value) − {(2 (number of BBAG repeating units) × 7 (number of protons of BBAG except *t*-butyl)}]/5 (number of protons of the G monomer (5H)) = 56; M_n = 74.08 (molecular weight of the G monomer) × 56 + 245.32 (molecular

ULSAN NATIONAL INSTITUTE OF SCIENCE AND TECHNOLOGY

weight of the BBAG monomer) × 2 + 134.17 (molecular weight of TMP) = 4773.29 g/mol. Considering the error range of NMR integration, we used 4800 g/mol as the M_n value of the polymer 1.

Synthesis of P(G_{56}-co-BAG_2)

The Boc-protected P(G_{56}-*co*-$BBAG_2$) copolymer (polymer 1) was dissolved in CH_2Cl_2 with trifluoroacetic acid (TFA) (1.0 mL) and stirred at room temperature for 1 h. The reaction mixture was concentrated under reduced pressure and the resulting deprotected polymer was dissolved in 1.0 mL of methanol; the homogeneous polymer solution was then precipitated in excess diethyl ether, and the precipitate was washed twice using diethyl ether. The resulting deprotected P(G_{56}-*co*-BAG_2) polymer was dried under vacuum at 90 °C for one day.

^{13}C NMR Kinetics

To generate the initiator, TMP (20 mg, 0.204 mmol) and potassium methoxide in methanol (25 wt %, 23 μL, 0.082 mmol) were reacted in a round-bottom flask under an argon atmosphere at 50 °C. Excess methanol was removed using a rotary evaporator, and the resulting product was dried in a vacuum oven at 90 °C for 3 h to yield a white salt of the initiator. The initiator was added to the comonomer mixture of G (0.151 g, 2.04 mmol) and BBAG (0.500 g, 2.04 mmol), which was placed in a 4.0 mL vial and stirred over an ice bath. The mixture was transferred to a conventional NMR tube under an argon atmosphere and then sealed with a septum over an ice bath. The kinetic measurements using ^{13}C NMR spectroscopy were recorded on a 600 MHz VNMRS system with a 5 mm PFG AutoXDB probe in neat solutions. A standard kinetic ^{13}C NMR experiment required 64 transients, which were obtained with a 13.7 μs 90° pulse, the spectral width of 1894 Hz, and recycling delay of 10 s for each kinetic run; 43 experiments were performed over a period of 12 h with a flip angle of 45° and inverse gated decoupling.

Rhodamine B Conjugated Hyperbranched P(G_{113}-co-BAG_{21}) Polymer

Rhodamine B conjugated polymer was synthesized according to a method previously described in the literature.[36] *N*-Hydroxysuccinimide (2.3 mg, 0.02 mmol) and rhodamine B (9.6 mg, 0.02 mmol) were dissolved in 1.5 mL of DMF, and then *N*,*N*′-dicyclohexylcarbodiimide (6.2 mg, 0.03 mmol) and 4-dimethylaminopyridine (2.4 mg, 0.02 mmol) were added to the solution. The mixture was stirred at room temperature for 30 min, and then, 70 mg of P(G_{113}-*co*-BAG_{21}) (polymer 7) in 1.5 mL of DMF was added to the solution. After stirring for 48 h at room temperature the insoluble residue was filtered off and the solvent was removed by a rotary evaporator. The residues were dissolved in deionized water to dialyze against water for seven days, followed by lyophilization to give the

ULSAN NATIONAL INSTITUTE OF SCIENCE AND TECHNOLOGY

rhodamine B-conjugated polymer in a quantitative yield.

Cytotoxicity Assay

Murine macrophage cell line, RAW264.7, was purchased from the Korean Cell Line Bank (Seoul, Korea). Cytotoxicity assays were performed using the traditional MTT assay. Cells were seeded in 24-well plates at a density of 1×10^5 cells per well and incubated for 24 h in 5% CO_2 at 37 °C. The RAW264.7 cells were cultured with Dulbecco's Modified Eagle's Medium (DMEM, Hyclone) containing 10% fetal bovine serum (FBS) and 1% penicillin−streptomycin. After removing the culture medium, the wells were washed with phosphate-buffered saline (PBS). Each well was then treated with various concentrations of P(G-*co*-BAG) solutions (polymer 3, 6, and 7) and incubated for an additional 18 h. For the MTT assays, each well was washed with PBS then filled with 60 μL of a thiazolyl blue tetrazolium bromide (MTT, Sigma-Aldrich) stock solution (5.0 mg/mL) and 940 μL of fresh media. After incubation for 3 h, 1.0 μL of DMSO was added to the polymer solution to solubilize the MTT-formazan product, after which the plates were gently agitated for 15 min at room temperature. After transferring 100 μL of each sample into the 96-well plates, the absorbance of the solution was recorded at a wavelength of 540 nm using 620 nm as the reference.

Cellular Uptake Imaging

Cellular uptake of the rhodamine B-conjugated polymers was tested by using HEK-293T cells. Cells were seeded on a coverslip in a 24-well tissue culture plate at a density of 1×10^5 cells per well and incubated for 24 h. After the initial cell culture, the rhodamine B-conjugated polymer (polymer 7) dissolved in water (0.50 mg/mL) was added to each well and incubated at 37 °C for an additional 24 h. After washing with PBS (pH 7.4), a solution of 4',6-diamidino-2-phenylindole (DAPI, Sigma-Aldrich) (20 mg/mL in MEM media) was incubated at 37 °C. After incubation for 30 min, the cells were fixed with 4% formaldehyde at room temperature. Confocal laser scanning microscopy (CLSM) images were taken using an Olympus FV1000 confocal microscope equipped with 405, 473, and 559 nm laser with fluorescence detection channels.

ULSAN NATIONAL INSTITUTE OF SCIENCE AND TECHNOLOGY

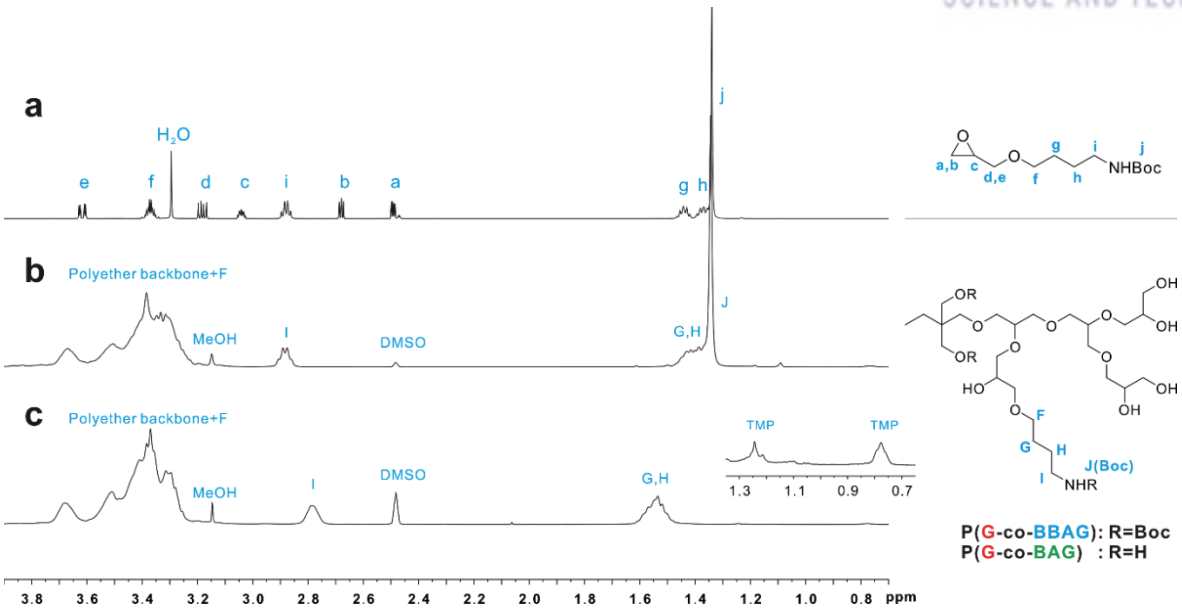

Figure 3.2. ^{1}H NMR spectra of (a) BBAG monomer, (b) P(G_{113}-*co*-$BBAG_{21}$) copolymer (polymer 7), and (c) deprotected P(G_{113}-*co*-BAG_{21}) copolymer measured in DMSO-d_6.

ULSAN NATIONAL INSTITUTE OF SCIENCE AND TECHNOLOGY

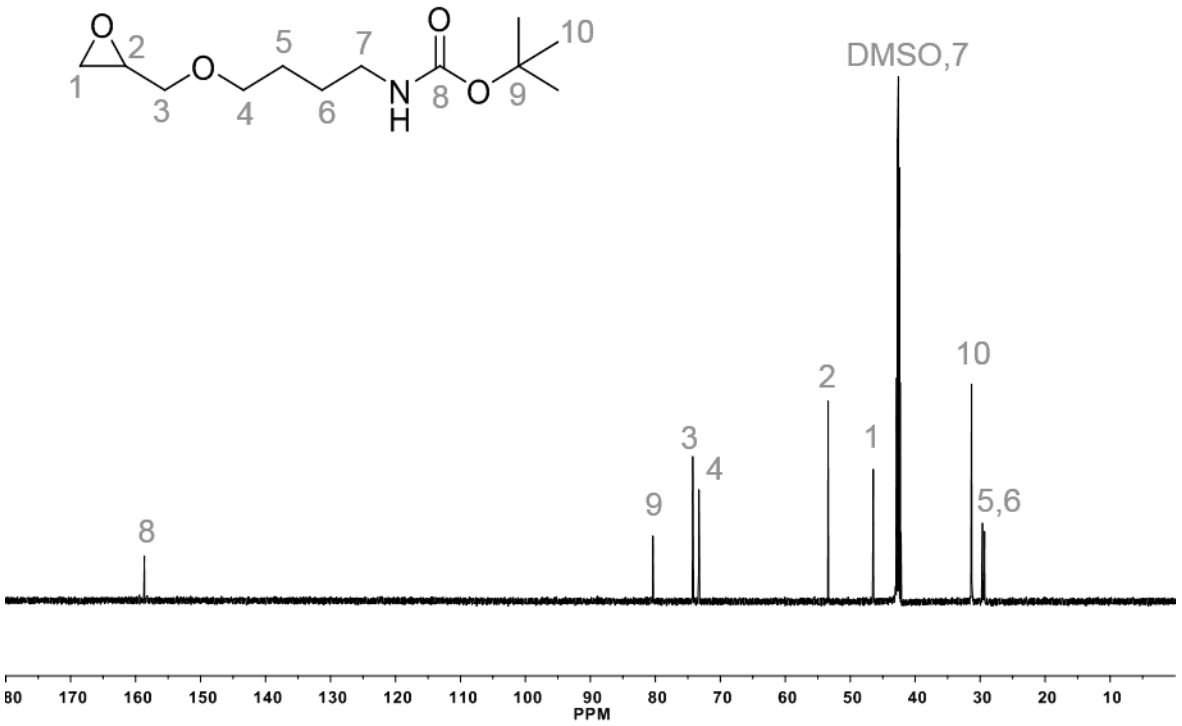

Figure 3.3. ^{13}C NMR spectrum of BBAG monomer in DMSO-d_6.

ULSAN NATIONAL INSTITUTE OF SCIENCE AND TECHNOLOGY

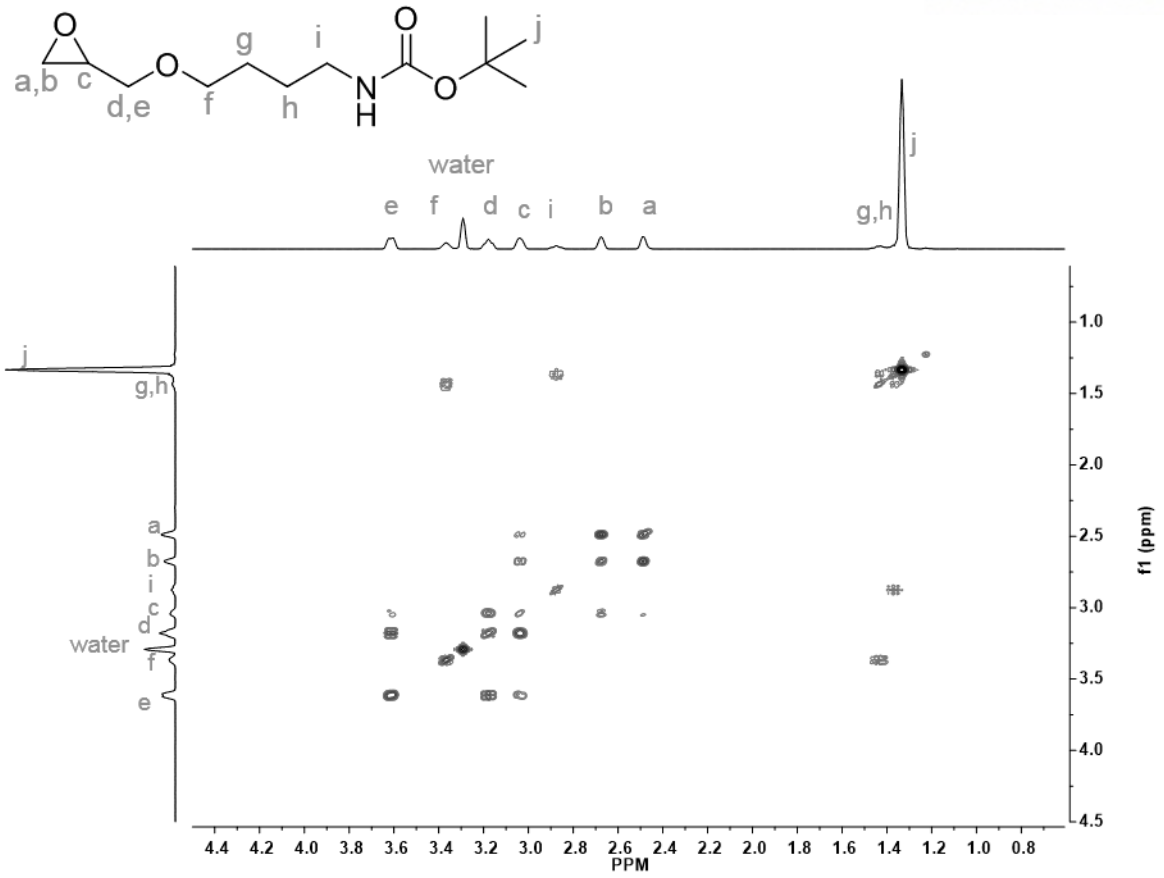

Figure 3.4. COSY spectrum of BBAG monomer in DMSO-d_6.

ULSAN NATIONAL INSTITUTE OF SCIENCE AND TECHNOLOGY

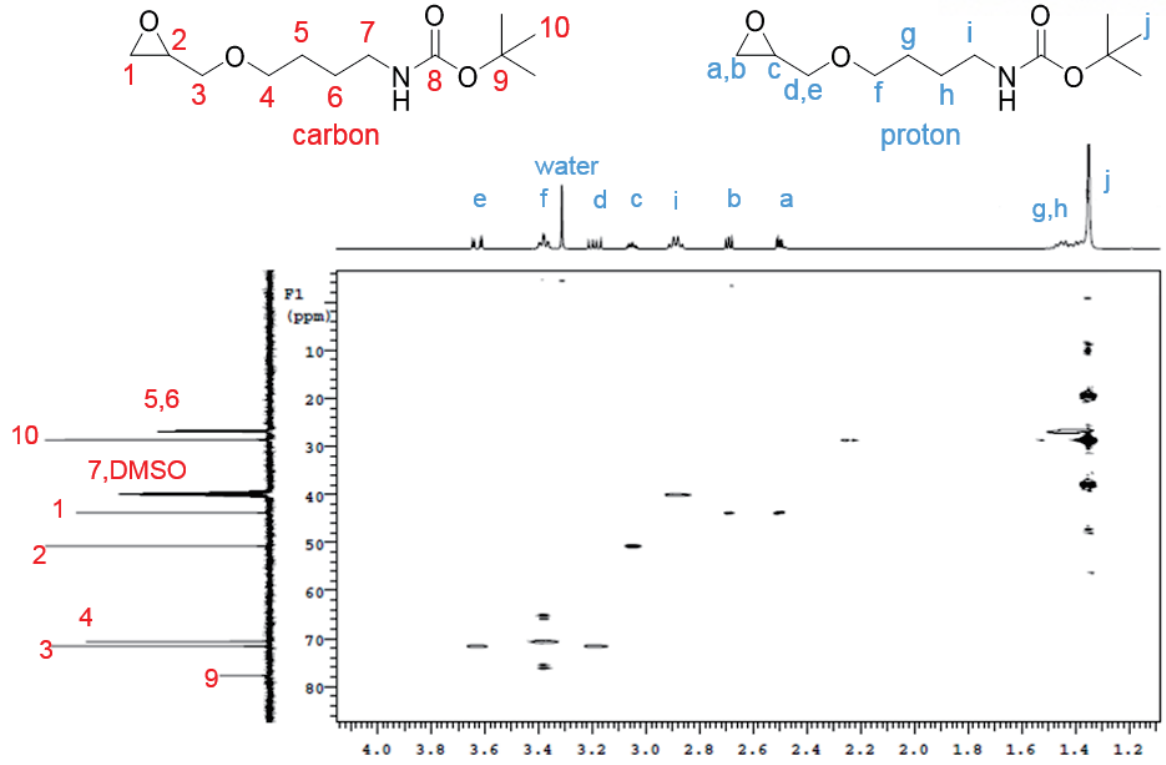

Figure 3.5. HMQC spectrum of BBAG monomer in DMSO-d_6.

ULSAN NATIONAL INSTITUTE OF SCIENCE AND TECHNOLOGY

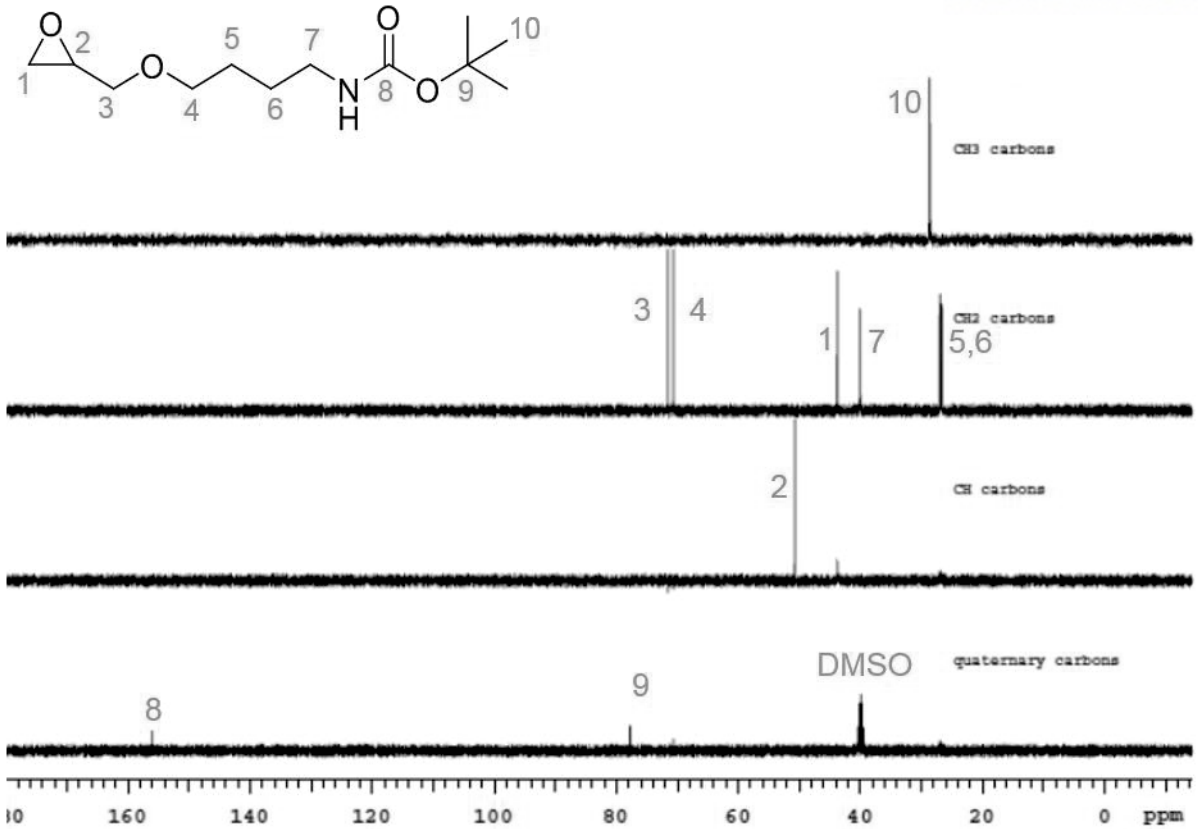

Figure 3.6. DEPT spectra of BBAG monomer in DMSO-d_6.

ULSAN NATIONAL INSTITUTE OF SCIENCE AND TECHNOLOGY

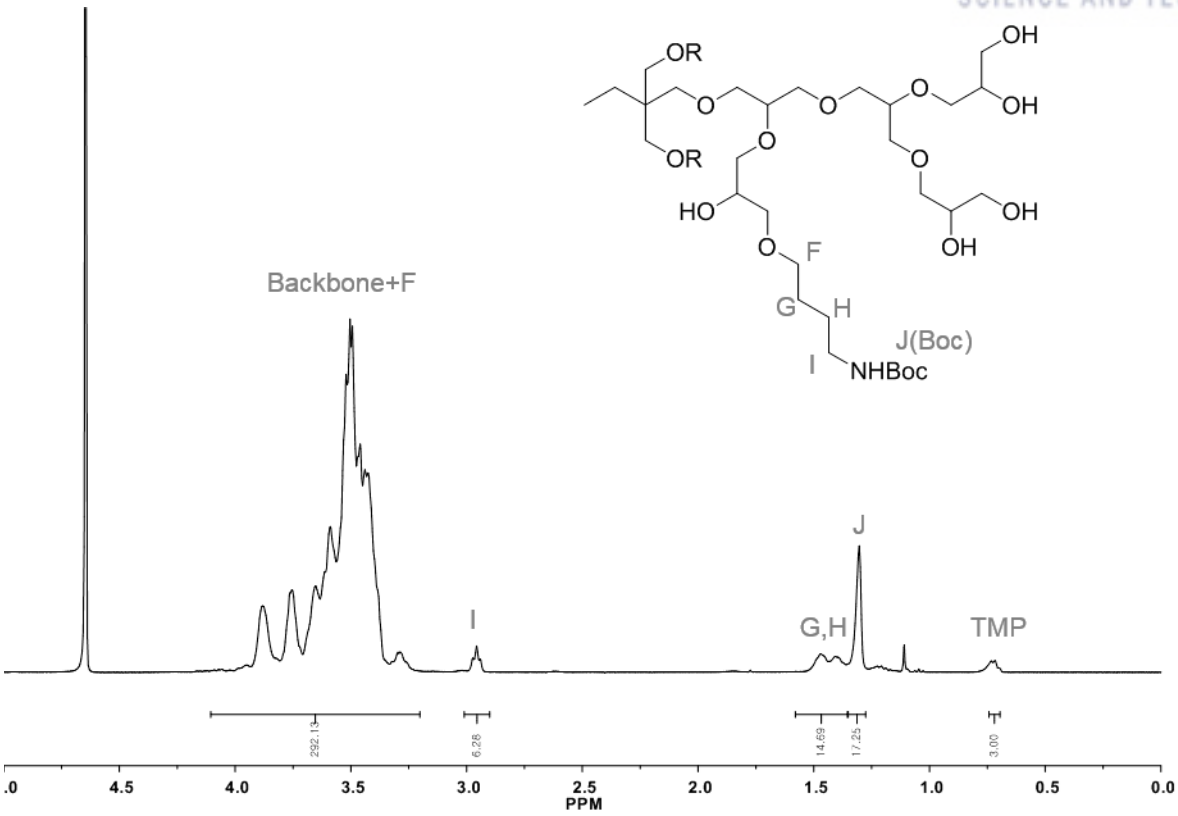

Figure 3.7. ^{1}H NMR spectrum of P(G_{56}-*co*-$BBAG_2$) polymer (polymer 1) in D_2O.

ULSAN NATIONAL INSTITUTE OF SCIENCE AND TECHNOLOGY

3.4 Results and Discussion

The general synthetic routes toward the BBAG monomer and copolymers are outlined in Figure 3.1. In the first step, 4-amino-1-butanol was protected with di-*t*-butyl dicarbonate (Boc_2O) and triethylamine (TEA) in dichloromethane (DCM) to generate *t*-butyl *N*-(4-hydroxybutyl)carbamate. The intermediate was then coupled with epichlorohydrin to obtain a Boc-protected butanolamine glycidyl ether (BBAG) monomer, *t*-butyl-4-(oxiran-2-ylmethoxy)butylcarbamate. The successful synthesis of the BBAG monomer was confirmed through various characterizations including ^{1}H and ^{13}C NMR, COSY, HMQC and DEPT spectroscopy, and ESI-MS (see Figures 3.2–3.6).

After the successful synthesis of the BBAG monomer, we studied its anionic ring-opening multibranching polymerization using a potassium alkoxide initiator that was formed via the reaction of trimethylolpropane (TMP) and a potassium methoxide solution.[19] As demonstrated previously, we employed slow monomer addition of a mixture of G and BBAG monomer to the deprotonated TMP initiator and copolymerized at 90 °C for 17 h for controlled synthesis of the polymers. The molecular weight of the copolymers was controlled by the monomer-to-initiator ratio and the comonomer feed ratio of BBAG to G monomers, which was varied from 5 to 20% to yield different degrees of BBAG incorporation within the copolymer.

The successful synthesis of P(G-*co*-BBAG) copolymers was characterized by ^{1}H NMR and GPC measurements (Figures 3.2, 3.8, 3.9, and Table 3.1). As shown in Figure 3.2, the ^{1}H NMR spectra of the BBAG monomer and synthesized polymers indicated the corresponding characteristic proton peaks. Specifically, the M_n value was calculated by the ratio of the peak integrals between the methyl and methylene groups of the TMP initiator (peaks at 0.8 and 1.3 ppm, respectively) and polyether backbone (peaks at 3.3–3.8 ppm) (see the Experimental Section for detailed calculations). In addition, the incorporation ratio of BBAG within the P(G-*co*-BBAG) copolymers was determined by integrating the unique distinguishable protons of the *t*-butyl group on BBAG (peak at 1.34 ppm) against the signal of the initiator and polyether backbone. Overall, we found reasonable agreement between the target molecular weight and composition and those obtained from the ^{1}H NMR results (Table 3.1).

The hyperbranched nature of the P(G-*co*-BBAG) copolymers was further confirmed by measuring the degree of branching (DB) via a detailed analysis of the ^{13}C NMR spectra (Figures 3.10, 3.11 and Table 3.2). The resulting DB indicated the ratio of the branched dendritic segment within the PG backbones, which were composed of both AB-type linear (BBAG block) and AB_2-type branched (G block) segments. The DBs of the selected polymers, polymer 5 and 7, were determined to be about 0.63 and 0.56, which were in a similar range with those of other hyperbranched systems.[15,33,37]

The GPC results showed controlled molecular weight values with a monomodal distribution (Table 3.1 and Figure 3.12). The M_n of the copolymers was found to be 6800–12600 with a

ULSAN NATIONAL INSTITUTE OF SCIENCE AND TECHNOLOGY

polydispersity index (M_w/M_n) value of 1.2–1.6 determined by GPC using polystyrene as a standard. It is of note that there is an observable discrepancy between the molecular weights determined by ^{1}H NMR and GPC; however, this could be attributed to the hyperbranched architecture and presence of multiple hydroxyl functional groups because these globular hyperbranched structures do not contribute to the overall hydrodynamic radius of the polymers. Additionally, the use of linear polystyrene as a molecular weight reference could lead to deviation.

The Boc-protected copolymers were treated with trifluoroacetic acid (TFA) for 1 h to yield the desired P(G-*co*-BAG) copolymers. The elimination of the Boc moiety was clearly monitored in the ^{1}H NMR spectrum with the disappearance of the strong *t*-butyl group at 1.34 ppm (Figure 3.2c). Moreover, the ^{13}C NMR analysis supported the removal of Boc group as well (Figure 3.13). Besides these spectroscopic analyses, a simple ninhydrin assay confirmed the successful recovery of the primary amine groups. The synthesized P(G-*co*-BBAG) copolymers and deprotected P(G-*co*-BAG) copolymers were soluble in organic polar solvents such as methanol, DMSO, and DMF. The P(G-*co*-BBAG) copolymers were moderately soluble in water; however, P(G-*co*-BAG) copolymers became highly soluble in water after deprotection (Figure 3.9).

Analysis of polymers bearing primary amine groups with GPC is rather challenging due to the strong interaction between amine groups and GPC columns. However, acetylation of the amine groups allows the characterization of copolymers after the deprotection.[27] As a representative example, GPC analysis of polymer 7 after the treatment with excess acetic anhydride demonstrated a clear monomodal trace with a narrow polydispersity index of 1.15, further confirming the successful polymerization and subsequent functionality (Figure 3.14).

Along with the successful synthesis of the desired copolymers, we also attempted the homopolymerization of the novel BBAG monomer; however, the resulting BBAG homopolymer did not dissolve at all in many common solvents (i.e. chloroform, dichloromethane, THF, dioxane, ethyl acetate, methanol, ethanol, DME, DMSO, DMF, chlorobenzene, and trichlorobenzene) after recovering the precipitate, which limited the structural analysis of the homopolymers. The insoluble precipitate does not become soluble even after the treatment of TFA, suggesting possible cross-linking reaction during the homopolymerization of the BBAG monomer. A model reaction using *tert*-butyl 4-methoxybutylcarbamate, similar to the chemical structure of side chain of the butanolamine glycidyl ether, further suggested that there could be possible deprotection of Boc groups when both strong base and high temperature were employed together. We found that there was no significant change in the chemical structure of the model compound under high temperature treatment at 90 °C for 24 h (Figure 3.15). However, when both strong base and high temperature conditions were employed together, we found that a fraction of Boc group was degraded. Although the degree of deprotection was less than 5% under current polymerization condition (Figure 3.16), it increased with increasing equivalence of strong

ULSAN NATIONAL INSTITUTE OF SCIENCE AND TECHNOLOGY

base under high temperature (Figure 3.17). Nonetheless, when copolymerized with the G monomer, the relative fraction of the BBAG to G was relatively small within the range of 5−20%, thus, possible side reaction occurring on the Boc group could be reduced significantly. This postulation is further supported by comparison of the NMR integration of the two internal peaks such as polyether backbone and Boc peaks with respect to the TMP initiator, suggesting no considerable deprotection of the Boc group during the copolymerization.

As we developed the novel BBAG monomer, it was essential to investigate its copolymerization behavior with other monomers. In order to investigate the kinetics of two monomers during copolymerization, *in situ* ^{13}C NMR kinetic measurements were performed on the basis of recent developments reported by Frey and co-workers (Figure 3.18).[38,39] Specifically, the copolymerization of G and BBAG monomers at an equimolar ratio was performed in a conventional NMR tube at 75 °C. During bulk polymerization, a quantitative ^{13}C NMR spectrum could be obtained within a few minutes due to the sufficient abundance of the ^{13}C isotope. Figure 3.18 shows a series of ^{13}C NMR spectra collected during the copolymerization of G and BBAG monomers, which demonstrate the consumption of both monomers with the progress of polymerization. To evaluate the monomer consumption in a quantitative manner, the resonance peaks corresponding to the representative methine carbon for both epoxide monomers (at 54.9 and 53.2 ppm for G and BBAG, respectively) were compared during copolymerization. The disappearance of the G monomer was very rapid, and it was difficult to evaluate the initial consumption, even after 15 min of the reaction at 75 °C. The reduced reactivity of BBAG can be attributed to the structure of the long alkyl spacer within BBAG, which could have hindered the ring-opening from other epoxide monomers, as has been similarly observed in other studies involving functional epoxide monomers.[17,19] In addition, the stability of ring-opening product of secondary alkoxide chain end from the BBAG monomer is considerably lower than that of primary alkoxide resulting from the fast proton transfer reaction of the G monomer. Thus, more stable alkoxide chain end generated from the G monomer suppresses the backward reaction, which in turn increases the rate of G conversion.

The monomer conversion ratio of both G and BBAG monomers was plotted against the total conversion ratio during copolymerization (Figure 3.19). The monomer conversion in the first ^{13}C NMR spectra was set to 0% and the conversion ratio was calculated from the integration values of the methine group of each monomer against the signal from the Boc-protecting group, which remained constant during polymerization. As shown clearly in Figure 3.19, the molar ratio of the BBAG unit in the polymer chain was considerably lower than the monomer feed at the initial stage and increased rapidly upon consumption of the G monomer near the final stages of the reaction; for instance, at a total conversion of ~50%, the conversions of G and BBAG were 78% and 19%, respectively. Thus, there is a gradient of monomer incorporation during copolymerization of P(G-*co*-BBAG). However, it should

ULSAN NATIONAL INSTITUTE OF SCIENCE AND TECHNOLOGY

be noted that the kinetic experiments were conducted in a batch polymerization, which typically highlights the difference in the kinetics of the two different monomers during the copolymerization. On the other hand, in our actual copolymerization process in which the slow monomer addition method for a long period of time in a solution was employed could reduce this difference considerably, as reported similarly in literature.[40] Thus, we postulate that the gradient nature of the copolymerization will be significantly reduced and the chain ends will be in a statistical mixture of alcohols (from G monomer) and amines (from BBAG monomer).

MALDI-ToF spectrometry was performed to confirm the incorporation of G and BAG monomers within the copolymer backbone and the successful deprotection of the Boc group as well (Figure 3.20). Moreover, it augments the GPC analysis due to the inherent limitation in the characterization of free amine groups within the P(G-*co*-BAG) copolymers. The presence of functional monomer segments in P(G-*co*-BAG) copolymers is revealed by peak analysis as shown in Figure 3.20. For example, the spacing of the signals corresponds to the mass of a linear combination of the respective monomers in the copolymer in varying degrees, which unambiguously demonstrates the successful copolymerization and deprotection of P(G-*co*-BAG) copolymers.

Upon successful demonstration of the deprotection to release the free amino groups within the polymers, we evaluated the charge density by zeta potential measurement. As expected, the synthesized P(G-*co*-BAG) copolymers displayed highly positive charges between 24.4 and 34.9 mV, which suggested potential applications as prospective DNA and siRNA carriers (Table 3.3). We observed that the higher amount of amine functional groups in P(G-*co*-BAG) generally led to higher zeta potential. Moreover, the thermal properties and microstructure of the copolymers were investigated with differential scanning calorimetry (DSC) as summarized in Table 3.3. The glass transition temperature (T_g) for the P(G-*co*-BBAG) copolymers were ranged between −52.7 and −31.8 °C, which increased to between −30.9 and −5.6 °C upon deprotection to afford the P(G-*co*-BAG) copolymers. The T_g of the copolymers increased generally with increasing BAG contents and decreasing molecular weights. The additional intermolecular interactions present in the BAG group affect the T_g value of hyperbranched copolymers, as compared with pure PGs synthesized in our previous study (i.e., PG_{75}: −27.2 °C and PG_{150}: −32.2 °C). In addition, the appearance of a single T_g for copolymers in the DSC curves suggests successful copolymerization without phase separation between the comonomers.

Encouraged by the successful synthesis of P(G-*co*-BAG) copolymers with active amine groups, we evaluated their cytotoxicity to investigate their potential in biomedical settings. Three representative polymers with varying degree of amine contents (from 3.8%, 8.6% to 15.7% for polymer 3, polymer 6, and polymer 7, respectively) were treated with the murine macrophage cell line, RAW264.7 as a model normal cell. The cytotoxicity of each polymer was examined using an MTT assay based on the mitochondrial dehydrogenase activity. As shown in Figure 3.21a, the cell viability of each cell line

ULSAN NATIONAL INSTITUTE OF SCIENCE AND TECHNOLOGY

treated with various concentrations of the polymer solution was greater than 95%, even up to a concentration of 500 μg mL^{-1}, which is usually beyond the common concentration ranges tested. Although many polyamines are reported to display significant cytotoxicity due to the free amine groups associated with tight cell binding,[41,42] our P(G-*co*-BAG) copolymers exhibited considerably low cell toxicity; this is attributed to the protected amine groups sheathed by the hyperbranched PG shell, yielding optimum cell viability.

The facile functionalization of amine groups sheathed within the framework of hyperbranched PG could provide a useful platform for further modification with other organic or biological molecules.[43,44] Toward this end, the available amine groups within the P(G-*co*-BAG) copolymers were further utilized to conjugate with a model dye, rhodamine, via a carbodiimide intermediate to yield the rhodamine B-conjugated P(G-*co*-BAG) copolymers. After preparation, their cellular uptake was further evaluated by confocal laser scanning microscopy (CLSM). Figure 3.21b clearly shows that the red fluorescence of the rhodamine B-conjugated copolymer stems from the localization of P(G_{113}-*co*-BAG_{21}) primarily within the perinuclear cytoplasm region, whereas the polymer is not located within the cell nucleus. This result indicates that the cellular uptake of hyperbranched P(G-*co*-BAG) is based on endocytosis. Taken together these cellular assay results with a high potential of conjugation chemistry, the hyperbranched P(G-*co*-BAG) copolymer with the novel amine moieties will offer a compelling platform for next-generation biological and biomedical materials.

ULSAN NATIONAL INSTITUTE OF SCIENCE AND TECHNOLOGY

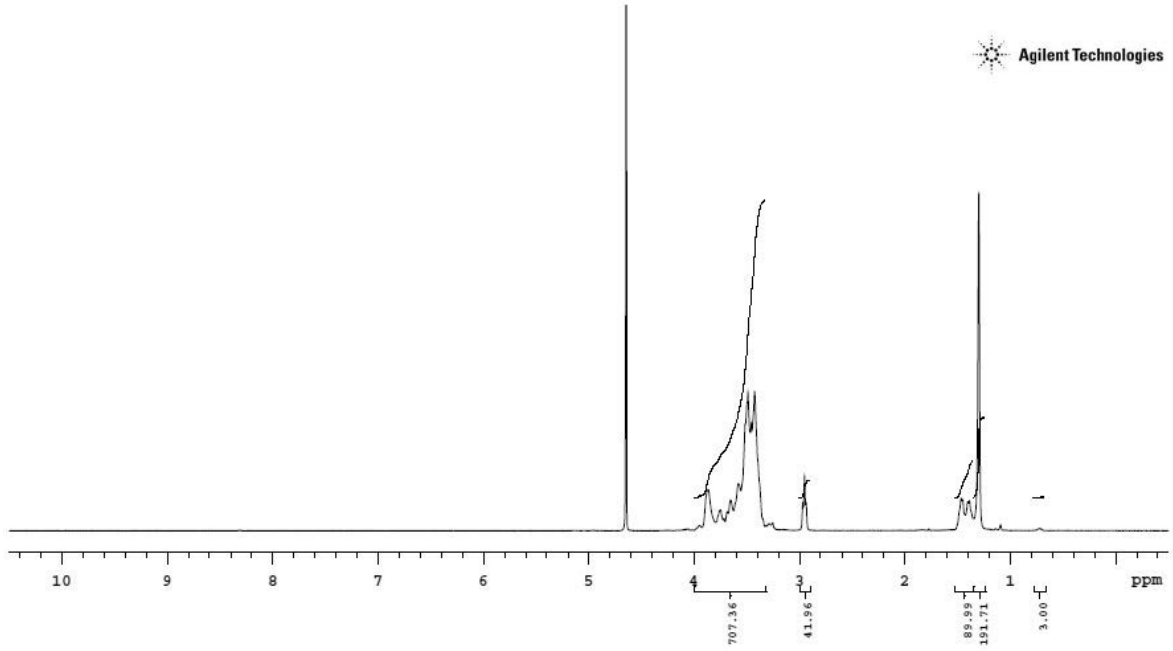

Figure 3.8. ^{1}H NMR spectrum of P(G_{113}-*co*-$BBAG_{21}$) polymer (polymer 7) in D_2O.

ULSAN NATIONAL INSTITUTE OF SCIENCE AND TECHNOLOGY

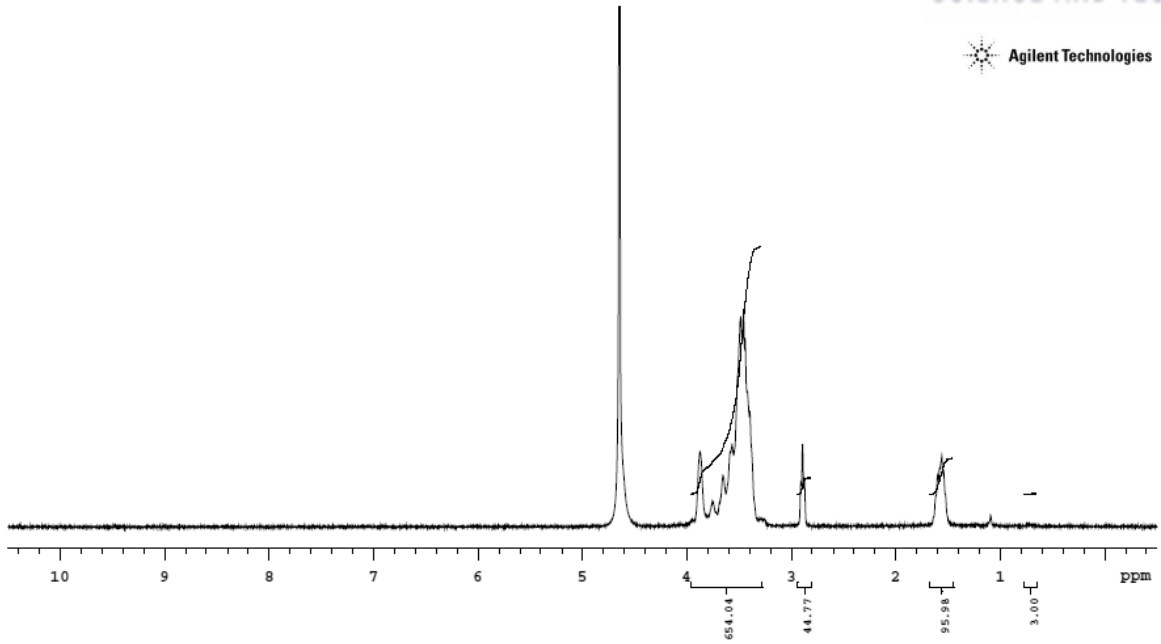

Figure 3.9. ^{1}H NMR spectrum of P(G_{113}-*co*-BAG_{21}) polymer (deprotected polymer 7) in D_2O.

ULSAN NATIONAL INSTITUTE OF SCIENCE AND TECHNOLOGY

Table 3.1. Characterization Data for the Synthesized P(G-*co*-BBAG) Copolymers

No	Polymer composition (target)	Polymer composition (NMR)[a]	M_n (target)	%BBAG (target)	M_n (NMR)[a]	%BBAG (NMR)[a]	M_n (GPC)[b]	M_w/M_n[b] (GPC)[b]
1	$P(G_{57}\text{-co-}BBAG_3)$	$P(G_{56}\text{-co-}BBAG_2)$	5093	5	4800	3.4	9000	1.3
2	$P(G_{52}\text{-co-}BBAG_6)$	$P(G_{61}\text{-co-}BBAG_8)$	5458	10	6600	11.6	10000	1.4
3	$P(G_{114}\text{-co-}BBAG_6)$	$P(G_{125}\text{-co-}BBAG_5)$	10051	5	10600	3.8	10000	1.4
4	$P(G_{100}\text{-co-}BBAG_{10})$	$P(G_{100}\text{-co-}BBAG_8)$	9995	10	9500	7.4	12200	1.6
5	$P(G_{228}\text{-co-}BBAG_{12})$	$P(G_{149}\text{-co-}BBAG_{11})$	19968	5	13900	6.9	8500	1.3
6	$P(G_{200}\text{-co-}BBAG_{22})$	$P(G_{170}\text{-co-}BBAG_{16})$	20347	10	16700	8.6	12600	1.5
7	$P(G_{100}\text{-co-}BBAG_{25})$	$P(G_{113}\text{-co-}BBAG_{21})$	13675	20	13700	15.7	6800	1.2

[a]Determined via ^{1}H NMR spectroscopy. [b]Measured using GPC-RI in DMF with a polystyrene standard.

ULSAN NATIONAL INSTITUTE OF SCIENCE AND TECHNOLOGY

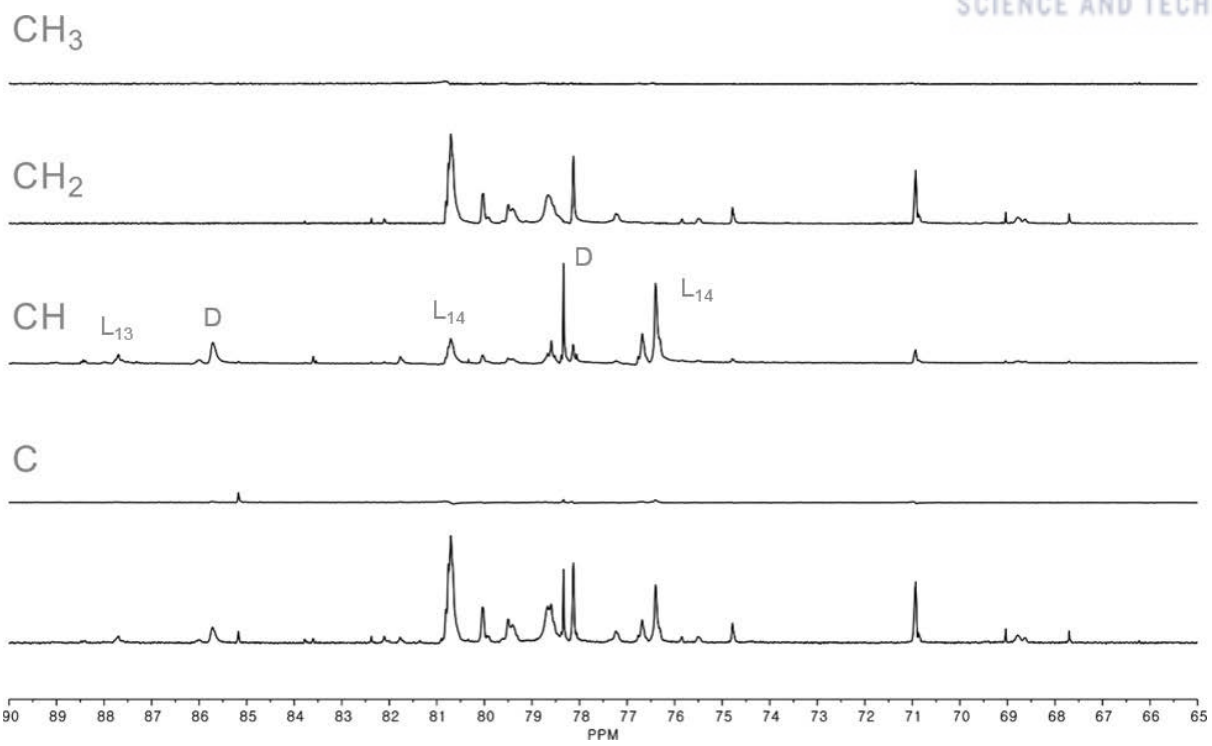

Figure 3.10. DEPT spectra of P(G_{113}-*co*-$BBAG_{21}$) polymer (polymer 7) in DMSO-d_6.

ULSAN NATIONAL INSTITUTE OF SCIENCE AND TECHNOLOGY

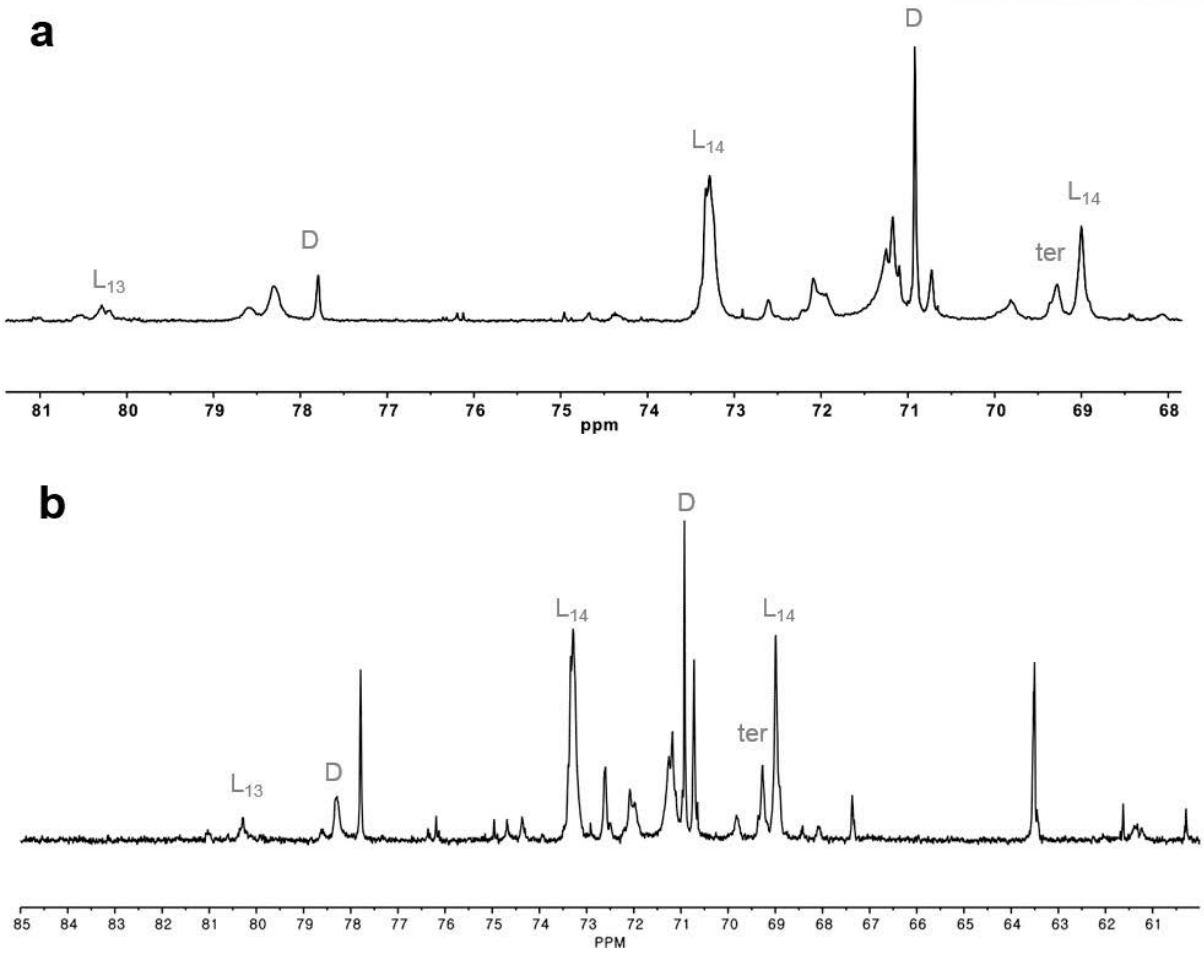

Figure 3.11. Detailed ^{13}C NMR spectrum of (a) P(G_{149}-*co*-$BBAG_{11}$) polymer (polymer 5) and (b) P(G_{113}-*co*-$BBAG_{21}$) polymer (polymer 7) in DMSO-d_6.

ULSAN NATIONAL INSTITUTE OF SCIENCE AND TECHNOLOGY

Calculation of Degree of Branching

Using relative integral values from ^{13}C NMR in Table 3.2, degree of branching (DB) of the copolymers was determined according to the equation for AB/AB_2 systems below.

$$DB_{AB/AB_2} = \frac{2D}{2D + \sum L}$$

Table 3.2. Calculation of Degree of Branching Based on the ^{13}C NMR Spectra of Copolymers.

Region	Chemical Shift (ppm)	Relative Integral Values	
		Polymer 5	Polymer 7
L_{13}	80.0-81.5	1.00	1.00
D	78.0-78.5	3.19	3.53
L_{14}	73.0-73.5	4.22	4.80
D	70.5-71.0	6.13	8.42
Terminal	68.7-69.2	2.60	5.13
L_{14}	69.2-69.5	5.54	13.7

$$DB_{polymer\ 5} = \frac{\{2 \times (3.19 + 6.13)\}}{\{2 \times (3.19 + 6.13) + (1 + 4.22 + 5.54\}} = 0.63$$

$$DB_{polymer\ 7} = \frac{\{2 \times (3.53 + 8.42)\}}{\{2 \times (3.53 + 8.42) + (1 + 4.80 + 13.07\}} = 0.56$$

ULSAN NATIONAL INSTITUTE OF
SCIENCE AND TECHNOLOGY

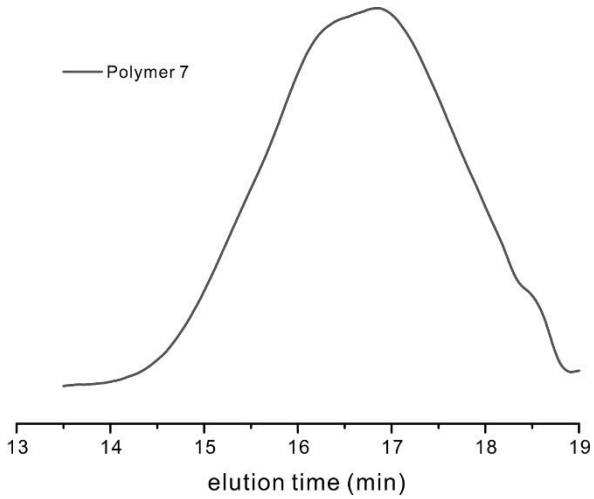

Figure 3.12. Representative gel permeation chromatogram of P(G_{113}-*co*-$BBAG_{21}$) polymer (polymer 7).

ULSAN NATIONAL INSTITUTE OF SCIENCE AND TECHNOLOGY

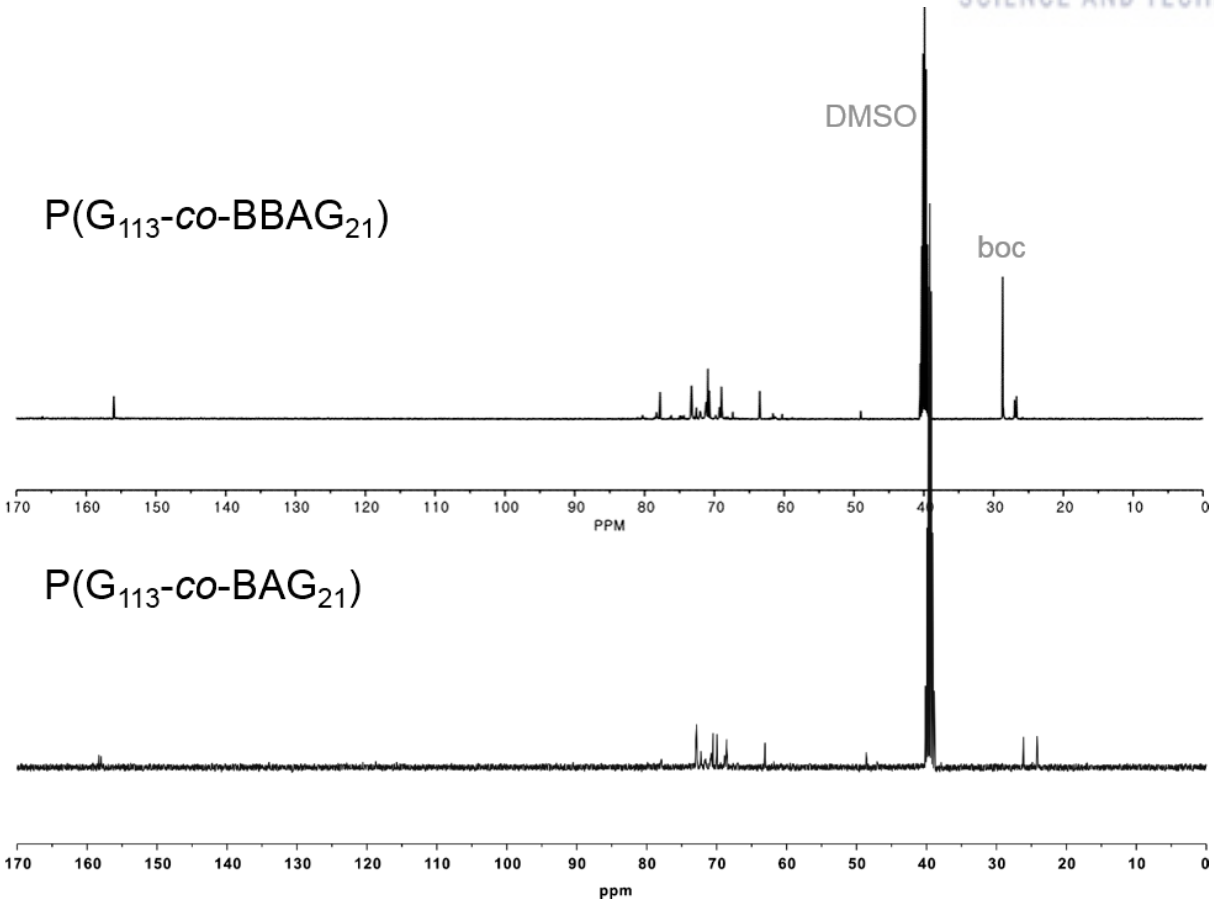

Figure 3.13. ^{13}C NMR spectrum of P(G_{113}-*co*-$BBAG_{21}$) polymer (polymer 7) and P(G_{113}-*co*-BAG_{21}) polymer in DMSO-d_6.

ULSAN NATIONAL INSTITUTE OF SCIENCE AND TECHNOLOGY

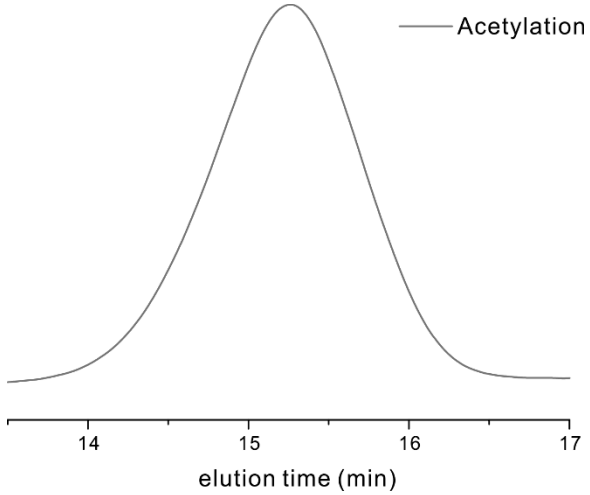

Figure 3.14. Gel permeation chromatogram of acetylated P(G_{113}-*co*-BAG_{21}) polymer (polymer 7).

ULSAN NATIONAL INSTITUTE OF SCIENCE AND TECHNOLOGY

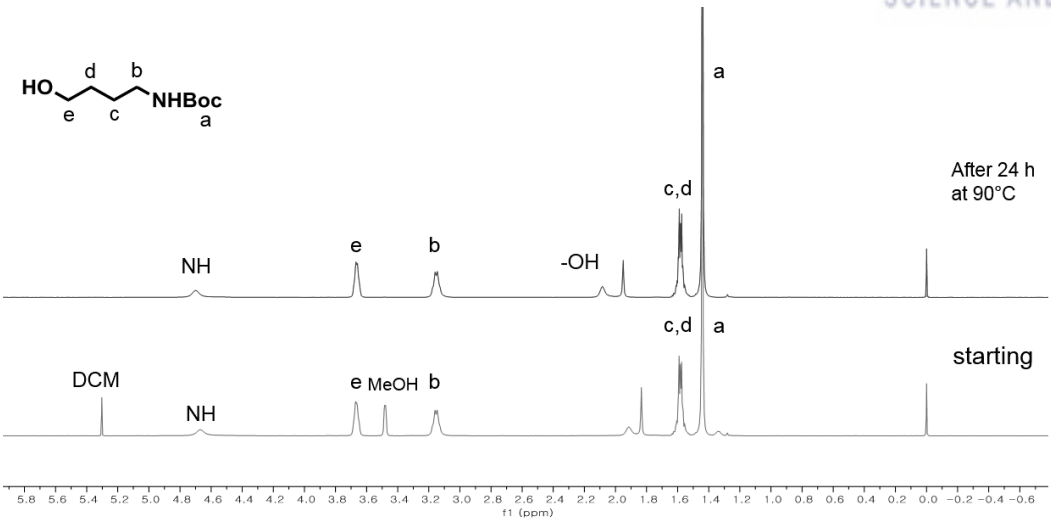

Figure 3.15. ^{1}H NMR spectra of Boc-protected 1-aminobutanol before and after heating over 24 h at 90 °C.

ULSAN NATIONAL INSTITUTE OF SCIENCE AND TECHNOLOGY

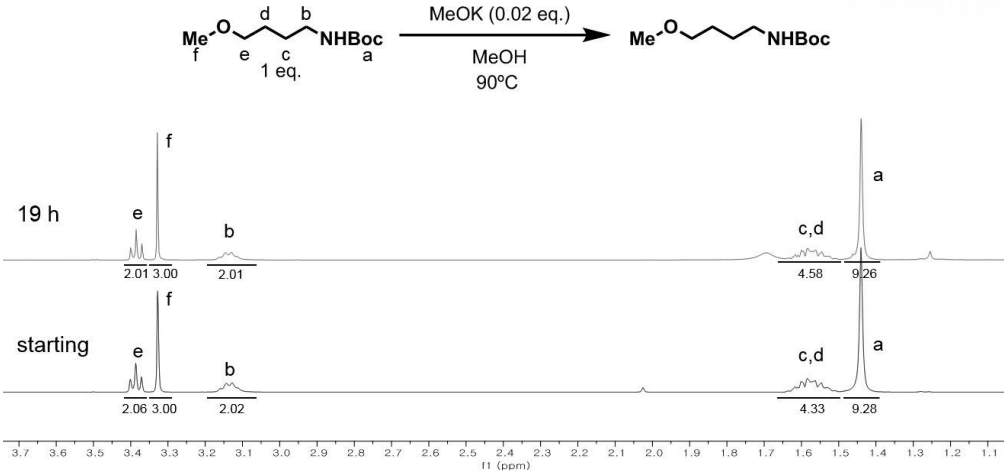

Figure 3.16. ^{1}H NMR spectra of the reaction of model compound with a strong base at 90 °C.

ULSAN NATIONAL INSTITUTE OF SCIENCE AND TECHNOLOGY

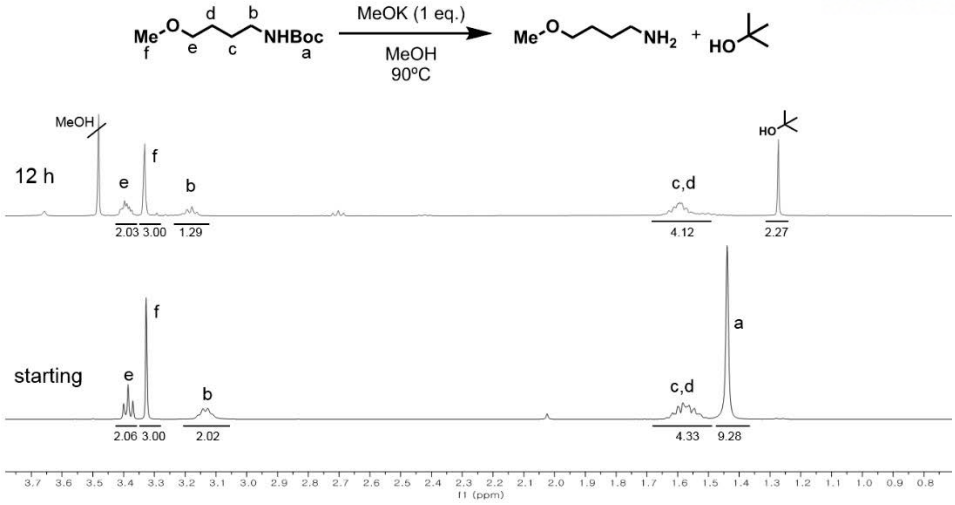

Figure 3.17. ^{1}H NMR spectra of the reaction of model compound with a strong base (1.0 equiv) at 90 °C.

ULSAN NATIONAL INSTITUTE OF SCIENCE AND TECHNOLOGY

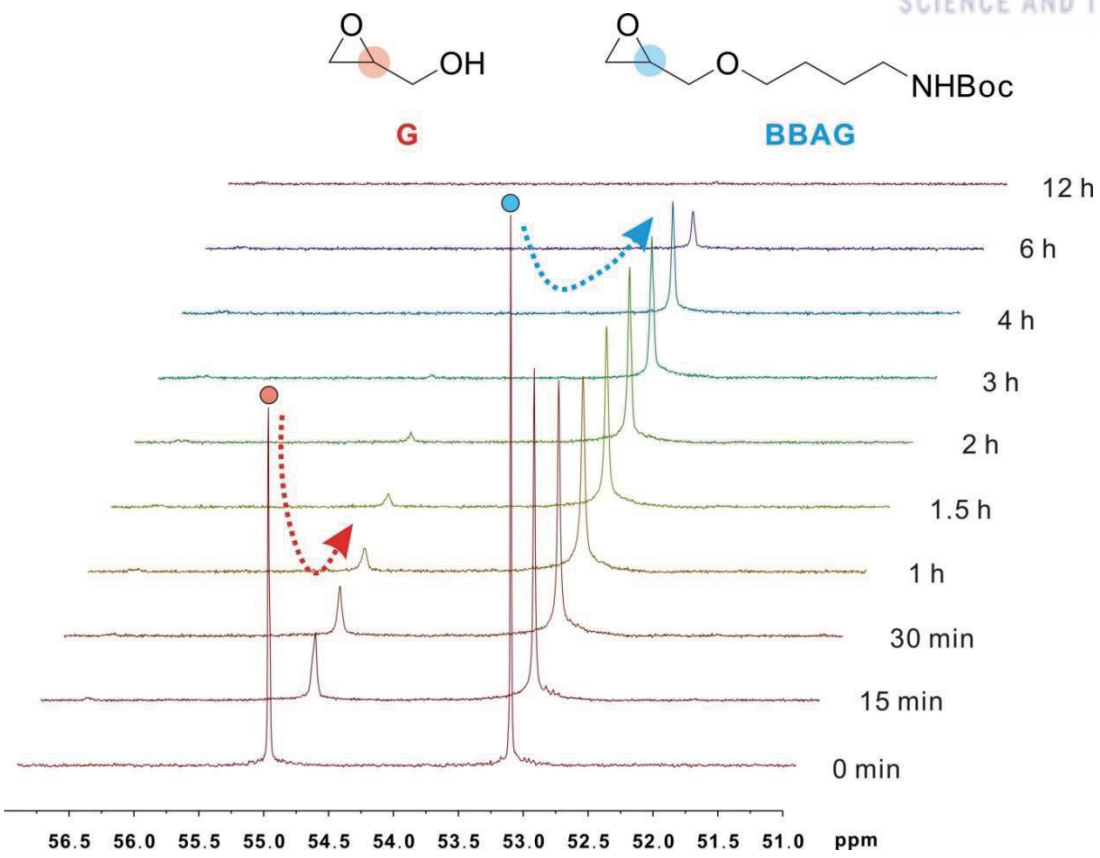

Figure 3.18. ^{13}C NMR spectra of the *in situ* copolymerization kinetics of G and BBAG monomers (initial monomer ratio of 1:1). Overlay of the spectra showing the signals for the methine carbons of the epoxide at 54.9 and 53.2 ppm, which correspond to the G and BBAG monomers, respectively, collected after the designated time period (DMSO-d_6, 150 MHz, 75 °C).

ULSAN NATIONAL INSTITUTE OF
SCIENCE AND TECHNOLOGY

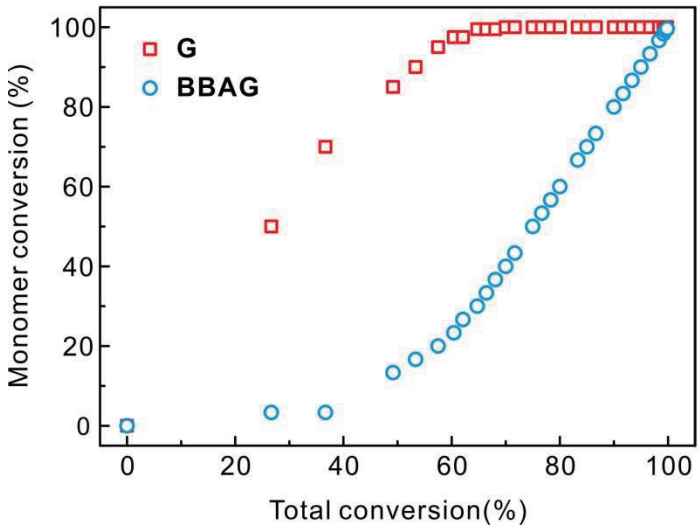

Figure 3.19. Monomer conversion percentage versus total conversion for copolymerization of G (red square) and BBAG (blue circle) (initial monomer ratio of 1:1) determined from quantitative ^{13}C NMR kinetics at 75 °C.

ULSAN NATIONAL INSTITUTE OF SCIENCE AND TECHNOLOGY

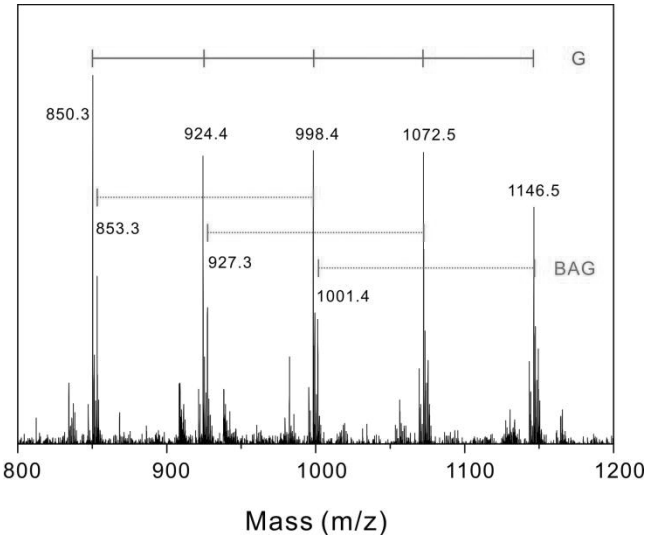

Figure 3.20. Expanded MALDI-ToF mass spectrum of the P(G_{125}-*co*-BAG_5) copolymer (polymer 3) from 800 to 1200 Da. The spacing of the signals corresponds to the mass of the respective monomers in the copolymer (G:74.08 g/mol and BAG: 145.2 g/mol).

ULSAN NATIONAL INSTITUTE OF SCIENCE AND TECHNOLOGY

Table 3.3. Characterization Data for the Synthesized P(G-co-BAG) Copolymers

No	Polymer composition (target)	Polymer composition (NMR)		T_g / °C (DSC)		Zeta potential / mV
		before	after deprotection	before	after	
1	$P(G_{57}\text{-co-}BBAG_3)$	$P(G_{56}\text{-co-}BBAG_2)$	$P(G_{56}\text{-co-}BAG_2)$	-31.8	-18.7	24.4±0.7
2	$P(G_{52}\text{-co-}BBAG_6)$	$P(G_{61}\text{-co-}BBAG_8)$	$P(G_{61}\text{-co-}BAG_8)$	-39.5	-25.1	27.7±1.5
3	$P(G_{114}\text{-co-}BBAG_6)$	$P(G_{125}\text{-co-}BBAG_5)$	$P(G_{125}\text{-co-}BAG_5)$	-52.7	-30.9	24.0±2.2
4	$P(G_{100}\text{-co-}BBAG_{10})$	$P(G_{100}\text{-co-}BBAG_8)$	$P(G_{100}\text{-co-}BAG_8)$	-39.2	-26.0	25.9±5.3
5	$P(G_{228}\text{-co-}BBAG_{12})$	$P(G_{149}\text{-co-}BBAG_{11})$	$P(G_{149}\text{-co-}BAG_{11})$	-34.5	-7.1	34.9±1.1
6	$P(G_{200}\text{-co-}BBAG_{22})$	$P(G_{170}\text{-co-}BBAG_{16})$	$P(G_{170}\text{-co-}BAG_{16})$	-33.2	-22.9	25.5±2.0
7	$P(G_{100}\text{-co-}BBAG_{25})$	$P(G_{113}\text{-co-}BBAG_{21})$	$P(G_{113}\text{-co-}BAG_{21})$	-33.2	-5.6	31.3±3.1

ULSAN NATIONAL INSTITUTE OF SCIENCE AND TECHNOLOGY

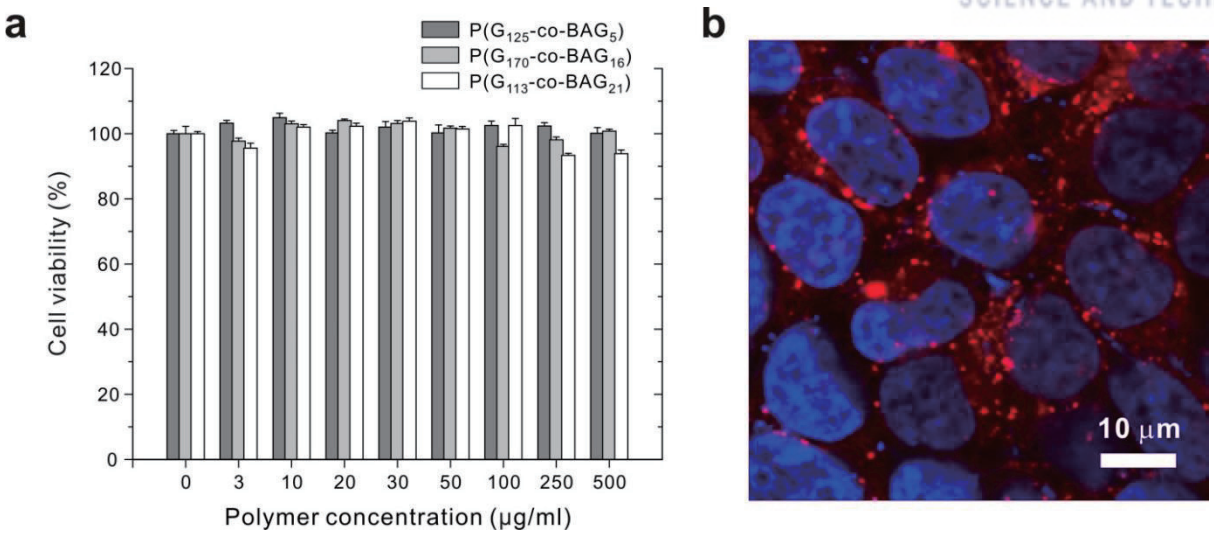

Figure 3.21. (a) *In vitro* cell viability assay of copolymers. P(G_{125}-*co*-BAG_5) (polymer 3) (dark gray), P(G_{170}-*co*-BAG_{16}) (polymer 6) (light gray), and P(G_{113}-*co*-BAG_{21}) (polymer 7) (white) polymers determined by MTT assays using RAW264.7 cell lines. (b) CLSM image of HEK293T cells incubated with rhodamine B-conjugated P(G_{113}-*co*-BAG_{21}) (polymer 7). DAPI was used to stain the cell nucleus.

ULSAN NATIONAL INSTITUTE OF SCIENCE AND TECHNOLOGY

3.5 Conclusion

In summary, we present a one-pot synthesis of a series of hyperbranched PGs possessing amino functionality. A novel glycidyl amine as a monomer, Boc-protected butanamine glycidyl ether monomer (BBAG), was designed and polymerized with glycidol (G) through anionic ring-opening multibranching polymerization to yield a well-defined P(G-*co*-BBAG) with an adjustable comonomer ratio, which was subsequently deprotected with TFA to yield the desired P(G-*co*-BAG) copolymers. The polymerization was successfully characterized by ^{1}H NMR and GPC, and the copolymerization kinetics between the two monomers was further revealed by an *in situ* ^{13}C NMR study. The possible side reaction of Boc protecting group was carefully investigated by the model reaction of tert-butyl 4-methoxybutylcarbamate under high temperature and strongly basic condition. The high zeta-potential and *in vitro* biocompatibility assay results of P(G-*co*-BAG), together with its efficiency in conjugating functional molecules, clearly demonstrate its significant potential in bioconjugation chemistry, which takes advantage of the free amine groups sheathed in hyperbranched PGs. We anticipate that the new class of amine functional monomer and polymers developed in this study will contribute to the advancement and understanding of PG-based polymers and will be a promising candidate for emerging materials and biomedical applications.

ULSAN NATIONAL INSTITUTE OF SCIENCE AND TECHNOLOGY

3.6 References

(1) Albertazzi, L.; Mickler, F. M.; Pavan, G. M.; Salomone, F.; Bardi, G.; Panniello, M.; Amir, E.; Kang, T.; Killops, K. L.; Bräuchle, C.; Amir, R. J.; Hawker, C. J. Enhanced Bioactivity of Internally Functionalized Cationic Dendrimers with PEG Cores. *Biomacromolecules* **2012**, *13*, 4089–4097.

(2) Dey, P.; Adamovski, M.; Friebe, S.; Badalyan, A.; Mutihac, R.-C.; Paulus, F.; Leimkühler, S.; Wollenberger, U.; Haag, R. Dendritic Polyglycerol–Poly(ethylene glycol)-Based Polymer Networks for Biosensing Application. *ACS Appl. Mater. Interfaces* **2014**, *6*, 8937–8941.

(3) Knop, K.; Hoogenboom, R.; Fischer, D.; Schubert, U. S. Poly(ethylene glycol) in Drug Delivery: Pros and Cons as Well as Potential Alternatives. *Angew. Chem. Int. Ed.* **2010**, *49*, 6288–6308.

(4) Larson, N.; Ghandehari, H. Polymeric Conjugates for Drug Delivery. *Chem. Mater.* **2012**, *24*, 840–853.

(5) Senevirathne, S. A.; Washington, K. E.; Biewer, M. C.; Stefan, M. C. PEG Based Anti-Cancer Drug Conjugated Prodrug Micelles for The Delivery of Anti-Cancer Agents. *J. Mater. Chem. B* **2016**, *4*, 360–370.

(6) Pelegri-O'Day, E. M.; Lin, E.-W.; Maynard, H. D. Therapeutic Protein-Polymer Conjugates: Advancing Beyond PEGylation. *J. Am. Chem. Soc.* **2014**, *136*, 14323–14332.

(7) Thomas, A.; Müller, S. S.; Frey, H. Linear Polyglycerol as a Multifunctional Polyether for Biomedical and Pharmaceutical Applications. *Biomacromolecules* **2014**, *15*, 1935–1954.

(8) Du, W.; Li, Y.; Nyström, A. M.; Cheng, C.; Wooley, K. L. Synthesis, Characterization, and Aqueous Self-Assembly of Amphiphilic Poly(ethylene oxide)-Functionalized Hyperbranched Fluoropolymers. *J. Polym. Sci. Part A Polym. Chem.* **2010**, *48*, 3487–3496.

(9) Saville, P. M.; Reynolds, P. A.; White, J. W.; Hawker, C. J.; Frechet, J. M. J.; Wooley, K. L.; Penfold, J.; Webster, J. R. P. Neutron Reflectivity and Structure of Polyether Dendrimers as Langmuir Films. *J. Phys. Chem.* **1995**, *99*, 8283–8289.

(10) Herzberger, J.; Niederer, K.; Pohlit, H.; Seiwert, J.; Worm, M.; Wurm, F. R.; Frey, H. Polymeri zation of Ethylene Oxide, Propylene Oxide, and Other Alkylene Oxides: Synthesis, Nov el Polymer Architectures, and Bioconjugation. *Chem. Rev.* **2016**, *116*, 2170–2243.

(11) Kainthan, R. K.; Muliawan, E. B.; Hatzikiriakos, S. G.; Brooks, D. E. Synthesis, Characterization, and Viscoelastic Properties of High Molecular Weight Hyperbranched Polyglycerols. *Macromolecules* **2006**, *39*, 7708–7717.

(12) Sisson, A. L.; Papp, I.; Landfester, K.; Haag, R. Functional Nanoparticles from Dendritic Precursors: Hierarchical Assembly in Miniemulsion. *Macromolecules* **2009**, *42*, 556–559.

(13) Wilms, D.; Stiriba, S.-E.; Frey, H. Hyperbranched Polyglycerols: From the Controlled

ULSAN NATIONAL INSTITUTE OF SCIENCE AND TECHNOLOGY

Synthesis of Biocompatible Polyether Polyols to Multipurpose Applications. *Acc. Chem. Res.* **2010**, *43*, 129–141.

(14) Zheng, Y.; Li, S.; Weng, Z.; Gao, C. Hyperbranched Polymers: Advances from Synthesis to Applications. *Chem. Soc. Rev.* **2015**, *44*, 4091–4130.

(15) Schömer, M.; Seiwert, J.; Frey, H. Hyperbranched Poly(propylene oxide): A Multifunctional Backbone-Thermoresponsive Polyether Polyol Copolymer. *ACS Macro Lett.* **2012**, *1*, 888–891.

(16) Christ, E.-M.; Hobernik, D.; Bros, M.; Wagner, M.; Frey, H. Cationic Copolymerization of 3,3-Bis(hydroxymethyl)oxetane and Glycidol: Biocompatible Hyperbranched Polyether Polyols with High Content of Primary Hydroxyl Groups. *Biomacromolecules* **2015**, *16*, 3297–3307.

(17) Niederer, K.; Schüll, C.; Leibig, D.; Johann, T.; Frey, H. Catechol Acetonide Glycidyl Ether (CAGE): A Functional Epoxide Monomer for Linear and Hyperbranched Multi-Catechol Functional Polyether Architectures. *Macromolecules* **2016**, *49*, 1655–1665.

(18) Thomas, A.; Bauer, H.; Schilmann, A.-M.; Fischer, K.; Tremel, W.; Frey, H. The "Needle in the Haystack" Makes the Difference: Linear and Hyperbranched Polyglycerols with a Single Catechol Moiety for Metal Oxide Nanoparticle Coating. *Macromolecules* **2014**, *47*, 4557–4566.

(19) Son, S.; Shin, E.; Kim, B.-S. Redox-Degradable Biocompatible Hyperbranched Polyglycerol s: Synthesis, Copolymerization Kinetics, Degradation, and Biocompatibility. *Macromolecules* **2015**, *48*, 600–609.

(20) Son, S.; Park, H.; Shin, E.; Shibasaki, Y.; Kim, B.-S. Architecture-Controlled Synthesis of Redox-Degradable Hyperbranched Polyglycerol Block Copolymers and The Structural Implications of Their Degradation. *J. Polym. Sci. Part A Polym. Chem.* **2016**, *54*, 1752–1761.

(21) Meyer, J.; Keul, H.; Möller, M. Poly(glycidyl amine) and Copolymers with Glycidol and Glycidyl Amine Repeating Units: Synthesis and Characterization. *Macromolecules* **2011**, *44*, 4082–4091.

(22) Wurm, F.; Dingels, C.; Frey, H.; Klok, H.-A. Squaric Acid Mediated Synthesis and Biological Activity of a Library of Linear and Hyperbranched Poly(glycerol)–Protein Conjugates. *Biomacromolecules* **2012**, *13*, 1161–1171.

(23) Moore, E.; Delalat, B.; Vasani, R.; Thissen, H.; Voelcker, N. H. Patterning and Biofunctionalization of Antifouling Hyperbranched Polyglycerol Coatings. *Biomacromolecules* **2014**, *15*, 2735–2743.

(24) Pant, K.; Gröger, D.; Bergmann, R.; Pietzsch, J.; Steinbach, J.; Graham, B.; Spiccia, L.; Berthon, F.; Czarny, B.; Devel, L.; Dive, V.; Stephan, H.; Haag, R. Synthesis and Biodistribution Studies of ^{3}H- and ^{64}Cu-Labeled Dendritic Polyglycerol and Dendritic Polyglycerol Sulfate. *Bioconjugate Chem.* **2015**, *26*, 906–918.

ULSAN NATIONAL INSTITUTE OF SCIENCE AND TECHNOLOGY

(25) Su, Z.; Jiang, X. Multi-Stimuli Responsive Amine-Containing Polyethers: Novel Building Blocks for Smart Assemblies. *Polymer* **2016**, *93*, 221–239.

(26) Koyama, Y.; Umehara, M.; Mizuno, A.; Itaba, M.; Yasukouchi, T.; Natsume, K.; Suginaka, A.; Watanabe, K. Synthesis of Novel Poly(ethylene glycol) Derivatives Having Pendant Amino Groups and Aggregating Behavior of Its Mixture with Fatty Acid in Water. *Bioconjugate Chem.* **1996**, *7*, 298–301.

(27) Obermeier, B.; Wurm, F.; Frey, H. Amino Functional Poly(ethylene glycol) Copolymers via Protected Amino Glycidol. *Macromolecules* **2010**, *43*, 2244–2251.

(28) Reuss, V. S.; Obermeier, B.; Dingels, C.; Frey, H. N,N-Diallylglycidylamine: A Key Monomer for Amino-Functional Poly(ethylene glycol) Architectures. *Macromolecules* **2012**, *45*, 4581–4589.

(29) Herzberger, J.; Frey, H. Epicyanohydrin: Polymerization by Monomer Activation Gives Ac cess to Nitrile-, Amino-, and Carboxyl-Functional Poly(ethylene glycol). *Macromolecules* **2015**, *48*, 8144–8153.

(30) Isono, T.; Asai, S.; Satoh, Y.; Takaoka, T.; Tajima, K.; Kakuchi, T.; Satoh, T. Controlled/Living Ring-Opening Polymerization of Glycidylamine Derivatives Using *t*-Bu-P_4 /Alcohol Initiating System Leading to Polyethers with Pendant Primary, Secondary, and Tertiary Amino Groups. *Macromolecules* **2015**, *48*, 3217–3229.

(31) Lee, A.; Lundberg, P.; Klinger, D.; Lee, B. F.; Hawker, C. J.; Lynd, N. A. Physiologically Rele vant pH-Responsive PEG-Based Block and Statistical Copolymers with N,N-Diisopropyl Amine Units. *Polym. Chem.* **2013**, *4*, 5735.

(32) Son, S.; Shin, E.; Kim, B.-S. Light-Responsive Micelles of Spiropyran Initiated Hyperbranc hed Polyglycerol for Smart Drug Delivery. *Biomacromolecules* **2014**, *15*, 628–634.

(33) Oikawa, Y.; Lee, S.; Kim, D. H.; Kang, D. H.; Kim, B.-S.; Saito, K.; Sasaki, S.; Oishi, Y.; Shibasaki, Y. One-Pot Synthesis of Linear-Hyperbranched Amphiphilic Block Copolymers Based on Polyglycerol Derivatives and Their Micelles. *Biomacromolecules* **2013**, *14*, 2171–2178.

(34) Lee, S.; Saito, K.; Lee, H.-R.; Lee, M. J.; Shibasaki, Y.; Oishi, Y.; Kim, B.-S. Hyperbranched Double Hydrophilic Block Copolymer Micelles of Poly(ethylene oxide) and Polyglycerol for pH-Responsive Drug Delivery. *Biomacromolecules* **2012**, *13*, 1190–1196.

(35) Nguyen, C.; Ruda, G. F.; Schipani, A.; Kasinathan, G.; Leal, I.; Musso-Buendia, A.; Kaiser, M.; Brun, R.; Ruiz-Pérez, L. M.; Sahlberg, B.-L.; Johansson, N. G.; González-Pacanowska, D.; Gilbert, I. H. Acyclic Nucleoside Analogues as Inhibitors of *Plasmodium falciparum* dUTPase. *J. Med. Chem.* **2006**, *49*, 4183–4195.

(36) Pang, Y.; Zhu, Q.; Liu, J.; Wu, J.; Wang, R.; Chen, S.; Zhu, X.; Yan, D.; Huang, W.; Zhu, B. Design and Synthesis of Cationic Drug Carriers Based on Hyperbranched Poly(amine-ester)s

ULSAN NATIONAL INSTITUTE OF SCIENCE AND TECHNOLOGY

Biomacromolecules **2010**, *11*, 575–582.

(37) Sunder, A.; Hanselmann, R.; Frey, H.; Mülhaupt, R. Controlled Synthesis of Hyperbranched Polyglycerols by Ring-Opening Multibranching Polymerization. *Macromolecules* **1999**, *32*, 4240–4246.

(38) Wolf, F. K.; Frey, H. Ferrocene-Containing Multifunctional Polyethers: Monomer Sequence Monitoring via Quantitative ^{13}C NMR Spectroscopy in Bulk. *Macromolecules* **2009**, *42*, 9443–9456.

(39) Alkan, A.; Natalello, A.; Wagner, M.; Frey, H.; Wurm, F. R. *Macromolecules* **2014**, *47*, 2242–2249.

(40) Seiwert, J.; Leibig, D.; Kemmer-Jonas, U.; Bauer, M.; Perevyazko, I.; Preis, J.; Frey, H. Hyperbranched Polyols via Copolymerization of 1,2-Butylene Oxide and Glycidol: Comparison of Batch Synthesis and Slow Monomer Addition. *Macromolecules* **2016**, *49*, 38–47.

(41) Deng, Y.; Saucier-Sawyer, J. K.; Hoimes, C. J.; Zhang, J.; Seo, Y.-E.; Andrejecsk, J. W.; Saltzman, W. M. The Effect of Hyperbranched Polyglycerol Coatings on Drug Delivery Using Degradable Polymer Nanoparticles. *Biomaterials* **2014**, *35*, 6595–6602.

(42) Mehrabadi, F. S.; Hirsch, O.; Zeisig, R.; Posocco, P.; Laurini, E.; Pricl, S.; Haag, R.; Kemmner, W.; Calderón, M. Structure–activity relationship study of dendritic polyglycerolamines for efficient siRNA transfection. *RSC Adv.* **2015**, *5*, 78760–78770.

(43) Gröger, D.; Paulus, F.; Licha, K.; Welker, P.; Weinhart, M.; Holzhausen, C.; Mundhenk, L.; Gruber, A. D.; Abram, U.; Haag, R. Synthesis and Biological Evaluation of Radio and Dye Labeled Amino Functionalized Dendritic Polyglycerol Sulfates as Multivalent Anti-Inflammatory Compounds. *Bioconjugate Chem.* **2013**, *24*, 1507–1514.

(44) Zeng, H.; Schlesener, C.; Cromwell, O.; Hellmund, M.; Haag, R.; Guan, Z. Amino Acid-Functionalized Dendritic Polyglycerol for Safe and Effective siRNA Delivery. *Biomacromolecules* **2015**, *16*, 3869–3877.

ULSAN NATIONAL INSTITUTE OF SCIENCE AND TECHNOLOGY

Chapter 4

Anionic Polymerization of Azidoalkyl Glycidyl Ethers and Post-Polymerization Modification*

4.1 Abstract

Polyethers like poly(ethylene glycol) have been widely used for a variety of valuable applications, though their functionalization still poses challenges due to the lack of functional handles along the polymer backbone. Herein, a series of novel azide-functionalized glycidyl ether monomers are presented as a universal approach to synthesize functional polyethers by post-polymerization modification. Three azide-functionalized glycidyl ether monomers possessing different alkyl spacers (ethyl, butyl, and hexyl) were designed and synthesized by a simple two-step substitution reaction. Organic superbase-catalyzed anionic ring-opening polymerization can proceed under mild conditions compatible with an azide-pendant group, affording well-controlled azide-functionalized polyethers with low dispersity ($Đ < 1.2$). The azide pendant groups on the resulting polymers were readily modified to a variety of functional groups via copper-catalyzed azide–alkyne cycloaddition reactions and Staudinger reduction. Furthermore, copolymerization of azidohexyl glycidyl ether with allyl glycidyl ether was demonstrated to provide an additional orthogonal functional handle. We anticipate that this work provides a new platform for the preparation of diverse functional polyethers.

*Chapter 4 is reproduced in part with permission from *Macromolecules* **2019**, published ASAP by Joonhee Lee, Sohee Han, Minseong Kim, and Byeong-Su Kim. Copyright 2019 American Chemical Society.

ULSAN NATIONAL INSTITUTE OF SCIENCE AND TECHNOLOGY

4.2 Introduction

The development of efficient and reliable methods to synthesize functional polymers with diverse properties and architectures is essential to satisfy the demands of various applications in materials science. Many functional polymers have been prepared by direct polymerization of readily polymerizable monomers accompanied by significant advances in controlled polymerization techniques with tolerable functional monomers.[1–3] However, there are still some monomers having reactive functional moieties that are not amenable to direct polymerization.

Alternatively, post-polymerization modification offers an avenue to access multi-functional polymers, while circumventing the incompatibility of desirable functional groups with polymerization conditions.[4,5] Many post-polymerization modification strategies are based on the increasing convergence of organic chemistry and polymer synthesis,[6] spearheaded by the introduction of click chemistry by Sharpless and colleagues.[7] For example, post-polymerization modification of many classes of polymers has been achieved through various chemical transformations, including azide–alkyne cycloaddition,[8,9] transesterification,[10] thiol-ene addition,[11] Diels-Alder reactions,[12] Suzuki-Miyaura coupling,[13] and sulfur fluoride exchange.[14] For this strategy, the development of a suitable monomer that is compatible with a polymerization needs to be accompanied. In this manner, BN 2-vinylnaphthalene has been introduced by the Klausen group to prepare poly(vinyl alcohol) derivatives via post-polymerization organoborane oxidation.[15] Hillmyer group has established a new route to prepare poly(allyl alcohol) by post-polymerization modification of the polymer precursor synthesized from bis(*tert*-butyloxycarbonyl) twisted acrylamide monomer.[16] These strategies highlight the importance of designing a functional monomer suitable for post-polymerization modification to access desired functional polymers that are otherwise inaccessible by direct polymerization.

Poly(ethylene glycol) (PEG) is a representative polymer among aliphatic polyethers, drawing considerable attention as one of the most valuable polymers in biomedical applications by virtue of their excellent biocompatibility and aqueous solubility.[17,18] However, they lack reactive functional handles along their backbone, which limits their implications in broader areas. The typical approach for the preparation of multi-functional PEGs involves anionic ring-opening polymerization (AROP) of functional epoxide monomers.[19,20] Conventional AROP is typically incompatible with most functional groups, such as hydroxyl, carboxylic acid, primary amine, nitrile, and halide groups, due to the highly reactive conditions, leading to undesirable side reactions. An alternative approach such as the activated monomer method has been suggested to avoid such difficulties.[21–23] Nonetheless, the development of epoxide monomers exhibiting functional groups that are tolerable to typical AROP conditions is still necessary to design a convenient post-polymerization modification strategy for polyethers.

To date, several monomers bearing functional groups stable to AROP conditions have been

ULSAN NATIONAL INSTITUTE OF SCIENCE AND TECHNOLOGY

reported.[19] As a representative example, allyl glycidyl ether (AGE) is an epoxide monomer widely used for imparting functionality to PEG. Not only are allyl groups stable under typical AROP conditions, but they can also react with functional thiols via the thiol–ene reaction, to decorate polyethers with myriad pendant functionalities.[24–26] Intensive studies and various applications of AGE-based polymers by the Hawker and Lynd group have made a significant impact on post-polymerization modification of various polyethers.[27–35] Recently, Frey and coworkers have also developed a novel epoxide monomer, 3,3-dimethoxypropanyl glycidyl ether, for homopolymerization or copolymerization with ethylene oxide to afford PEG displaying multiple aldehyde functionalities.[36]

Inspired by the advent of click chemistry, the azide functionality is regarded as a good candidate for the post-polymerization modification of polyethers due to its potential to undergo further modification by Cu-catalyzed azide-alkyne cycloaddition (CuAAC) or Staudinger reduction. As a part of our ongoing effort in the development of novel functional glycidyl ether monomer library,[37–43] herein, we introduce a series of new azide-functional glycidyl ether monomers, azidoethyl glycidyl ether (AEGE), azidobutyl glycidyl ether (ABGE), and azidohexyl glycidyl ether (AHGE) that can be polymerizable under organic superbase-catalyzed AROP condition. The homopolymerization of each monomer was compared using *in situ* ^{1}H NMR kinetics study. Among them, AHGE was selected as a model monomer for the generation of a modular and versatile synthetic route to post-polymerization modified polyethers (Figure 4.1). Polymerization of AHGE provides functional polyethers bearing pendant azide groups, which can be further reacted with functional alkynes to install a broad range of functionalities along the polymer backbone. In addition, Staudinger reduction of the azide group can afford a pendant primary amine group, which is otherwise not tolerable in typical AROP conditions.

ULSAN NATIONAL INSTITUTE OF SCIENCE AND TECHNOLOGY

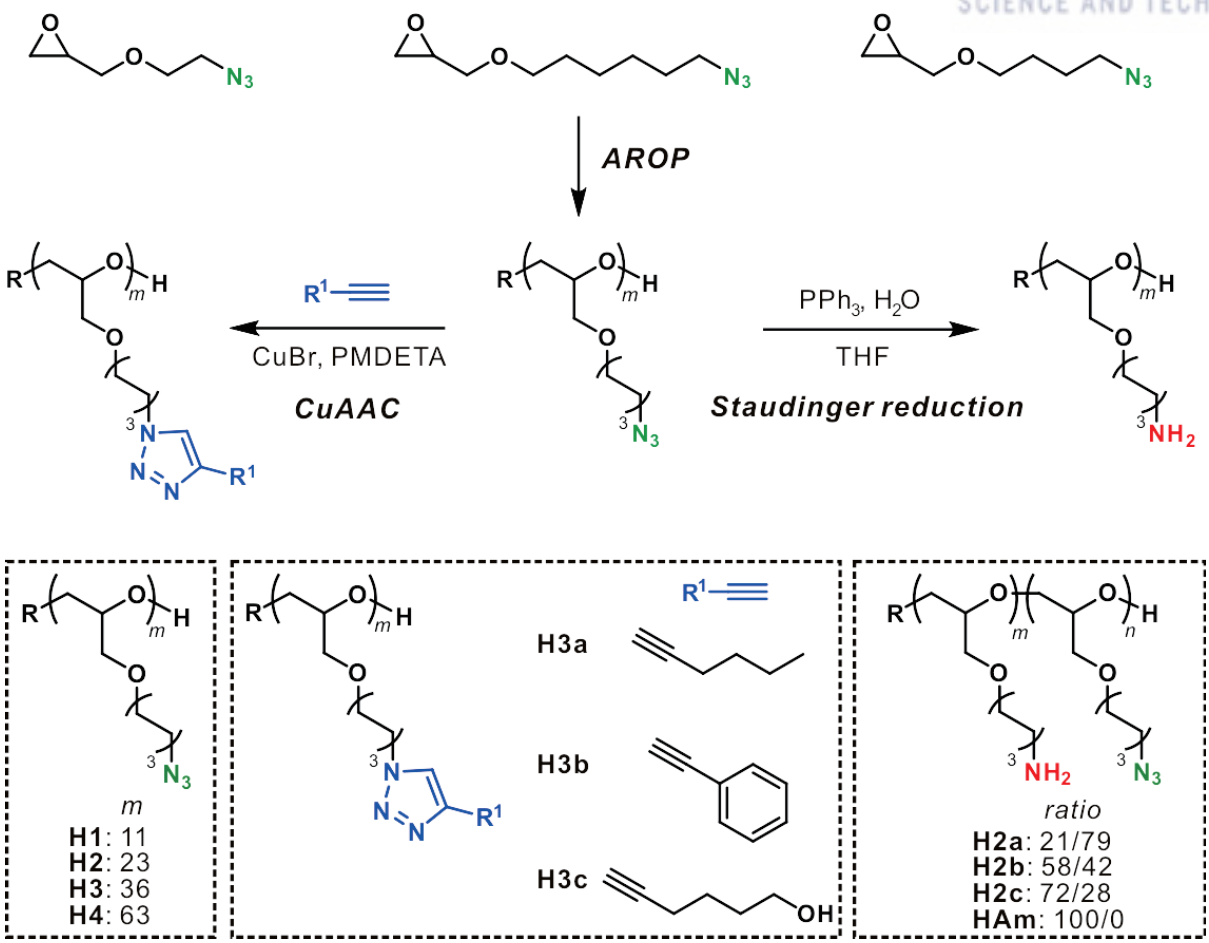

Figure 4.1. Post-polymerization modification of azide-functionalized polyethers via copper-catalyzed azide-alkyne cycloaddition (CuAAC) and Staudinger reduction.

ULSAN NATIONAL INSTITUTE OF SCIENCE AND TECHNOLOGY

4.3 Experimental Section

Materials

All reagents and solvents were purchased from Sigma-Aldrich, Alfa Aesar, or Tokyo Chemical Industry and used as received unless otherwise noted. Tetrahydrofuran (THF) and toluene were dried and degassed using a solvent purification system (Vac Atmospheres, USA) and collected to use immediately thereafter. $CDCl_3$, DMSO-d_6, toluene-d_8, and D_2O were purchased from Cambridge Isotope Laboratories. AEGE, ABGE, and AHGE were used for polymerization after the distillation over CaH_2.

Characterization

^1H and ^{13}C NMR spectra were recorded on an Agilent 400 MHz spectrometer or Bruker Avance III HD 400 MHz spectrometer at room temperature. Chemical shifts are reported in ppm relative to the signals corresponding to the residual non-deuterated solvents: $CDCl_3$, δH = 7.26 ppm and δC = 77.16 ppm; $(CD_3)_2SO$, δH = 2.50 ppm; D_2O, δH = 4.79 ppm; C_7D_8, δH = 2.09 ppm. Mass spectrometry was performed on a Bruker 1200 series and HCT Basic System using an electrospray ionization (ESI) source. The number and weight-averaged molecular weights (M_n and M_w) and molecular weight distributions (M_w/M_n) were measured using size exclusion chromatography (SEC). SEC analyses were performed on an Agilent 1260 Infinity setup with two PLgel 5 μm MIXED-D columns at 30 °C with either chloroform or THF as mobile phase. The columns were calibrated against standard poly(methyl methacrylate) samples (Sigma Aldrich, M_p 500 – 2,700,000). FT-IR spectra were recorded on an Agilent Cary 630 FTIR spectrometer equipped with an ATR module.

Synthesis of Azidoalkyl Glycidyl Ethers

Intermediates 2-azido-1-ethanol (**1b**), 4-azido-1-butanol (**2b**), and 6-azido-1-hexanol (**3b**) were prepared using a method derived by Hawker and coworkers.[44] We describe here a two-step synthesis of azidohexyl glycidyl ether (AHGE) as a representative example.

Synthesis of Azidohexyl Glycidyl Ether (AHGE)

*Synthesis of 6-azido-1-hexanol (**3b**).* A 250 mL round bottom flask was charged with 6-chloro-1-hexanol (**3a**) (15.0 g, 109.8 mmol), water (22.0 mL) and sodium azide (10.7 g, 164.7 mmol), then the solution was stirred overnight under reflux condition. The resulting solution was extracted with ethyl

ULSAN NATIONAL INSTITUTE OF SCIENCE AND TECHNOLOGY

acetate and the combined organic layers were washed with brine, dried over Na_2SO_4, and concentrated under reduced pressure to give (**3b**) as a yellowish liquid (15.0 g, 98%). The crude product was used for the next step without further purification. ^{1}H NMR (400 MHz, $CDCl_3$): δ 3.65 (t, J = 6.5 Hz, 2H), 3.27 (t, J = 6.9 Hz, 2H), 1.67 – 1.53 (m, 4H), 1.49 – 1.32 (m, J = 4.6, 3.8, 1.8 Hz, 5H). ^{13}C NMR (101 MHz, $CDCl_3$): δ 62.66, 51.42, 32.56, 28.84, 26.56, 25.38.

Synthesis of AHGE. A 40% solution of aqueous KOH was prepared by dissolving 38.18 g of KOH in 57.27 mL H_2O. Tetrabutylammonium hydrogensulfate ($TBAHSO_4$) (1.17 g, 3.44 mmol) and epichlorohydrin (29.96 mL, 343.85 mmol) were added to the completely dissolved KOH solution at 0 °C. The reaction mixture was stirred for 30 min and **3b** (9.85 g, 68.77 mmol) was added slowly at 0 °C. The reaction was allowed to proceed for 18 h at room temperature and reaction progress was monitored by TLC. The mixture was diluted with water and extracted with ethyl acetate (EtOAc). The organic layers were washed with brine, dried over Na_2SO_4 and evaporated to give a crude liquid. The residue was purified by column chromatography (EtOAc/Hexane, 1/3) to give the desired product as a colorless oil (7.59 g, 55%). The product was further purified by vacuum distillation over CaH_2. ^{1}H NMR (400 MHz, $CDCl_3$): δ 3.72 (dd, J = 11.5, 3.0 Hz, 1H), 3.58 – 3.41 (m, 2H), 3.37 (dd, J = 11.5, 5.8 Hz, 1H), 3.27 (t, J = 6.9 Hz, 2H), 3.19 – 3.08 (m, J = 5.8, 4.1, 2.9 Hz, 1H), 2.80 (dd, J = 5.0, 4.2 Hz, 1H), 2.61 (dd, J = 5.0, 2.7 Hz, 1H), 1.65 – 1.54 (m, 4H), 1.45 – 1.34 (m, 4H). ^{13}C NMR (101 MHz, $CDCl_3$): δ 71.57, 71.45, 51.44, 50.94, 44.32, 29.61, 28.85, 26.61, 25.75. ESI-MS (*m*/*z*): $[M+Na]^+$ calcd for $C_9H_{17}N_3O_2Na$, 222.12; found, 222.04

Synthesis of Azidoethyl Glycidyl Ether (AEGE) and Azidobutyl Glycidyl Ether (ABGE)

Azidoethyl glycidyl ether (AEGE) and azidobutyl glycidyl ether (ABGE) were prepared from 2-bromo-1-ethanol (**1a**) and 4-chloro-1-butanol (**2a**), respectively, by a two-step substitution reaction, as described in the synthesis of AHGE.

*Synthesis of 2-azido-1-ethanol (**1b**).* 2-azido-1-ethanol was prepared by using 2-bromo-1-ethanol (**1a**) as a starting material, according to the same procedure as described in the synthesis of **3b** in 85% yield. ^{1}H NMR (400 MHz, $CDCl_3$): δ 3.78 (dd, *J* = 10.2, 5.5 Hz, 2H), 3.49 – 3.39 (m, 2H), 2.44 (t, *J* = 5.8 Hz, 1H). ^{13}C NMR (101 MHz, $CDCl_3$): δ 61.52, 53.59.

Synthesis of AEGE. AEGE was prepared by using 2-azido-1-ethanol (**1b**) as a starting material, according to the same procedure as described in the synthesis of AHGE in 45% yield. ^{1}H NMR (400 MHz, $CDCl_3$): δ 3.84 (dd, *J* = 11.6, 2.8 Hz, 1H), 3.77 – 3.63 (m, 2H), 3.45 (dd, *J* = 11.6, 5.8 Hz, 1H), 3.41 (t, *J* = 5.0 Hz, 2H), 3.18 (m, 1H), 2.82 (dd, *J* = 5.0, 4.2 Hz, 1H), 2.65 (dd, *J* = 5.0, 2.7 Hz, 1H). ^{13}C NMR (101 MHz, $CDCl_3$): δ 71.90, 70.31, 50.90, 50.88, 44.18. ESI-MS (*m*/*z*): $[M+Na]^+$ calcd for

ULSAN NATIONAL INSTITUTE OF SCIENCE AND TECHNOLOGY

$C_5H_9N_3O_2Na$, 166.06; found, 166.06

*Synthesis of 4-azido-1-butanol (**2b**).* 4-azido-1-butanol was prepared by using distilled 4-chloro-1-ethanol (**2a**) as a starting material, according to the same procedure as described in the synthesis of **3b** in 60% yield. ^{1}H NMR (400 MHz, $CDCl_3$): δ 3.65 (t, J = 6.2 Hz, 2H), 3.32 (t, J = 6.6 Hz, 2H), 2.52 (s, 1H), 1.74 – 1.58 (m, 4H). ^{13}C NMR (101 MHz, $CDCl_3$): δ 62.00, 51.30, 29.73, 25.39.

Synthesis of ABGE. ABGE was prepared by using 4-azido-1-butanol (**2b**) as a starting material, according to the same procedure as described in the synthesis of AHGE in 41% yield. ^{1}H NMR (400 MHz, $CDCl_3$): δ 3.73 (dd, J = 11.5, 2.9 Hz, 1H), 3.59 – 3.45 (m, 2H), 3.36 (dd, J = 11.5, 5.9 Hz, 1H), 3.33 – 3.27 (m, 2H), 3.13 (m, 1H), 2.79 (dd, J = 5.0, 4.2 Hz, 1H), 2.60 (dd, J = 5.1, 2.7 Hz, 1H), 1.75 – 1.60 (m, 4H). ^{13}C NMR (101 MHz, $CDCl_3$): δ 71.45, 70.69, 51.21, 50.77, 44.09, 26.81, 25.68. ESI-MS (m/z): $[M+Na]^+$ calcd for $C_7H_{13}N_3O_2Na$, 194.09; found, 194.16

Homopolymerization of Azidoalkyl Glycidyl Ethers

The syntheses of all the homopolymers (**E1** – **E3**, **B1** – **B3**, and **H1** – **H4**) were carried out by Schlenk technique under Ar in flame-dried glass tubes. An exemplary synthetic protocol is described as follows.

*Homopolymerization of AHGE (Table 4.1, **H2**).* *t*-BuP_4 (0.8 M in hexane, 125.5 μL, 0.1 mmol) was added to a solution of benzyl alcohol (10.39 μL, 0.1 mmol) in toluene (0.6 mL) and stirred for 30 min. AHGE (500 mg, 2.51 mmol) was then slowly added to the solution to initiate the polymerization. The reaction was monitored by ^{1}H NMR to determine residual epoxide signals and if the reaction was complete. When reaction completion was determined, an excess amount of benzoic acid was added to terminate the polymerization. The mixture was passed through a basic alumina pad using THF to remove *t*-BuP_4. The polymer solution was concentrated in vacuo to obtain poly(azidohexyl glycidyl ether), P(AHGE) (312 mg, 61%). ^{1}H NMR (**H2**) (400 MHz, $CDCl_3$): δ 7.37 – 7.33 (m, 5H), 4.56 (s, 2H), 3.70 – 3.38 (m, 161H), 3.28 (t, J = 6.9 Hz, 46H), 1.69 – 1.50 (m, 92H), 1.47 – 1.34 (m, 92H). ^{13}C NMR (**H2**) (101 MHz, $CDCl_3$): δ 79.08, 78.96, 78.82, 71.49, 71.10, 70.25, 70.01, 51.51, 29.76, 29.74, 28.97, 26.75, 25.90. *Đ* (**H2**) (SEC, $CHCl_3$, PMMA standard) = 1.15

*Homopolymerization of AEGE (Table 4.1, **E2**).* *t*-BuP_4 (0.8 M in hexane, 104.7 μL, 0.08 mmol) was added to a solution of benzyl alcohol (8.68 μL, 0.08 mmol) in toluene (0.84 mL) and stirred for 30 min. AEGE (300 mg, 2.1 mmol) was then slowly added to the solution to initiate the polymerization. The reaction was monitored by ^{1}H NMR to determine residual epoxide signals and if the reaction was complete. When reaction completion was determined, an excess amount of benzoic acid was added to terminate the polymerization. The mixture was passed through a basic alumina pad using THF to

ULSAN NATIONAL INSTITUTE OF SCIENCE AND TECHNOLOGY

remove *t*-BuP$_4$. The polymer solution was concentrated in vacuo to obtain poly(azidoethyl glycidyl ether), P(AEGE) (189 mg, 64%). ^{1}H NMR (**E2**) (400 MHz, $CDCl_3$): δ 7.39 – 7.28 (m, 5H), 4.54 (s, 2H), 3.78 – 3.49 (m, 175H), 3.42 – 3.29 (m, 25H). *Đ* (**E2**) (SEC, THF, PMMA standard) = 1.15

*Homopolymerization of ABGE (Table 4.1, **B2**).* *t*-BuP$_4$ (0.8 M in hexane, 73.01 μL, 0.06 mmol) was added to a solution of benzyl alcohol (6.04 μL, 0.06 mmol) in toluene (1.2 mL) and stirred for 30 min. ABGE (500 mg, 2.92 mmol) was then slowly added to the solution to initiate the polymerization. The reaction was monitored by ^{1}H NMR to determine residual epoxide signals and if the reaction was complete. When reaction completion was determined, an excess amount of benzoic acid was added to terminate the polymerization. The mixture was passed through a basic alumina pad using THF to remove *t*-BuP$_4$. The polymer solution was concentrated in vacuo to obtain poly(azidobutyl glycidyl ether), P(ABGE) (403 mg, 68%). ^{1}H NMR (**B2**) (400 MHz, $CDCl_3$): δ 4.54 (s, 2H), 3.68 – 3.39 (m, 399H), 3.30 (t, *J* = 6.4 Hz, 114H), 1.72 – 1.61 (m, 228H). *Đ* (**B2**) (SEC, THF, PMMA standard) = 1.09

Azide Stability Test

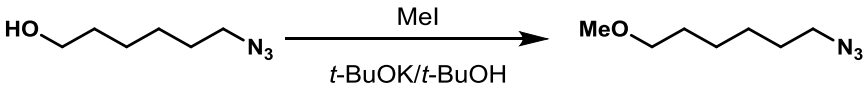

Preparation of 1-azido-6-methoxyhexane is described as follows. To a solution of potassium tert-butoxide (0.94 g, 8.38 mmol) dissolved in 30.0 mL of tert-butanol was added 6-azido-1-hexanol (1.0 g, 6.98 mmol). After the mixture was stirred for 30 min, methyl iodide (1.19 g, 8.38 mmol) was slowly added. The reaction was maintained for 24 h at room temperature, then the mixture was quenched by water and the aqueous phase was extracted with dichloromethane. The organic layers were washed with brine, dried over Na_2SO_4 and the solvent was evaporated. The crude liquid was purified by column chromatography (ethyl acetate/hexane 1:2) to yield 0.45 g (41%) of 1-azido-6-methoxyhexane. ^{1}H NMR (400 MHz, $CDCl_3$): δ 3.37 (t, J = 6.5 Hz, 2H), 3.33 (s, 3H), 3.27 (t, J = 6.9 Hz, 2H), 1.66 – 1.52 (m, 4H), 1.47 – 1.31 (m, 4H).

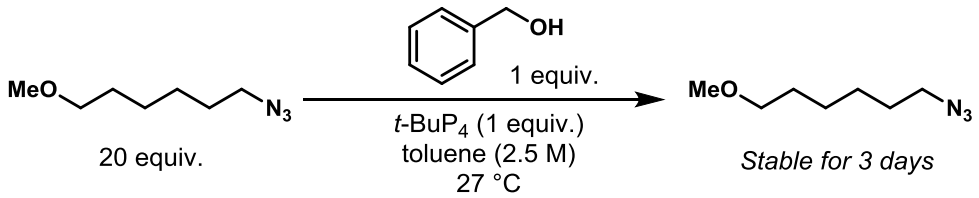

Procedure: In a 20 mL dried reaction vial, *t*-BuP$_4$ (40.0 μL, 0.032 mmol) was added to a solution of benzyl alcohol (3.35 μL, 0.032 mmol) and 1-azido-6-methoxyhexane (100 mg, 0.64 mmol) in toluene (0.3 mL) and stirred for 3 days at room temperature. Aliquots were drawn after 6 h, 1, and 3

ULSAN NATIONAL INSTITUTE OF SCIENCE AND TECHNOLOGY

days and analyzed by ^{1}H NMR.

In situ ^{1}H NMR Polymerization Kinetics Experiments

A mixture of benzyl alcohol (1.0 eq) and monomer (20 eq) in toluene-d_8 (1.0 M to the monomer) was transferred by a syringe to a conventional NMR tube sealed with a rubber septum. To the NMR tube was added *t*-BuP$_4$ (1.0 eq) and it was shaken to homogenize the mixture before placing in the NMR spectrometer. The sample temperature was set to 27 °C and spectra were recorded every 10 min with 16 scans for 4 or 5 hours. The integrals of methylene protons of monomer (δ = 2.28 and 2.15 for AEGE, δ = 2.31 and 2.16 for ABGE and δ = 2.32 and 2.18 for AHGE) were monitored to calculate monomer consumption, referenced to the residual signal of toluene (δ = 2.09 ppm).

Procedures for CuAAC Click Reactions

Click reaction for **H3a**, **H3b** and **H3c** proceeded using a method derived by Hawker and coworkers.[29] A typical procedure for the click reaction for **H3a** is as follows: **H3** (80 mg, 0.39 mmol of azides, 1.0 eq) and 5-hexyne (67.8 μL, 0.59 mmol, 1.5 eq) were dissolved in 3 mL of THF in a 20 mL reaction tube. The solution was degassed by N_2 bubbling for 30 min. CuBr (5.59 mg, 0.039 mmol, 0.10 eq) and *N*,*N*,*N'*,*N''*,*N''*-pentamethyldiethylenetriamine (PMDETA) (8.14 μL, 0.039 mmol, 0.10 eq) were added to the mixture and the solution was stirred for 2 h at room temperature. Saturated ammonium chloride aqueous solution (10 mL) was added to the solution, then the solution was extracted with dichloromethane (10 mL x 3). The organic layer was washed with brine, dried over Na_2SO_4, and concentrated under vacuum to yield 108 mg (99%) of a yellow polymer.

Procedures for Staudinger Reduction

Staudinger reductions for **H2a - H2c** and **HAm** proceeded using a method derived by Johnsson and coworkers.[45] A typical procedure for the Staudinger reduction for **H2a** is as follows: **H2** (100 mg, 0.49 mmol of azide, 1.0 eq) was dissolved in 1 mL of THF and the solution was degassed by N_2 bubbling for 20 min. PPh_3 (32.26 mg, 0.123 mmol, 0.25 eq) was completely dissolved in the solution. Water (0.05 mL) was added to the mixture and stirred 12 h at room temperature. THF was removed under reduced pressure and 1.0 M HCl solution was added to acidify and dissolve the polymer. The mixture was washed 3 times with diethyl ether to remove residual triphenylphosphine (TPP) and triphenylphosphine oxide (TPPO). The aqueous phase was lyophilized to give 80 mg of a viscous polymer.

ULSAN NATIONAL INSTITUTE OF SCIENCE AND TECHNOLOGY

Chain Extension Experiment for Diblock Copolymer Synthesis

The synthesis of the diblock copolymer of AHGE and AGE was carried out by Schlenk technique under Ar in flame-dried glass tubes. *t*-BuP_4 (0.8 M in hexane, 125.5 μL, 0.1 mmol) was added to a solution of benzyl alcohol (10.39 μL, 0.1 mmol) in toluene (1.0 mL) and stirred for 30 min. AHGE (600 mg, 3.0 mmol) was then slowly added to the solution to initiate the polymerization. The reaction was monitored by ^{1}H NMR spectroscopy to determine residual epoxide signals and once the reaction was completed, a small aliquot of the crude P(AHGE) polymer was taken for SEC analysis. Additional allyl glycidyl ether (AGE) (343.5 mg, 3.01 mmol) was added to the reaction mixture and the reaction was monitored by ^{1}H NMR to determine residual epoxide signals. When the reaction was determined to be complete, an excess amount of benzoic acid was added to terminate the polymerization. The mixture was passed through a basic alumina pad using THF to remove *t*-BuP_4. The polymer solution was concentrated in vacuo to obtain P(AHGE)-*b*-P(AGE) (480 mg). A small aliquot of the crude block copolymer was taken for NMR and SEC analysis to determine the degree of polymerization of each monomer ($M_{n,NMR}$: 10360, M_w/M_n: 1.09, DP_{NMR}: AHGE/AGE=32/34).

Copolymerization of AHGE and AGE

The synthesis of a statistical copolymer of AHGE and AGE was carried out by Schlenk technique under Ar in flame-dried glass tubes. *t*-BuP_4 (0.8 M in hexane, 375 μL, 0.3 mmol) was added to a solution of benzyl alcohol (31 μL, 0.3 mmol) in toluene (2.4 mL) and stirred for 30 min. A pre-mixed liquid of AHGE (600 mg, 3.0 mmol) and AGE (342 mg, 3.0 mmol) was then slowly added to the solution to initiate the polymerization. The reaction was monitored by ^{1}H NMR to determine residual epoxide signals. When the reaction was determined to be complete, an excess amount of benzoic acid was added to terminate the polymerization. The mixture was passed through a basic alumina pad using THF to remove *t*-BuP_4. The polymer solution was concentrated in vacuo to obtain P(AHGE-*co*-AGE) (630 mg). The degree of polymerization of each monomer was determined by ^{1}H NMR analysis ($M_{n,NMR}$: 3330, M_w/M_n: 1.10, DP_{NMR}: AHGE/AGE=11/9).

Copolymerization Kinetics of AHGE and AGE

A mixture of benzyl alcohol (1.0 eq), AHGE and AGE (20 eq. each) in toluene-d_8 (2.5 M to the total amount of monomers) was transferred by a syringe to a conventional NMR tube sealed with a rubber septum. To the NMR tube was added *t*-BuP_4 (1.0 eq) and it was shaken to homogenize the mixture before placing in the NMR spectrometer. The sample temperature was set to 27 °C and the first

ULSAN NATIONAL INSTITUTE OF SCIENCE AND TECHNOLOGY

spectrum was recorded 21 min after *t*-BuP_4 was added and continuously recorded every 16 min with 256 scans for 6 hours by inverse gated ^{13}C mode. The integrals of methine carbon of each monomer (δ = 50.77 for AHGE, and δ = 50.64 for AGE) were monitored to calculate monomer conversion, referenced to the residual signal of toluene (δ = 20.40 ppm).

Orthogonal Functionalization of P(AHGE-co-AGE)

*CuAAC of azide moieties with phenylacetylene (**H5**)*. The CuAAC of P(AHGE-*co*-AGE) was performed by using CuBr and PMDETA in THF as described above for **H3b**. P(AHGE-*co*-AGE) (50 mg, 0.16 mmol of azide, 1.0 eq) and phenylacetylene (26.3 μL, 0.24 mmol, 1.5 eq) were dissolved in 1.5 mL of THF in a 10 mL reaction tube. The solution was degassed by N_2 bubbling for 30 min. CuBr (2.3 mg, 0.016 mmol, 0.10 eq) and PMDETA (3.3 μL, 0.016 mmol, 0.10 eq) were added to the mixture and the solution was stirred for 2 h at room temperature. An aqueous solution of saturated ammonium chloride (8 mL) was added to the solution and the resulting mixture was extracted with dichloromethane (10 mL x 3). The organic layer was washed with brine, dried over Na_2SO_4 and concentrated under vacuum to yield 70 mg of a yellow polymer.

*Thiol-ene addition of allyl moieties with thioacetic acid (**H6**).* Thiol-ene addition of **H5** by using thioacetic acid and 2,2-dimethoxy-2-phenylacetophenone (DMPA) under UV irradiation to give **H6** was proceeded using a method derived by Hawker and coworkers.[34] **H5** (30 mg, 86 μmol of alkene, 1.0 eq), thioacetic acid (12.3 μL, 4.3 μmol, 0.05 eq) and DMPA (1.1 mg, 172 μmol, 2.0 eq) were dissolved in 1.0 mL of THF in a 10 mL reaction tube. The solution was degassed by N_2 bubbling for 30 min. The reaction mixture was stirred under UV light (λ = 365 nm) for 4 h. The reaction was monitored by ^1H NMR to determine the complete disappearance of the alkene peaks at 5.22 and 5.91 ppm. The reaction mixture was precipitated in hexane and recovered by dissolving in chloroform. The organic layer was concentrated under vacuum to yield 25 mg of a dark yellow polymer.

ULSAN NATIONAL INSTITUTE OF SCIENCE AND TECHNOLOGY

4.4 Results and Discussion

Design and Synthesis of Azide-Functionalized Glycidyl Ethers

The simplest glycidyl monomer containing azide functionality for the synthesis of polyethers with multiple azides is glycidyl azide (GA). Initially, we prepared GA as a monomer to demonstrate the versatility of azide-functional polyethers. However, the direct polymerization of simple glycidyl azide under organic superbase-catalyzed highly basic AROP condition was found to suffer from side reactions, such as elimination, in agreement with the previous report (Figure 4.2a and Figure 4.3).[46] In this regard, the synthesis of azide-functionalized polyethers has been achieved by the post-polymerization of polyepichlorohydrin that can be converted to the poly(glycidyl azide).[22] Feng *et al*. recently introduced the direct polymerization of glycidyl azide under monomer-activated AROP condition only in the presence of an excess amount of triethyl borane.[47] In general, the hydrogens on the β-carbon of the epoxide monomer exhibit a different acidic character in relation to the type of the substituents. Thus, we designed several azide-functional glycidyl ether monomers possessing different lengths of alkyl spacers to avoid such side reactions wherein the alkyl chain and ether linkage reduce the acidity of the β-protons (Figure 4.2b).

The AEGE, ABGE and AHGE monomers were prepared by a two-step reaction from corresponding haloalkanols (Figure 4.4). The substitution reaction of haloalkanol with sodium azide under aqueous conditions yielded the azide-functionalized alcohol, which was subsequently coupled with epichlorohydrin to afford AEGE, ABGE, and AHGE after column chromatography purification. Various characterizations including ^{1}H and ^{13}C NMR, ^{1}H–^{1}H correlation spectroscopy (COSY), and ESI-MS supported the successful synthesis of azidoalkyl glycidyl ethers (Figures 4.5 – 4.21).

Polymerization of Azidoalkyl Glycidyl Ethers

Organic superbase *t*-BuP_4-catalyzed AROP of AEGE, ABGE, and AHGE were conducted using benzyl alcohol as an initiator in toluene at room temperature (Table 4.1). We employed a commercially available metal-free organic phosphazene as a base due to its high basicity and, most importantly, its facile polymerization at room temperature.[48] For AHGE, monomer conversion was monitored by ^{1}H NMR spectroscopy by observing the reduction of methine and methylene signals of the epoxides at 3.15, 2.80, and 2.60 ppm (Figure 4.22a). The AROP of AHGE (**H4**) proceeded successfully, achieving 99% conversion within 10 h. When the monomer was completely consumed, as evidenced by ^{1}H NMR, the polymerization was quenched by the addition of benzoic acid to protonate the chain end. Filtration through a short pad of basic aluminum oxide was used to remove phosphazene salts. Successful removal of *t*-BuP_4 was confirmed by completely disappeared ^{1}H NMR signals at 2.66

ULSAN NATIONAL INSTITUTE OF SCIENCE AND TECHNOLOGY

ppm (Figure 4.22b and Figure 4.23). According to ^{1}H NMR and FT-IR analysis, the azide groups remained intact after polymerization (Figure 4.24). Following this result, we evaluated the stability of azide group under the polymerization condition. We first prepared a model compound, 1-azido-6-methoxyhexane, to exclude ring-opening of epoxide by nucleophilic attack from alkoxide species. Surprisingly, treatment of 1-azido-6-methoxyhexane (20 eq) with *t*-BuP_4 (1.0 eq) in the presence of benzyl alcohol (1.0 eq) in toluene at room temperature did not result in any changes in the model compound for 3 days (Figure 4.25 and Table 4.2). The inertness of the azide group under AROP condition highlights the compatibility of azidoalkyl glycidyl ether monomers and thus provides potential to expand the functional polyether platform by attachment of azide moieties in the designer monomer. We also conducted AROP of AEGE and ABGE under identical reaction conditions and the resulting polymers were characterized by ^{1}H NMR analysis (Figures 4.26 and 4.27). The molecular weights of the homopolymers of AEGE, ABGE, and AHGE (**E1** – **E3**, **B1** – **B3**, and **H1 – H4**) were well-controlled in the range of 2300 – 17400 g/mol by adjusting the ratio of monomer to initiator as verified by ^{1}H NMR spectroscopy (Table 4.1 and Figure 4.28). Moreover, the azide-functionalized homopolymers exhibited a narrow dispersity (*Đ*) ranging from 1.03 to 1.21, as confirmed by size exclusion chromatography (SEC) (Table 4.1 and Figure 4.28). The small shoulder peak observed in the higher molecular weight region possibly originates from chain transfer reactions during anionic polymerization.[47] In general, AROP of certain glycidyl ether monomers is accompanied by a chain transfer reaction due to the abstraction of methylene proton adjacent to the epoxide ring by active propagating chain end, leading to the formation of allyl alkoxide which act as new initiating species. It has already been discussed in previous literatures for the polymerization of phenyl glycidyl ether, propylene oxide, and ethoxy ethyl glycidyl ether.[49,50] Furthermore, monomer purity is a critical consideration in chain transfer reaction as reported by Lynd *et al*.[33]

in situ ^{1}H NMR Polymerization Kinetics Study

The homopolymerizations of AEGE, ABGE, and AHGE were investigated by *in situ* ^{1}H NMR kinetics studies to evaluate the living characteristics and the effect of monomer structure. The polymerizations were conducted at monomer concentration of 1.0 M in deuterated toluene. The signals of methylene protons of the monomers (highlighted in Figures 4.29 – 4.31) were monitored to observe monomer conversion by calculating integration value in reference to the residual signal of toluene (δ = 2.09 ppm), which remained constant during polymerization. The linear correlation between $\ln([M]_0/[M]_t)$ and reaction time supported the successful living characteristics of the polymerization of azidoalkyl glycidyl ethers (Figure 4.32). Interestingly, the kinetic plots obtained by different monomers indicated the increasing order of AHGE, ABGE, and AEGE for the polymerization rate. As the only difference between monomers is the length of alkyl spacer, thus the faster polymerization rate of AEGE can be

ULSAN NATIONAL INSTITUTE OF SCIENCE AND TECHNOLOGY

attributed to the shorter alkyl spacer and larger polarity among three monomers. On the other hand, the longer AHGE monomer showed a lower polymerization rate possibly due to the steric effect of alkyl chain that might disturb the propagating chain end. Moreover, to explore a correlation between monomer hydrophobicity and polymerization rate, we calculated the octanol/water coefficient (log *P*) of the monomers using the computational software ALOGPS 2.1 (Table 4.3).[51,52] The hydrophobicity increased as the length of alkyl spacer increased as expected. Coincidentally, we found that the polymerization rate is inversely proportional to the hydrophobicity of monomer (Figure 4.33).

Copper-Catalyzed Azide-Alkyne Cycloaddition of P(AHGE)

Having synthesized the desired P(AHGE) homopolymers, the potential post-polymerization modification of the pendant azide moieties via CuAAC was demonstrated by reaction with 1-hexyne, phenylacetylene, and 5-hexyn-1-ol to give the functional polyethers **H3a**, **H3b**, and **H3c**, respectively (Figure 4.34). ^{1}H NMR confirmed the successful transformation of pendant azide groups into alkyl, phenyl, and hydroxyl functionalities (Figure 4.34a-c). The protons adjacent to the azide, corresponding to the peak at 3.26 ppm (Figure 4.22b, peak *f'*), clearly disappeared, whereas the peak around 4.30 ppm (Figure 4.34, peak *a'*) appeared after CuAAC, due to the inductive electron-withdrawing character of triazole.[53] The characteristic peak of the triazole proton (Figure 4.34, peak *b*) was observed, presenting a clear evidence supporting the successful formation of the triazole group by CuAAC. To further confirm the successful click reaction, FT-IR analysis was conducted (Figure 4.35). The FT-IR spectra revealed that the characteristic azide peak at 2088 cm^{-1} for **H3** clearly disappeared after the click reactions, in accordance with the ^{1}H NMR analysis.

Staudinger Reduction of P(AHGE)

Investigations of the synthesis of the polyethers having pendant primary amine groups along the polymer backbones are limited. Satoh and coworkers demonstrated the synthesis of primary amine-functionalized polyether by *t*-BuP$_4$-catalyzed AROP of dibenzyl protected monomer, followed by subsequent hydrogenation.[54] Frey *et al.* reported polymerization by monomer activation of epicyanohydrin that can convert to amine-functional PEG.[23] However, the drawback of both approaches is a time-consuming deprotection step after polymerization. Alternatively, the Staudinger reduction of azide-functional polyethers can yield pendant amines from the presented azides in this study. We demonstrated Staudinger reduction of **H2** as a representative example (Figure 4.36). The reaction of **H2** with triphenylphosphine (TPP) and water in THF under ambient conditions resulted in the successfully reduced product, **HAm**, within 12 h. Moreover, the degree of reduction was controlled by the

ULSAN NATIONAL INSTITUTE OF SCIENCE AND TECHNOLOGY

equivalency of TPP used during the reduction to afford polyethers with varying ratios of amine relative to azide, yielding orthogonal pendant groups for post-polymerization modification (**H2a** – **H2c**). As the equivalency of TPP was increased, the reduced amine to unreacted azide ratio also increased, correlating well to the relative peak integrations determined by ^{1}H NMR (Figure 4.36a and Figures 4.37 – 4.40). FT-IR analyses displayed the disappearance of the characteristic azide peak at 2088 cm^{-1}, providing further evidence supporting the successful reduction (Figure 4.36b).

Copolymerization of AHGE and AGE

As previously mentioned, AGE is by far the most widely used functional epoxide monomer for post-polymerization modification in polyethers. Thus, we demonstrated the copolymerization of AHGE with AGE to impart a second orthogonal functionality to facilitate further modification. First, the one-pot sequential addition of AGE after the polymerization of P(AHGE) was performed to obtain P(AHGE)-*b*-P(AGE) (Figure 4.41). The complete shift of the SEC traces to the higher molecular weight diblock copolymer P(AHGE)-*b*-P(AGE) was observed, without the presence of the unreacted chain end of P(AHGE) (Figure 4.42). This observation supports the livingness of the propagating chain end of P(AHGE)s.

Furthermore, a well-defined statistical copolymer, P(AHGE-*co*-AGE), was prepared by taking advantage of the living character of AROP with the use of two monomers in a one-pot reaction (Figure 4.41). The molecular weight and degree of polymerization of each monomer representative by SEC and ^{1}H NMR (Figures 4.41b and 4.43). As shown in Figure 4.43, the characteristic allyl peaks at 5.22 and 5.91 ppm (peaks *b* and *c*) were observed along with the peak corresponding to the proton adjacent to the azide (peak *a*), indicating successful incorporation of both monomers. Allyl groups often show a tendency towards isomerization under potassium alkoxide base-catalyzed polymerization conditions at high temperature,[28] however, no isomerized alkenes were observed under the organic superbase-catalyzed AROP conditions due to the relatively low reaction temperature. The polymerization of both block and statistical copolymers were conducted in a controlled manner, exhibiting minor deviations from the targeted monomer ratio (Table 4.4).

To determine the reactivity ratios of AHGE and AGE, we monitored the copolymerization using *in situ* ^{13}C NMR spectroscopy with inverse-gated decoupling. The copolymerization of AHGE and AGE at a total concentration of 2.5 M in toluene-d_8 was performed in the NMR tube at 27 °C. Both monomer conversions and total conversion as a function of time were measured and the reactivity ratios of AHGE and AGE were obtained based on the nonterminal model developed by Lynd and coworkers.[55] The methine peaks of AHGE (peak *a*, 50.77 ppm) and AGE (peak *b*, 50.64 ppm) were integrated to calculate the monomer conversion using toluene peak (20.40 ppm) as an internal standard (Figure 4.42).

ULSAN NATIONAL INSTITUTE OF SCIENCE AND TECHNOLOGY

The plot of total conversion against monomer conversion was presented to determine reactivity ratios for the pair of monomers: $r_{AHGE} = 0.77 \pm 0.01$ and $r_{AGE} = 1.31 \pm 0.02$ (Figure 4.42b). As shown in Figure 4.42b, the copolymerization of AHGE and AGE tends to yield random microstructure ($r_{PGE} \times r_{AGE} = 1.01 \pm 0.02$) of resulting copolymer. The slightly lower reactivity of AHGE compared to AGE possibly originated from the steric effect of the longer alkyl chain.

Orthogonal Modification of P(AHGE-co-AGE)

Finally, we demonstrated two selective sequential reactions utilizing the orthogonal azide and allyl functionalities of the copolymer. Using the conditions, we established for the CuAAC of P(AHGE), the copolymer was first derivatized via click reaction with phenylacetylene and then was subsequently modified by thiol–ene addition (Figure 4.44). ^{1}H NMR spectroscopy was used to verify the success of the CuAAC reaction by observing the large downshift of the peak corresponding to the methylene unit adjacent to the azide from 3.26 to 4.3 ppm (Figure 4.44a, peaks *a* and *a'*). The characteristic peaks corresponding to the allyl group (Figure 4.44a, peaks *b*–*d*) were not shifted, suggesting that the orthogonality of CuAAC leaves the allyl groups intact for subsequent modification by thiol–ene addition. To modify the allyl moieties, thiol–ene addition, using thioacetic acid and photoinitiator, proceeded in THF under UV-irradiation. ^{1}H NMR observation of the complete disappearance of the signals corresponding to the allyl group and the appearance of the new signal at 2.29 ppm (peak *f*) corresponding to the methyl group of the thioester confirmed the successful functionalization of the allyl groups.

FT-IR analysis indicated the smooth progress of the sequential reactions, evidenced by the disappearance of the band corresponding to the azide (2088 cm^{-1}) and the appearance of a new band at 1691 cm^{-1} corresponding to the thioester group (Figure 4.44b). These results suggested that azide and alkene can be orthogonally functionalized without any cross-reactivity. There are many reports demonstrating multifunctional polyethers,[19] however, synthesis and post-polymerization modification of polyethers with both azide and alkene pendant groups along the polymer backbone has not been introduced to date. These systems present a unique avenue for orthogonal post-polymerization modification, which is the subject of our ongoing research endeavor.

ULSAN NATIONAL INSTITUTE OF SCIENCE AND TECHNOLOGY

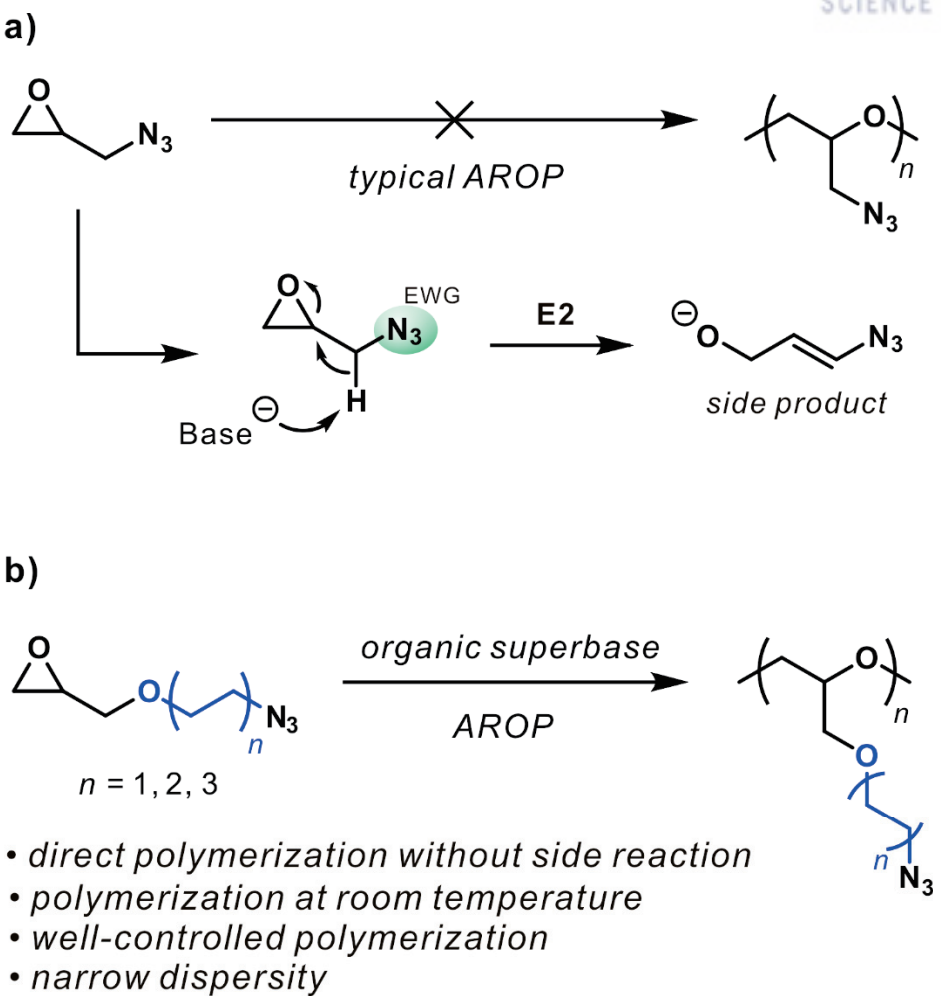

Figure 4.2. (a) Typical anionic ring-opening polymerization of glycidyl azide suffers from elimination side product. (b) Direct synthesis of azide-functionalized polyethers using a series of azidoalkyl glycidyl ethers.

ULSAN NATIONAL INSTITUTE OF SCIENCE AND TECHNOLOGY

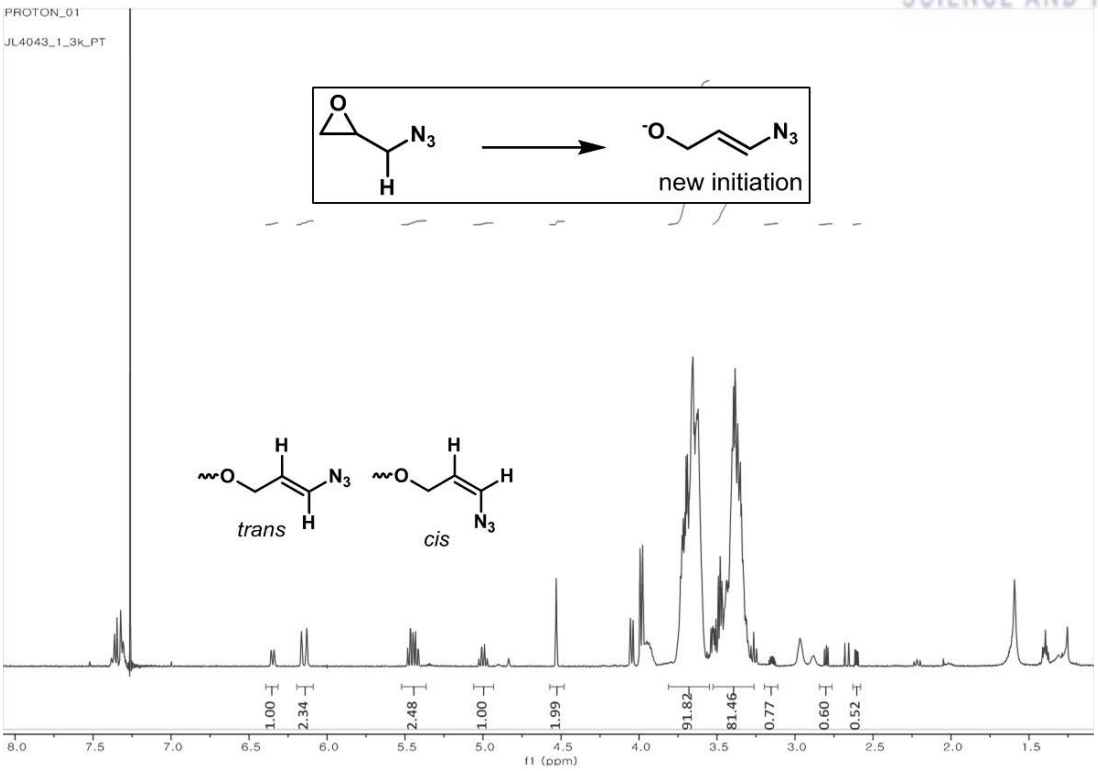

Figure 4.3. ^{1}H NMR spectrum of the polymerization of GA. The presence of olefinic protons around 5.0 – 6.5 ppm indicates that undesired elimination reaction of GA occurred.

ULSAN NATIONAL INSTITUTE OF SCIENCE AND TECHNOLOGY

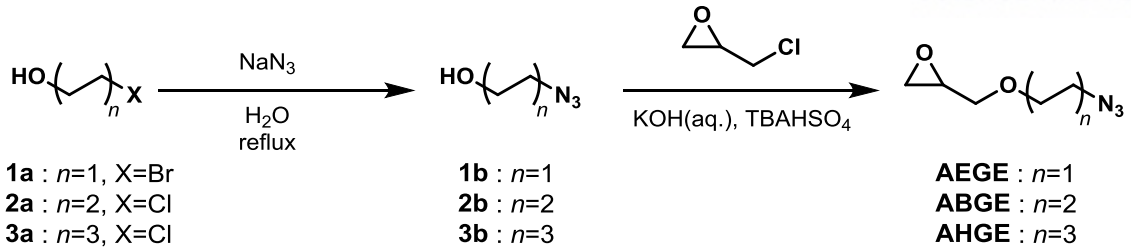

1a : *n*=1, X=Br
2a : *n*=2, X=Cl
3a : *n*=3, X=Cl

1b : *n*=1
2b : *n*=2
3b : *n*=3

AEGE : *n*=1
ABGE : *n*=2
AHGE : *n*=3

Figure 4.4. Synthesis of azidoalkyl glycidyl ether monomers

ULSAN NATIONAL INSTITUTE OF SCIENCE AND TECHNOLOGY

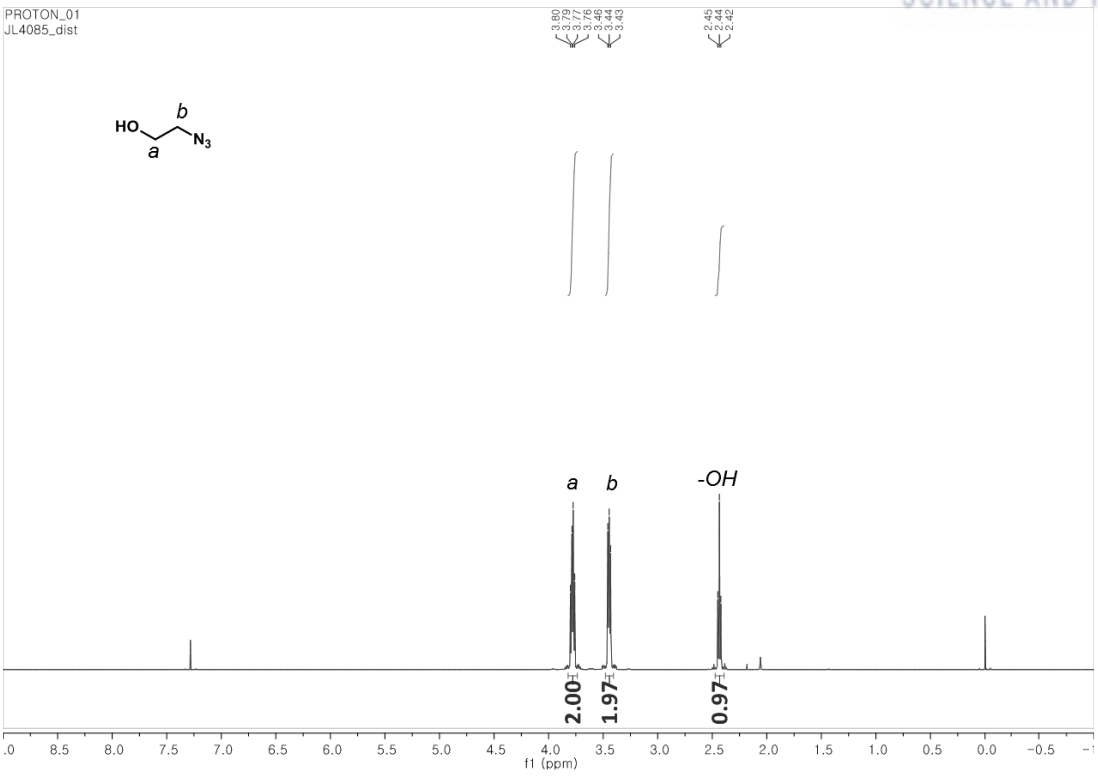

Figure 4.5. ^{1}H NMR spectrum of 2-azido-1-ethanol (**1b**) (400 MHz, $CDCl_3$, 298K)

ULSAN NATIONAL INSTITUTE OF SCIENCE AND TECHNOLOGY

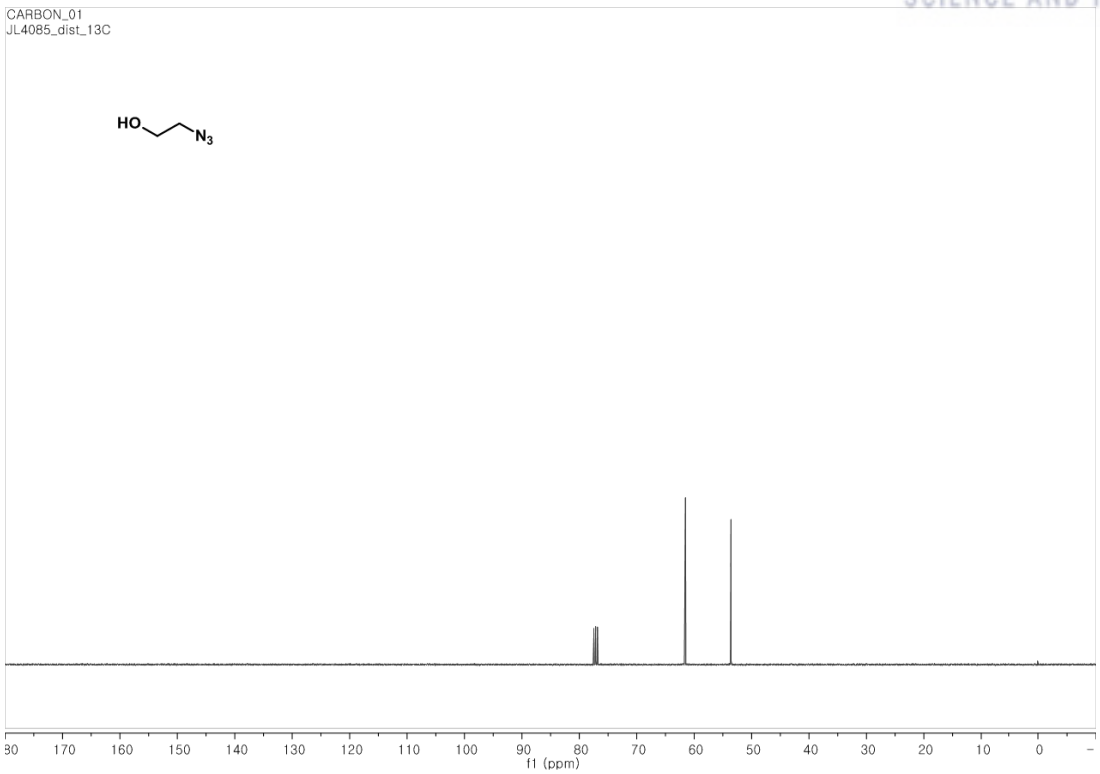

Figure 4.6. ^{13}C NMR spectrum of 2-azido-1-ethanol (**1b**) (101 MHz, $CDCl_3$, 298K)

ULSAN NATIONAL INSTITUTE OF SCIENCE AND TECHNOLOGY

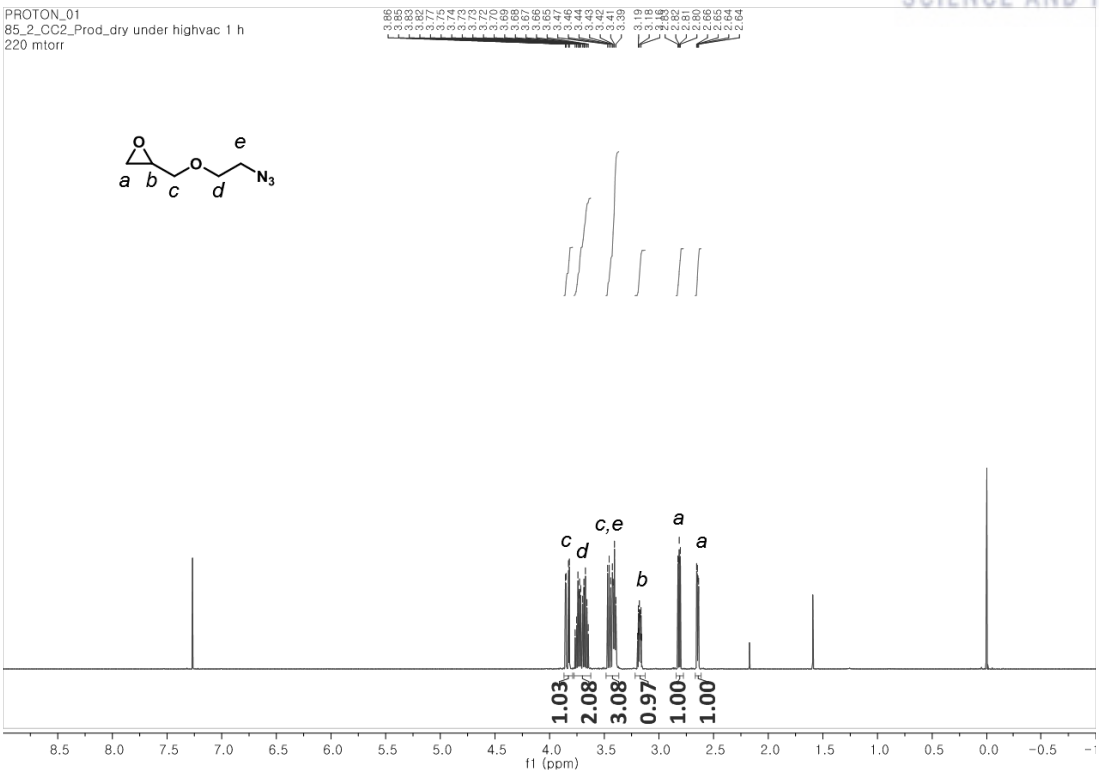

Figure 4.7. ^{1}H NMR spectrum of **AEGE** (400 MHz, $CDCl_3$, 298K).

ULSAN NATIONAL INSTITUTE OF SCIENCE AND TECHNOLOGY

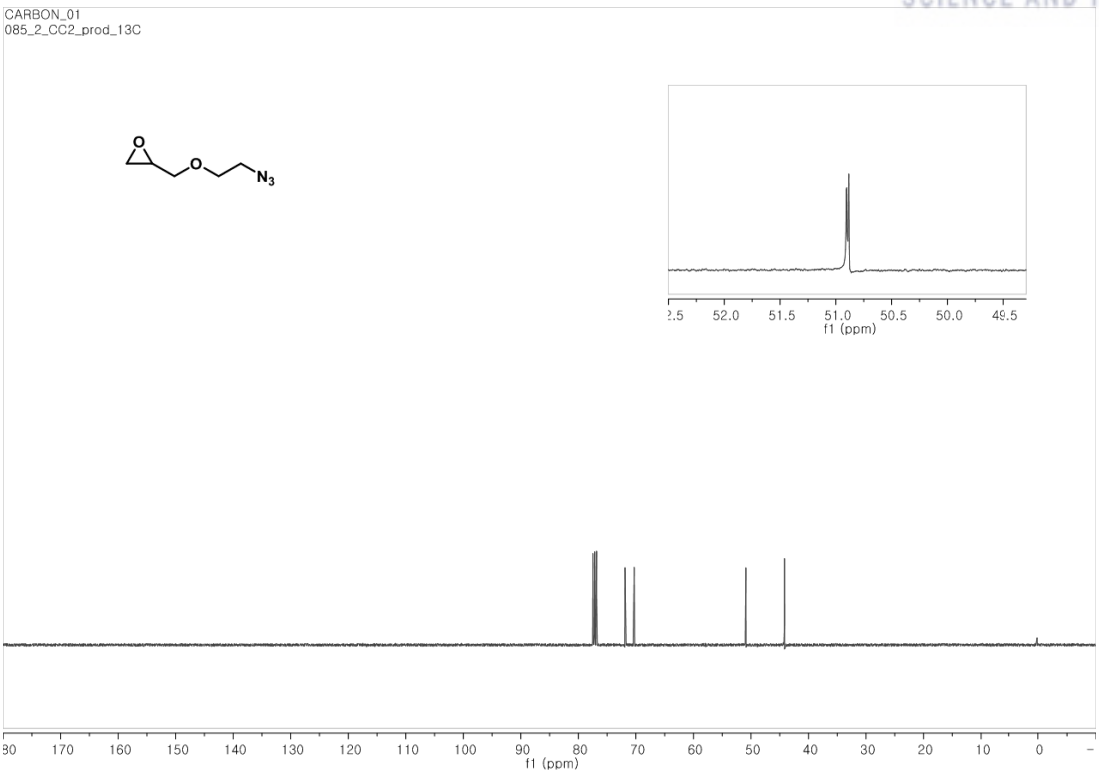

Figure 4.8. ^{13}C NMR spectrum of **AEGE** (101 MHz, $CDCl_3$, 298K).

ULSAN NATIONAL INSTITUTE OF SCIENCE AND TECHNOLOGY

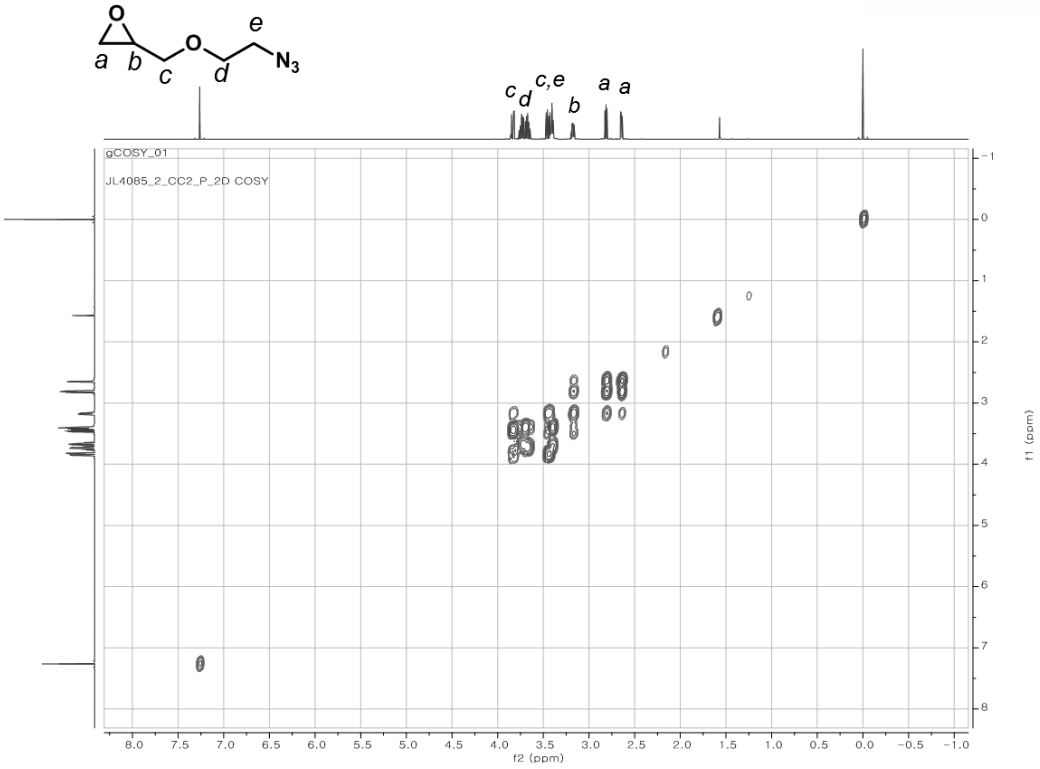

Figure 4.9. ^{1}H-^{1}H COSY NMR spectrum of **AEGE** in $CDCl_3$.

ULSAN NATIONAL INSTITUTE OF
SCIENCE AND TECHNOLOGY

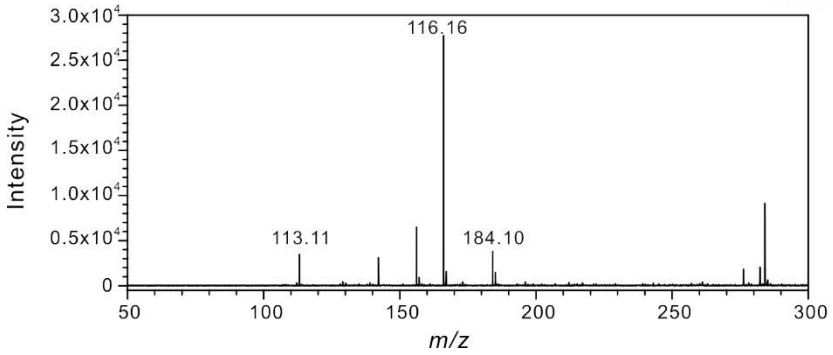

Figure 4.10. ESI-MS spectrum of **AEGE**.

ULSAN NATIONAL INSTITUTE OF SCIENCE AND TECHNOLOGY

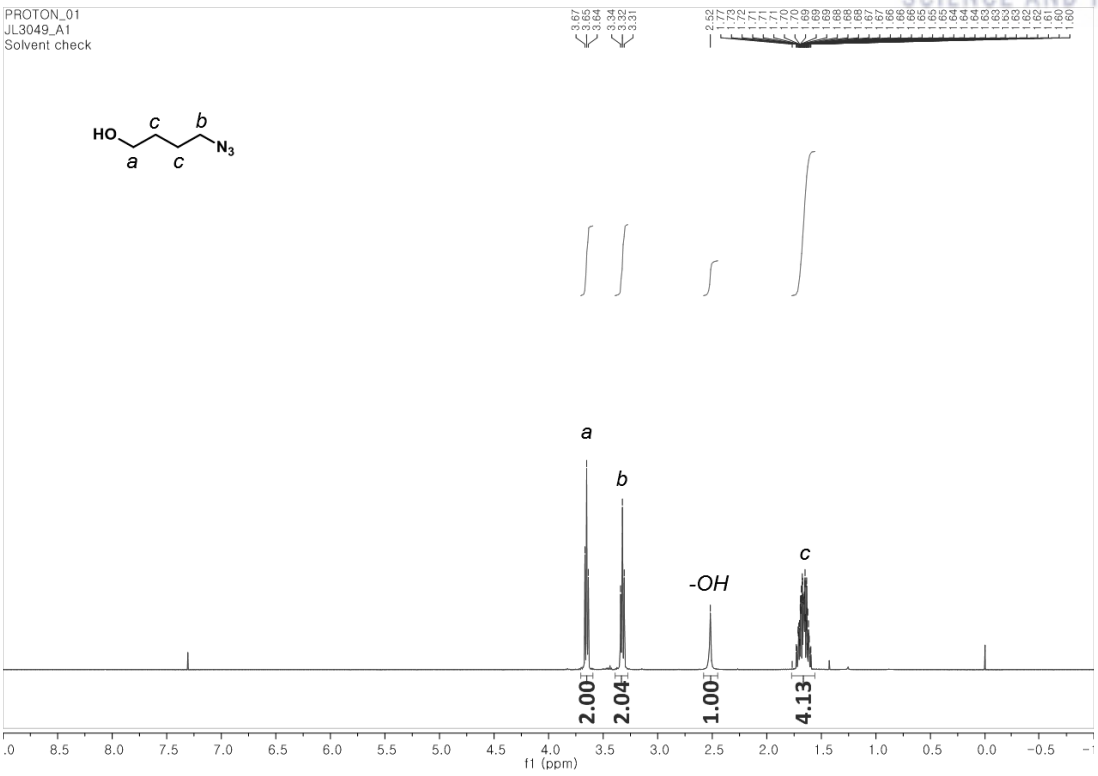

Figure 4.11. ^{1}H NMR spectrum of 4-azido-1-butanol (**2b**) (400 MHz, $CDCl_3$, 298K).

ULSAN NATIONAL INSTITUTE OF SCIENCE AND TECHNOLOGY

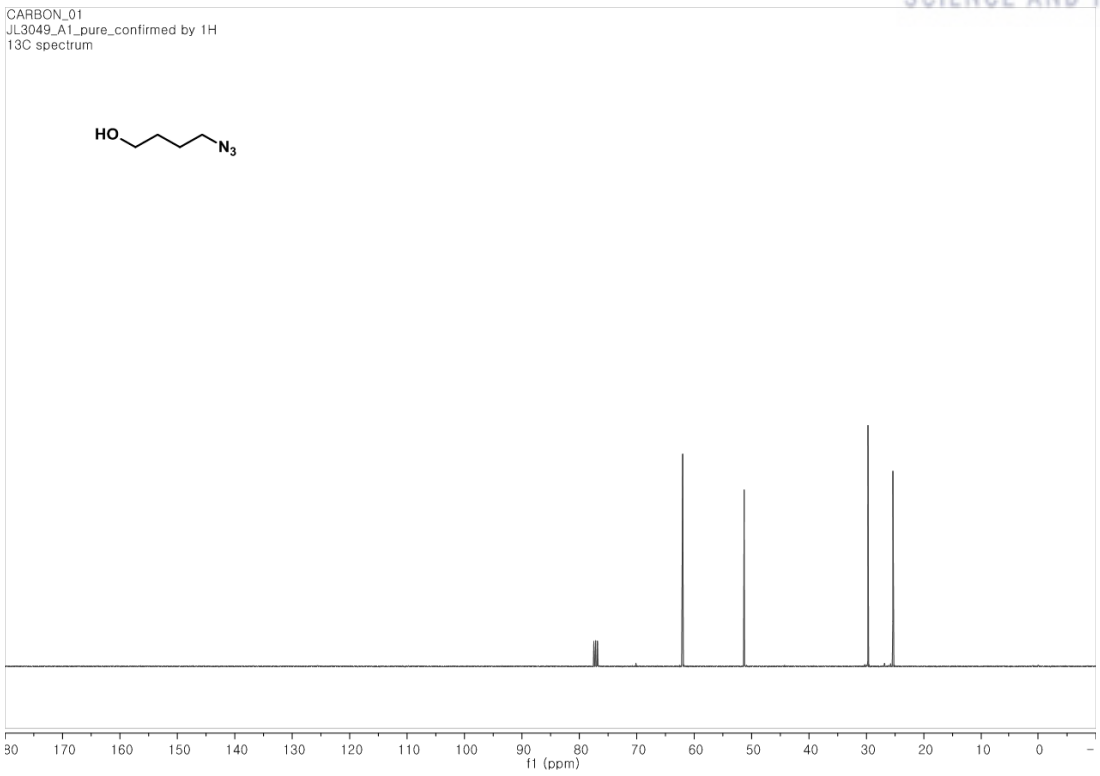

Figure 4.12. ^{13}C NMR spectrum of 4-azido-1-butanol (**2b**) (101 MHz, $CDCl_3$, 298K).

ULSAN NATIONAL INSTITUTE OF SCIENCE AND TECHNOLOGY

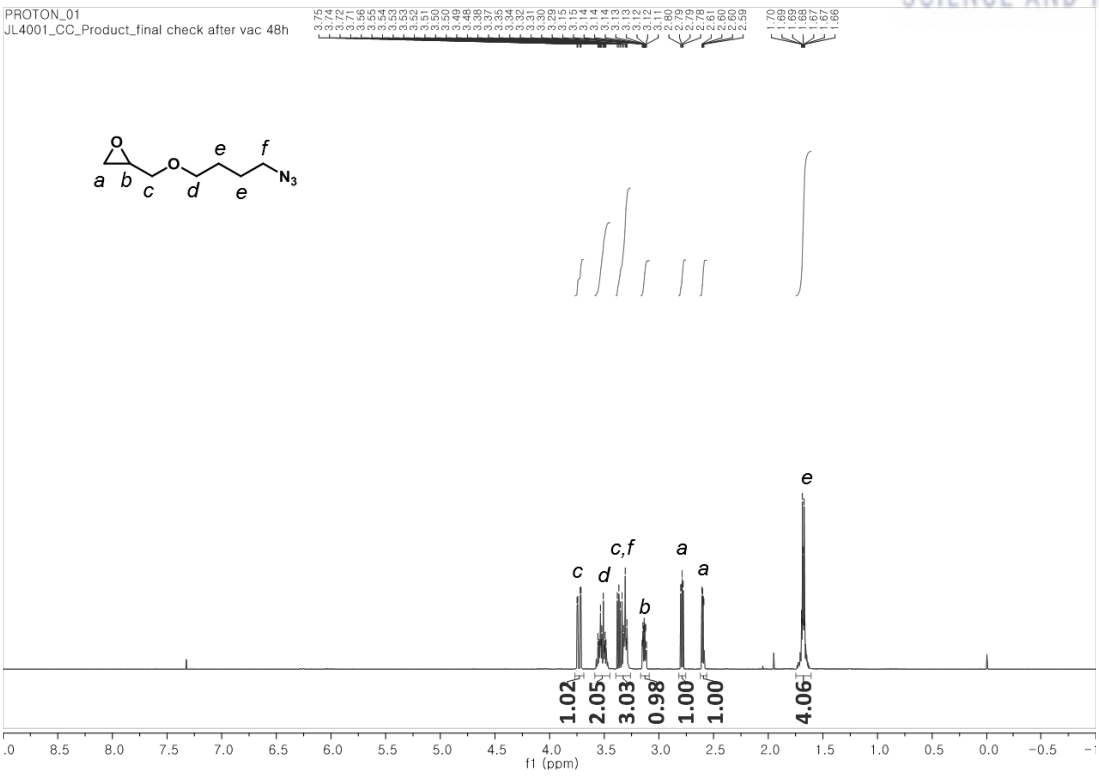

Figure 4.13. ^{1}H NMR spectrum of **ABGE** (400 MHz, $CDCl_3$, 298K).

ULSAN NATIONAL INSTITUTE OF SCIENCE AND TECHNOLOGY

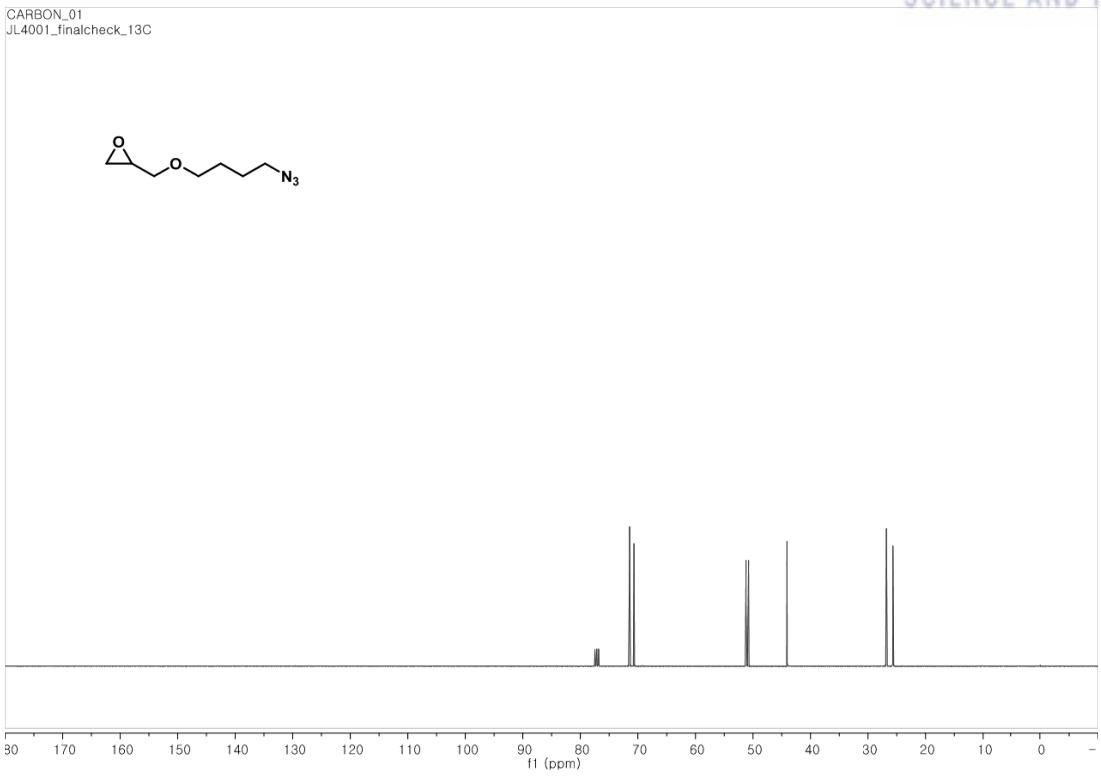

Figure 4.14. ^{13}C NMR spectrum of **ABGE** (101 MHz, $CDCl_3$, 298K).

ULSAN NATIONAL INSTITUTE OF SCIENCE AND TECHNOLOGY

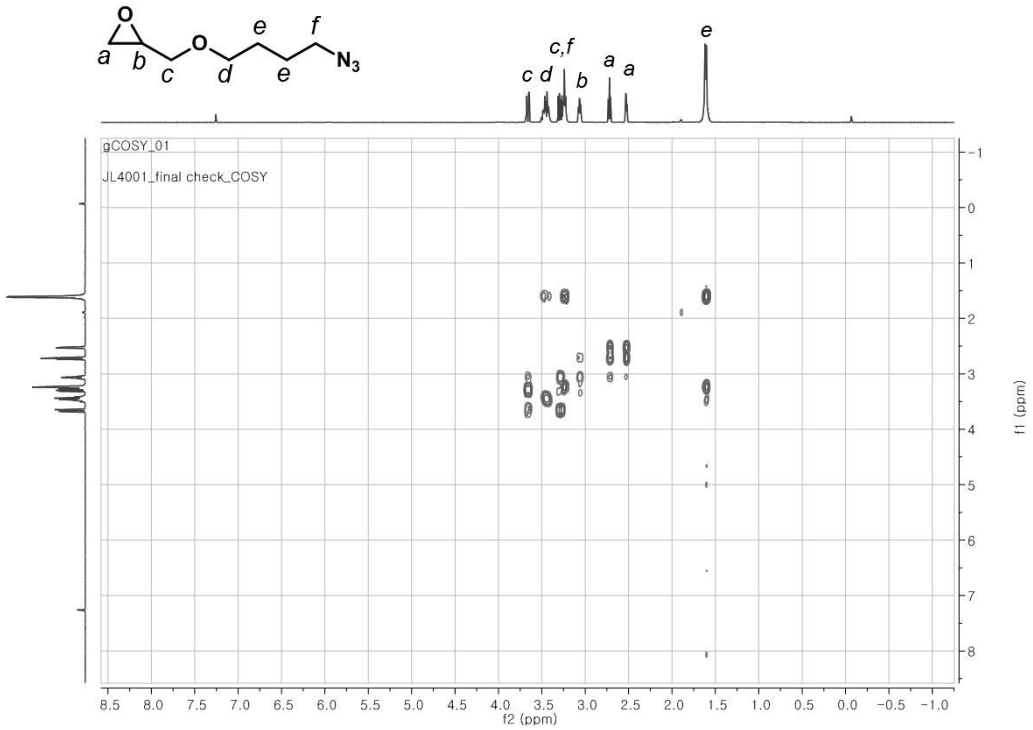

Figure 4.15. ^{1}H-^{1}H COSY NMR spectrum of **ABGE** in $CDCl_3$.

ULSAN NATIONAL INSTITUTE OF
SCIENCE AND TECHNOLOGY

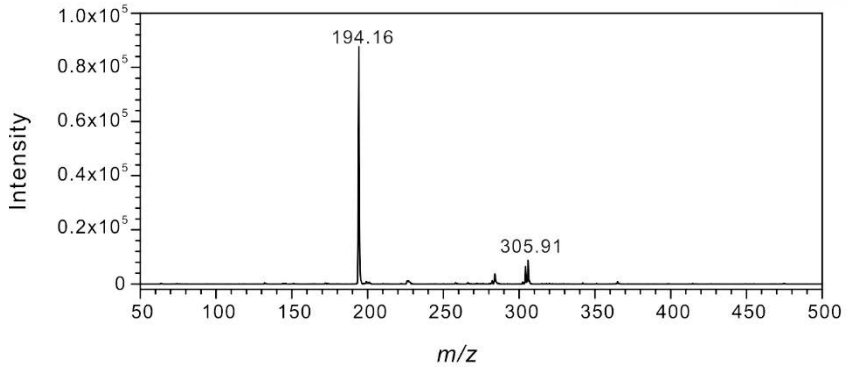

Figure 4.16. ESI-MS spectrum of **ABGE**.

ULSAN NATIONAL INSTITUTE OF SCIENCE AND TECHNOLOGY

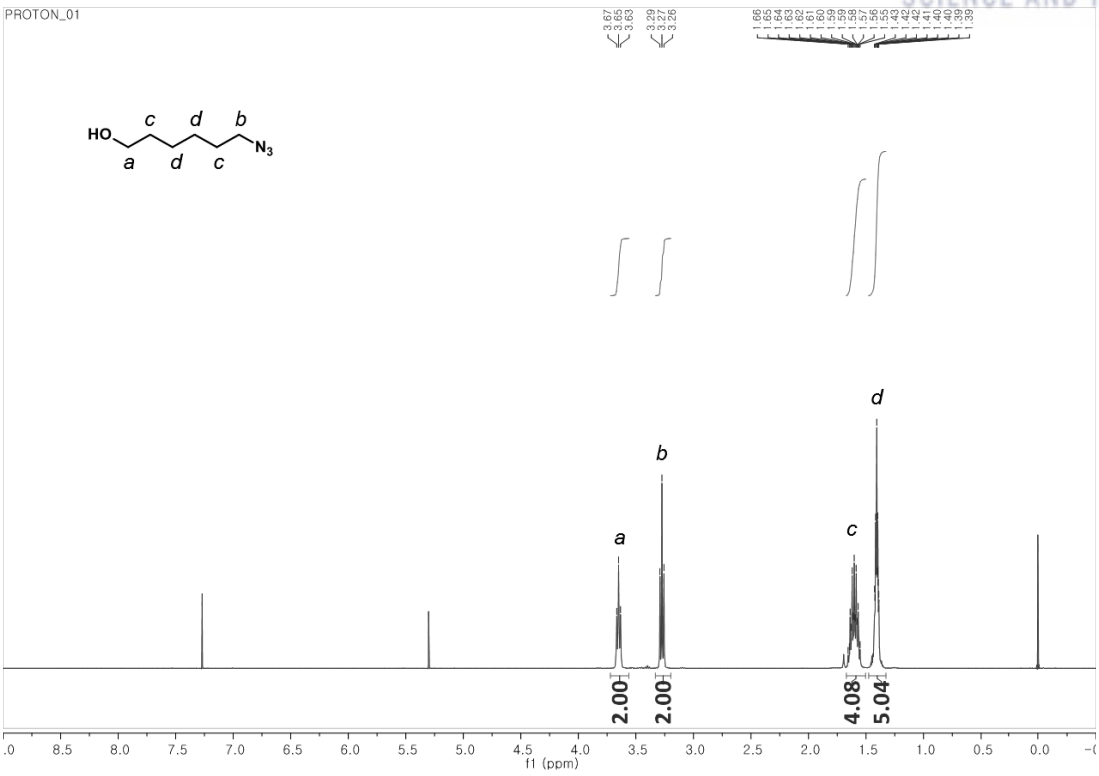

Figure 4.17. ^{1}H NMR spectrum of 6-azido-1-hexanol (**3b**) (400 MHz, $CDCl_3$, 298K).

ULSAN NATIONAL INSTITUTE OF SCIENCE AND TECHNOLOGY

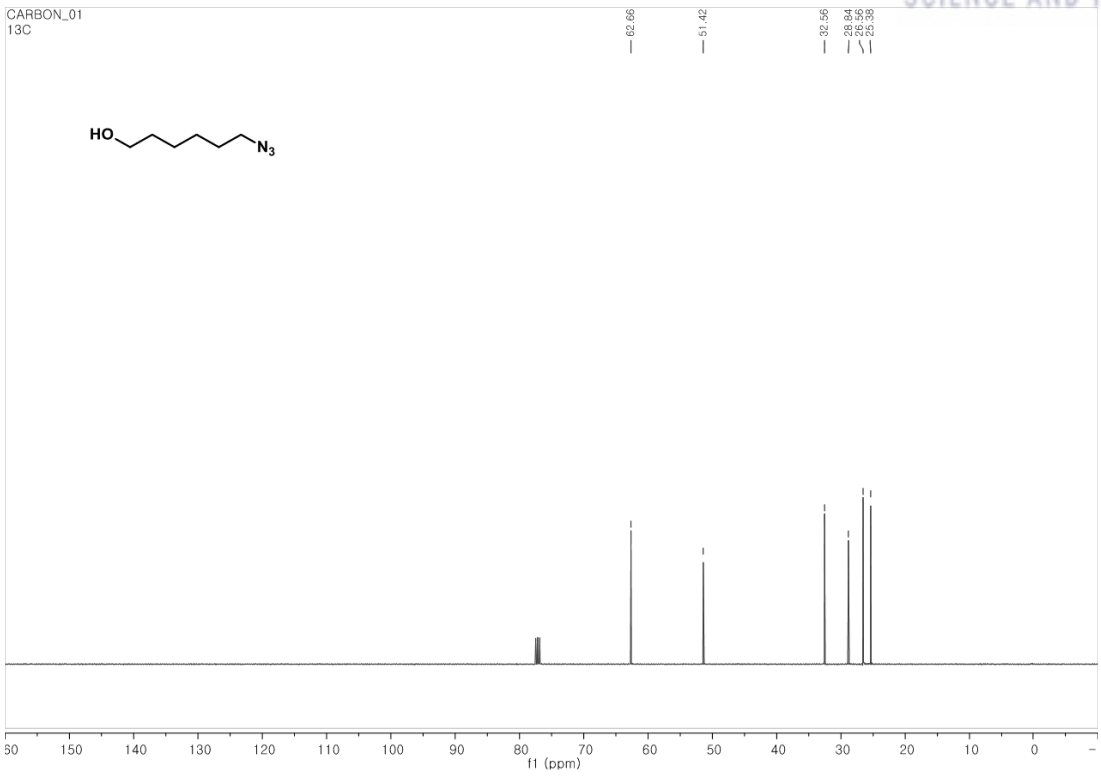

Figure 4.18. ^{13}C NMR spectrum of 6-azido-1-hexanol (**3b**) (101 MHz, $CDCl_3$, 298K).

ULSAN NATIONAL INSTITUTE OF SCIENCE AND TECHNOLOGY

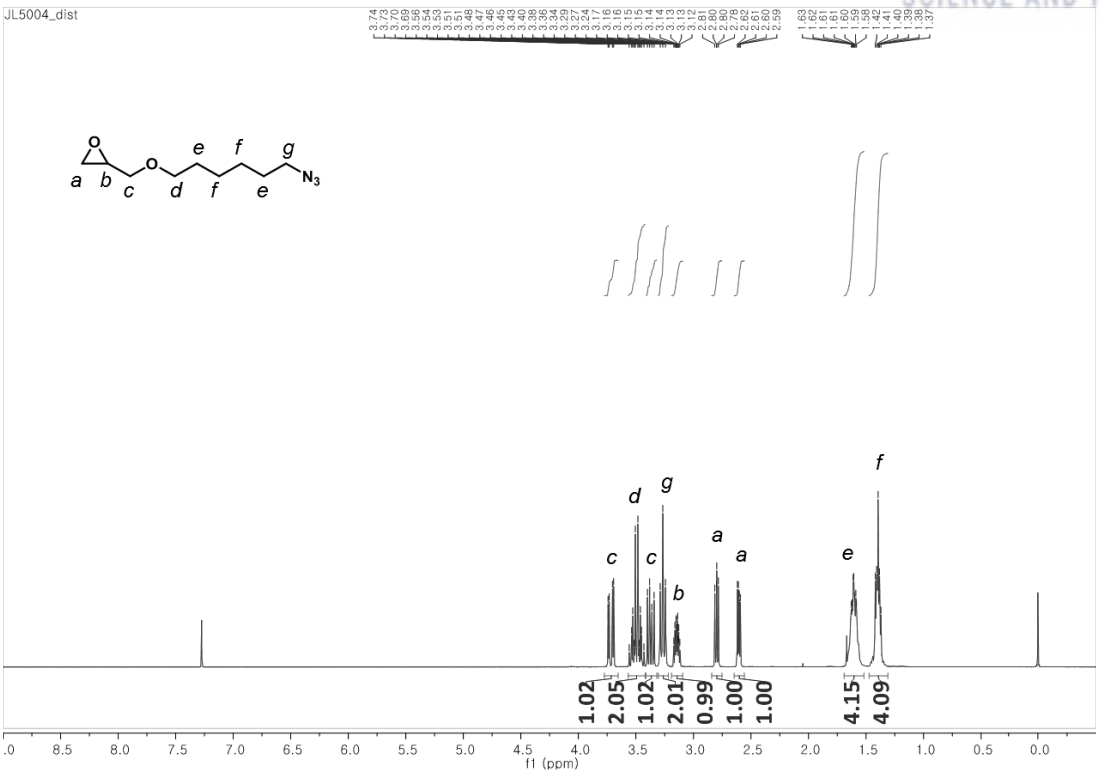

Figure 4.19. ^{1}H NMR spectrum of **AHGE** (400 MHz, $CDCl_3$, 298K).

ULSAN NATIONAL INSTITUTE OF SCIENCE AND TECHNOLOGY

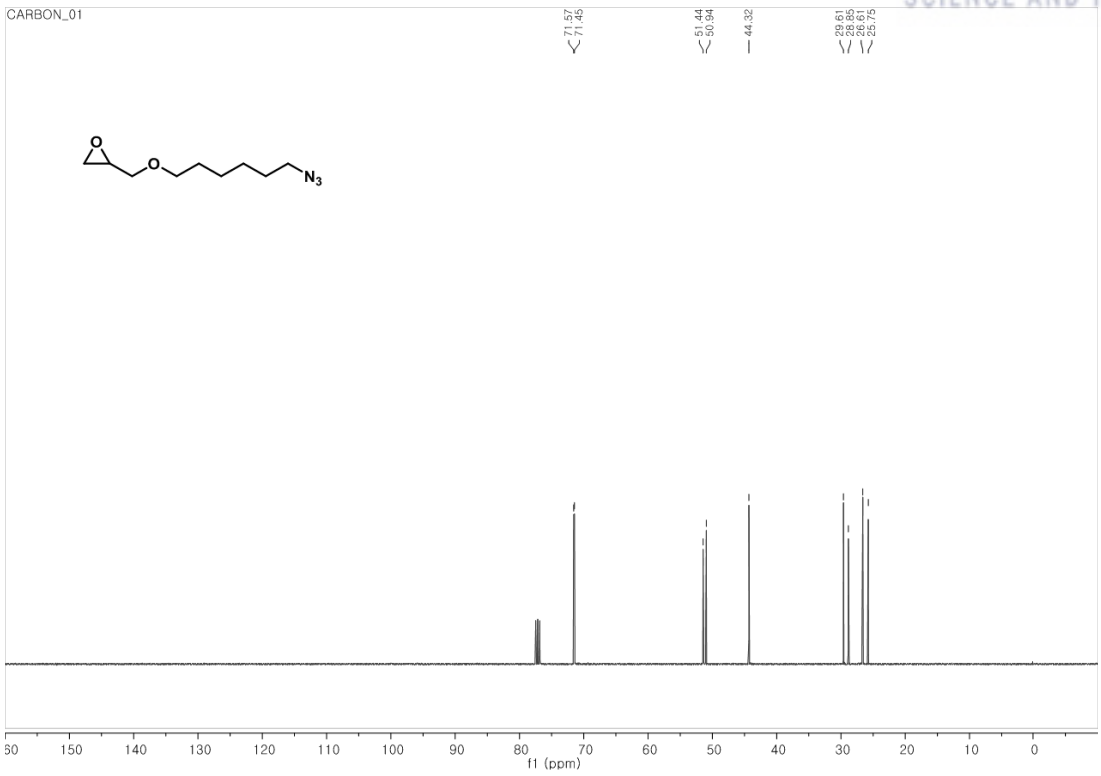

Figure 4.20. ^{13}C NMR spectrum of **AHGE** (101 MHz, $CDCl_3$, 298K).

ULSAN NATIONAL INSTITUTE OF SCIENCE AND TECHNOLOGY

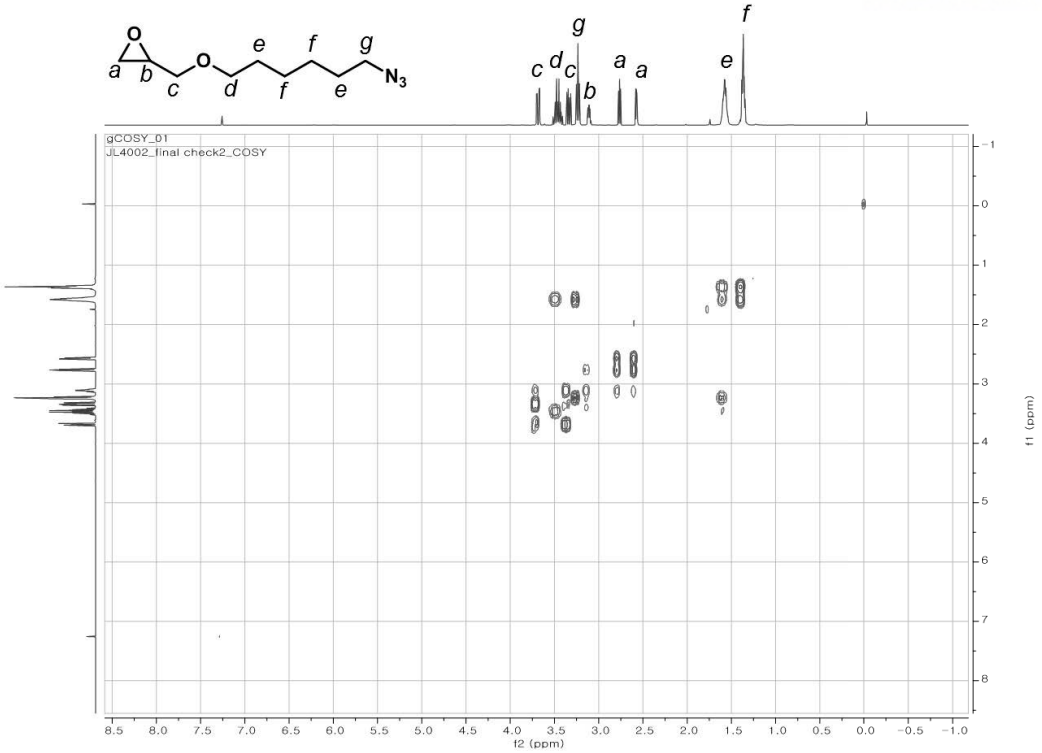

Figure 4.21. ^{1}H-^{1}H COSY NMR spectrum of **AHGE** in $CDCl_3$.

ULSAN NATIONAL INSTITUTE OF SCIENCE AND TECHNOLOGY

Table 4.1. Characterization Data of Poly(azidoalkyl glycidyl ether)s Prepared in This Study

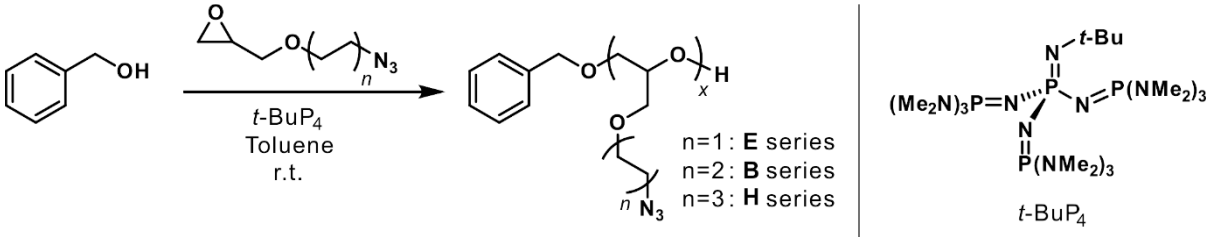

Entry	M_n (Target)	M_n (NMR)[a]	M_n (SEC)[b]	$Đ$ (SEC)[b]	Conv.[a] (%)	DP (Target)	DP[a]
E1	3000	2970	2700	1.13	>99	20	20
E2	3700	3690	3000	1.15	>99	25	25
E3	7300	6700	5600	1.11	>99	50	46
B1	3500	3880	4000	1.08	>99	20	22
B2	8700	9870	7400	1.09	>99	50	57
B3	17200	17400	11000	1.13	>99	100	101
H1	2100	2300	3000[c]	1.10[c]	>99	10	11
H2	5100	4690	4900[c]	1.15[c]	>99	25	23
H3	7100	7520	8400[c]	1.21[c]	>99	35	36
H4	13000	12660	11600[c]	1.03[c]	>99	65	63

[a]Determined from ^{1}H NMR spectra of resulting polymers. Number-average molecular weight (M_n) and dispersity ($Đ$) was measured by SEC in either [b]THF or [c]$CHCl_3$ with PMMA standard.

ULSAN NATIONAL INSTITUTE OF SCIENCE AND TECHNOLOGY

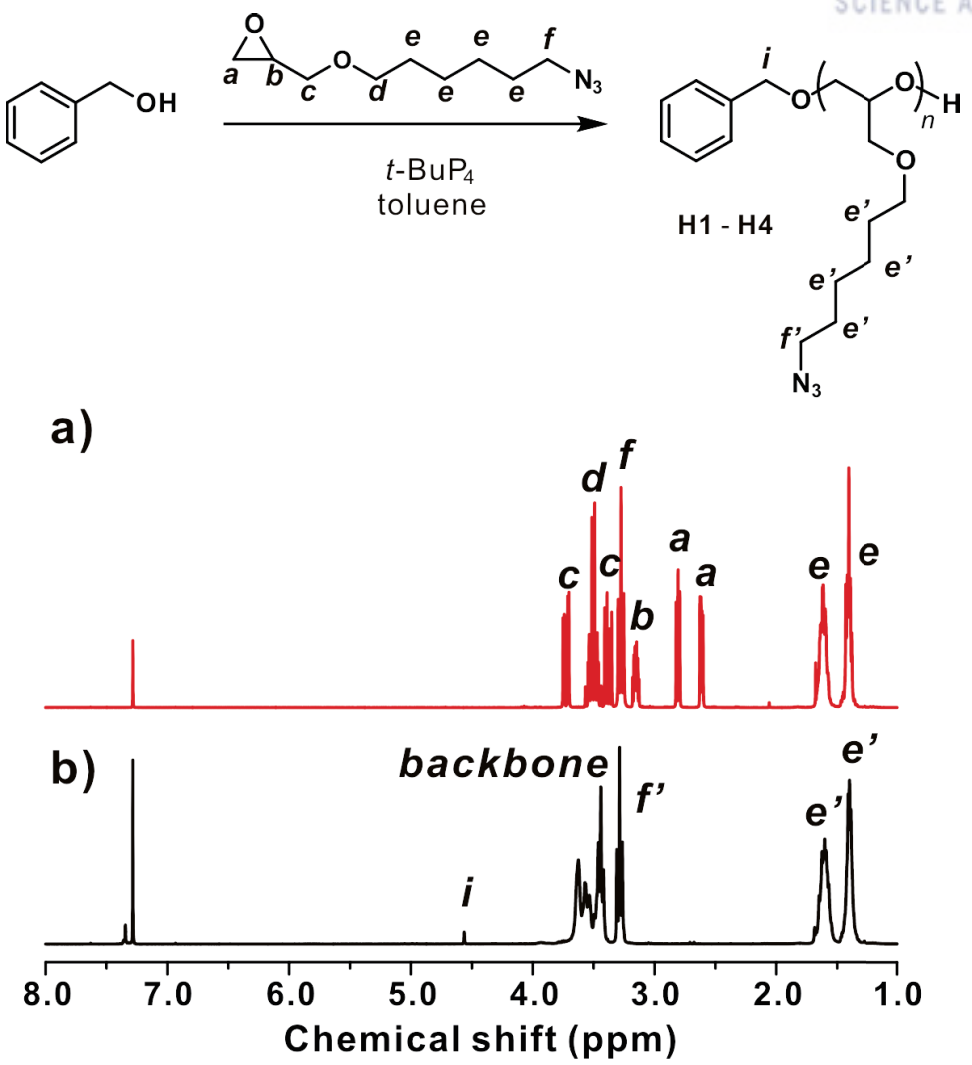

Figure 4.22. Synthesis of P(AHGE)s by AROP. Representative ^{1}H NMR spectra of (a) AHGE monomer and (b) P(AHGE) (**H4**) in $CDCl_3$ at 25 °C.

ULSAN NATIONAL INSTITUTE OF SCIENCE AND TECHNOLOGY

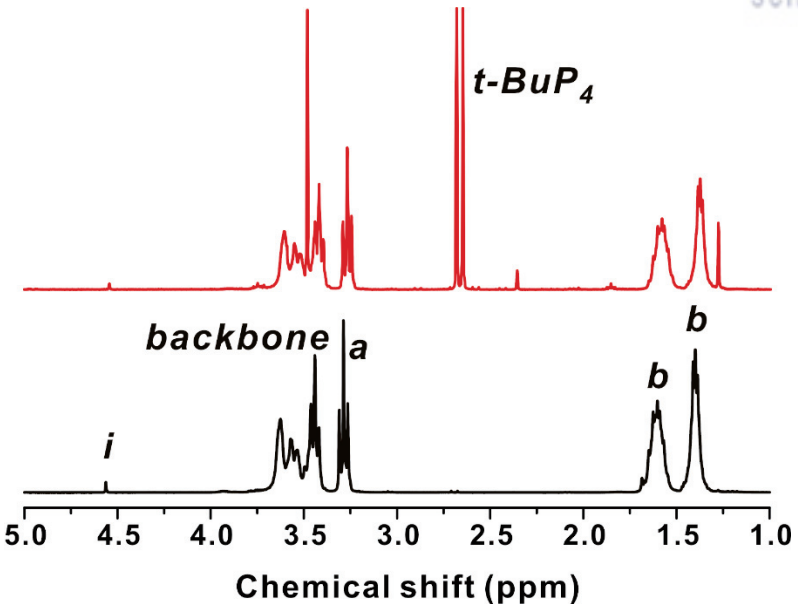

Figure 4.23. ^{1}H NMR spectrum of P(AHGE) (**H4**) before (top) and after purification (bottom) in $CDCl_3$.

ULSAN NATIONAL INSTITUTE OF SCIENCE AND TECHNOLOGY

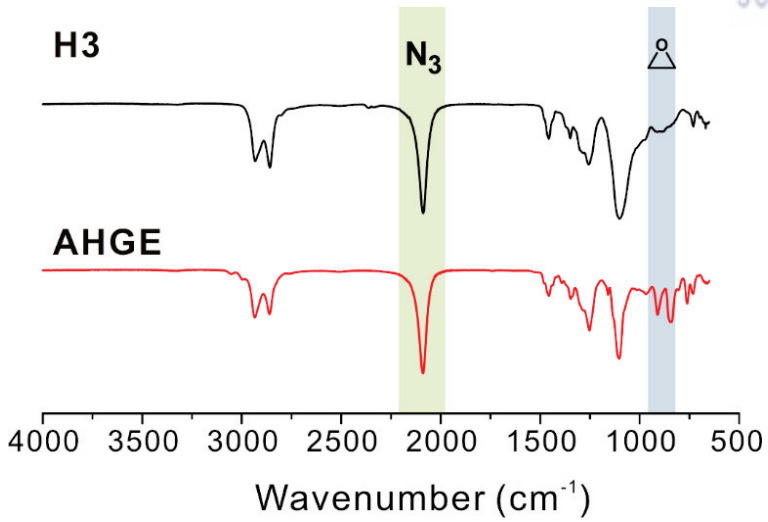

Figure 4.24. FT-IR spectra of **H3** and **AHGE** monomer.

ULSAN NATIONAL INSTITUTE OF SCIENCE AND TECHNOLOGY

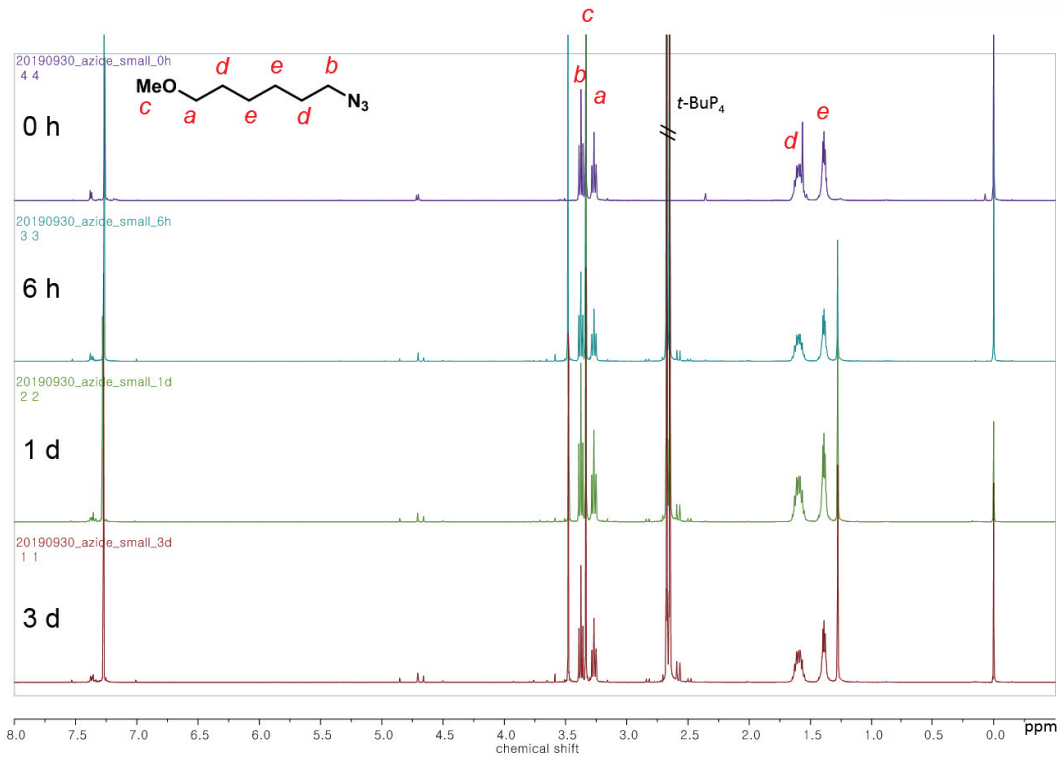

Figure 4.25. ^{1}H NMR spectra of the reaction mixture of 1-azido-6-methoxyhexane with *t*-BuP4 and benzyl alcohol over 3 days at room temperature (400 MHz, $CDCl_3$).

ULSAN NATIONAL INSTITUTE OF SCIENCE AND TECHNOLOGY

Table 4.2. ^{1}H NMR Integration Values of 1-Azido-6-Methoxyhexane Under AROP Condition

Peak	# of Protons	Integration region (ppm)	Integration value			
			0 h	6 h	1 d	3 d
a	2	3.302 – 3.229	2.15	2.08	2.10	2.06
b	2	3.045 – 3.349	2.05	2.05	2.07	2.04
c (ref.)	3	3.347 – 3.315	3.00	3.00	3.00	3.00
d	4	1.674 – 1.516	4.89	4.22	4.24	4.22
e	4	1.461 – 1.324	4.33	4.30	4.31	4.31

ULSAN NATIONAL INSTITUTE OF SCIENCE AND TECHNOLOGY

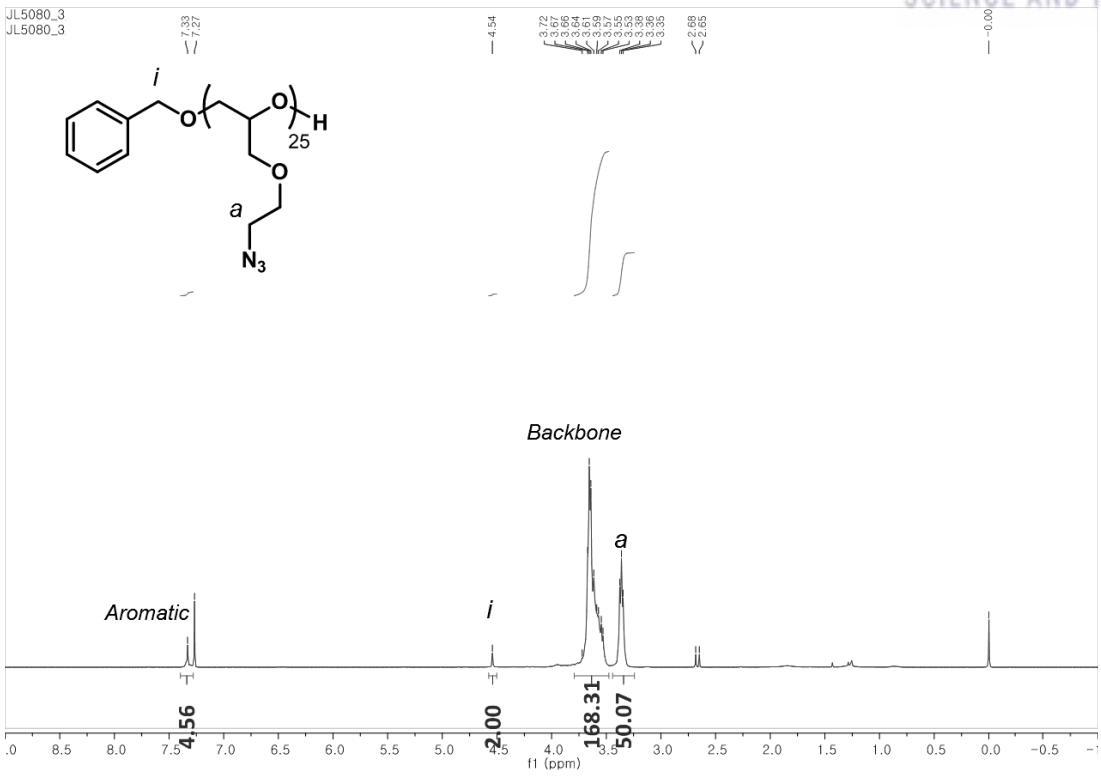

Figure 4.26. Representative ^{1}H NMR spectrum of **E2** in $CDCl_3$.

ULSAN NATIONAL INSTITUTE OF SCIENCE AND TECHNOLOGY

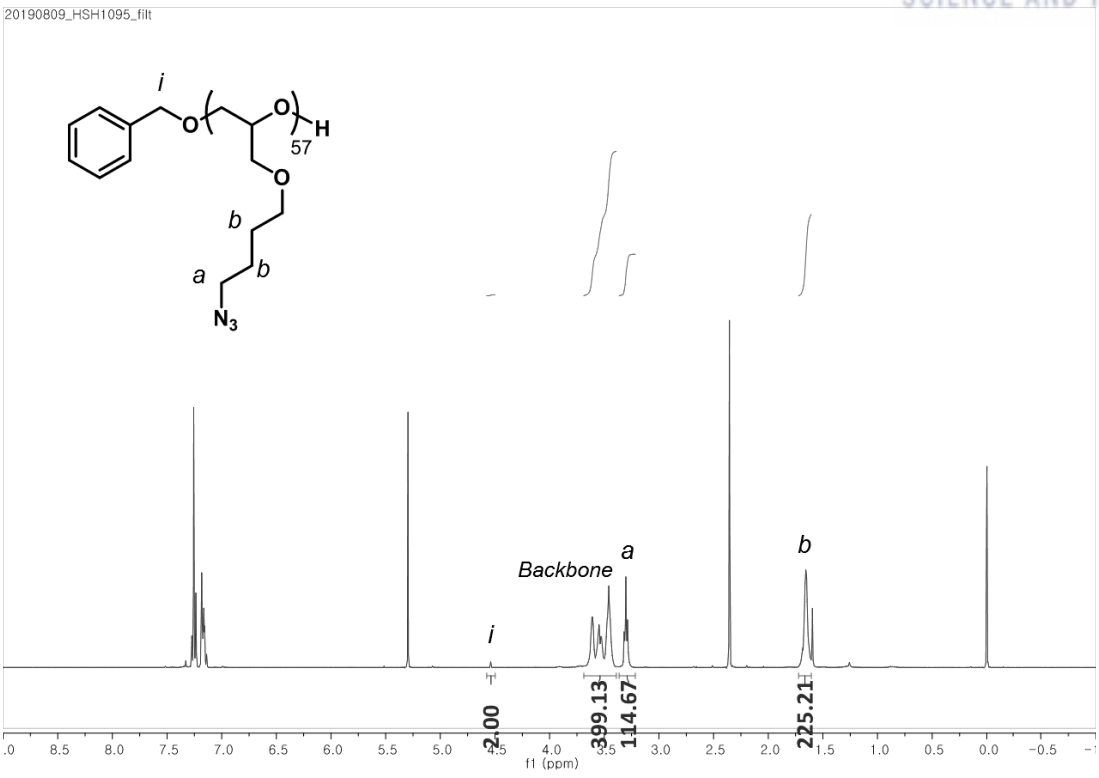

Figure 4.27. Representative ^{1}H NMR spectrum of **B2** in $CDCl_3$.

ULSAN NATIONAL INSTITUTE OF SCIENCE AND TECHNOLOGY

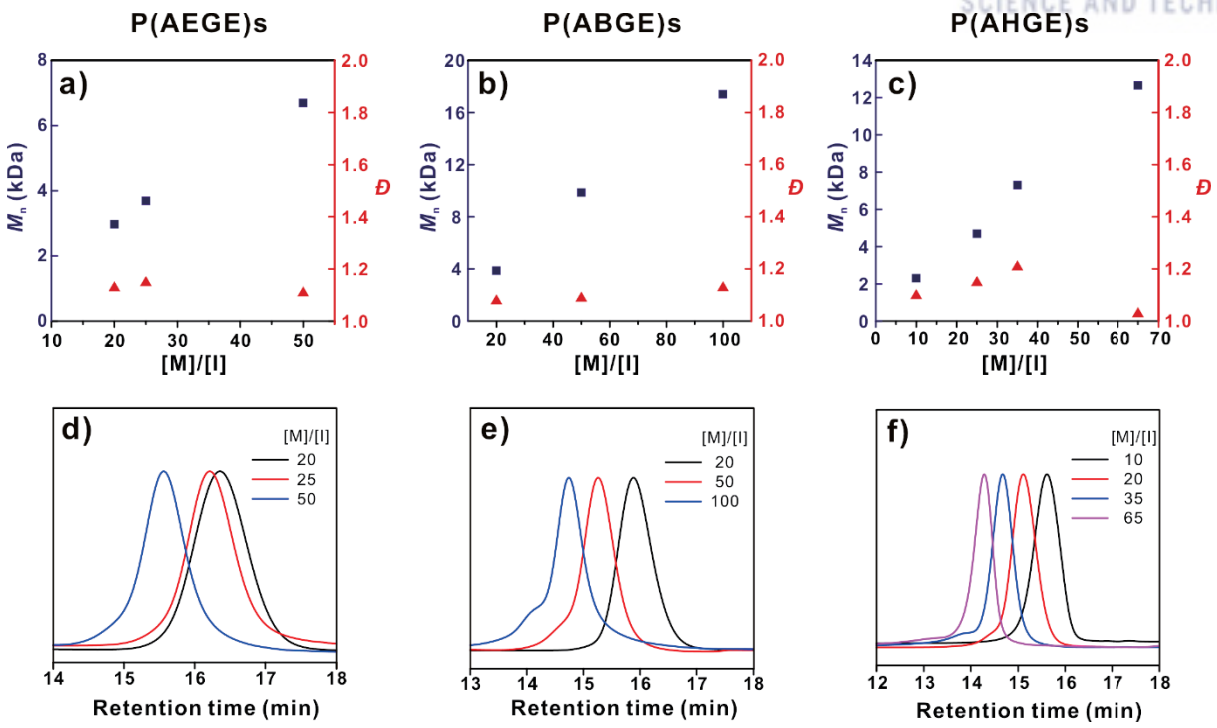

Figure 4.28. Demonstration of controlled AROP of azidoalkyl glycidyl ethers. (a – c) M_n and $Đ$ of (a) P(AEGE)s, (b) P(ABGE)s and (c) P(AHGE)s at various monomer-to-initiator ratios, [M]/[I]. (d – f) SEC chromatograms of (d) P(AEGE)s, (e) P(ABGE)s, and (f) P(AHGE)s.

ULSAN NATIONAL INSTITUTE OF SCIENCE AND TECHNOLOGY

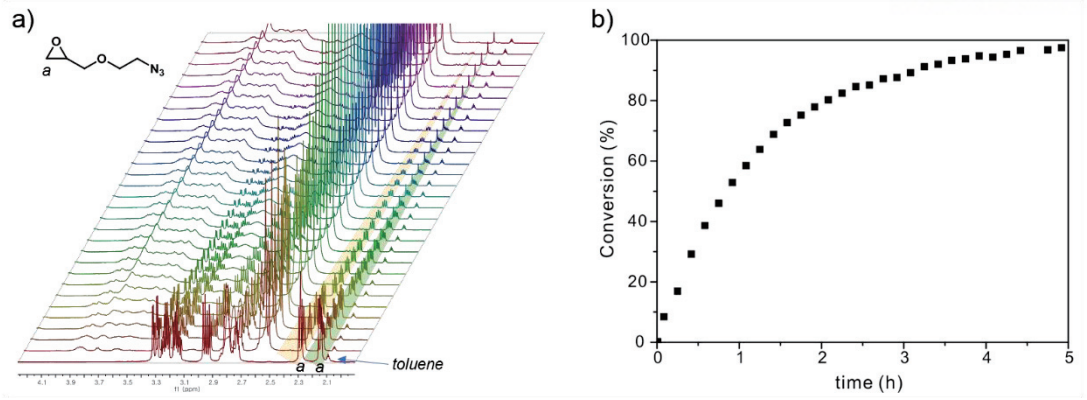

Figure 4.29. (a) *In situ* monitoring of the homopolymerization kinetics of AEGE. (b) Conversion versus time for the homopolymerization of AEGE.

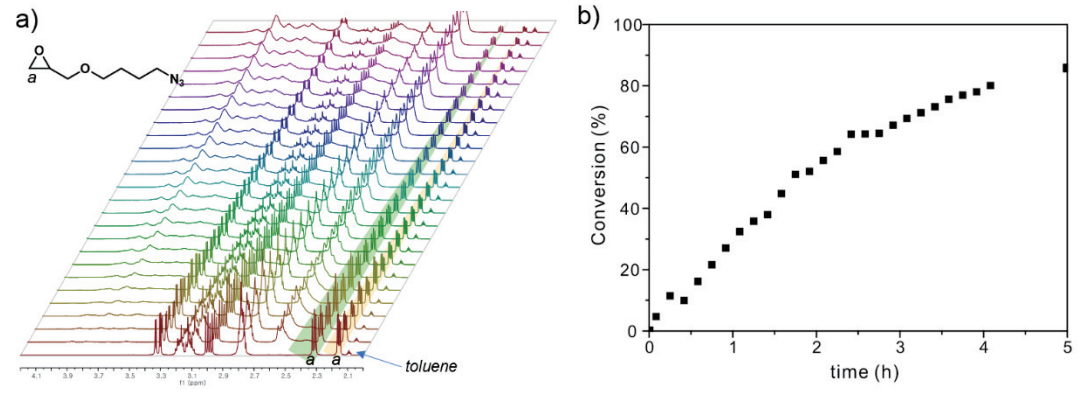

Figure 4.30. (a) *In situ* monitoring of the homopolymerization kinetics of ABGE. (b) Conversion versus time for the homopolymerization of ABGE.

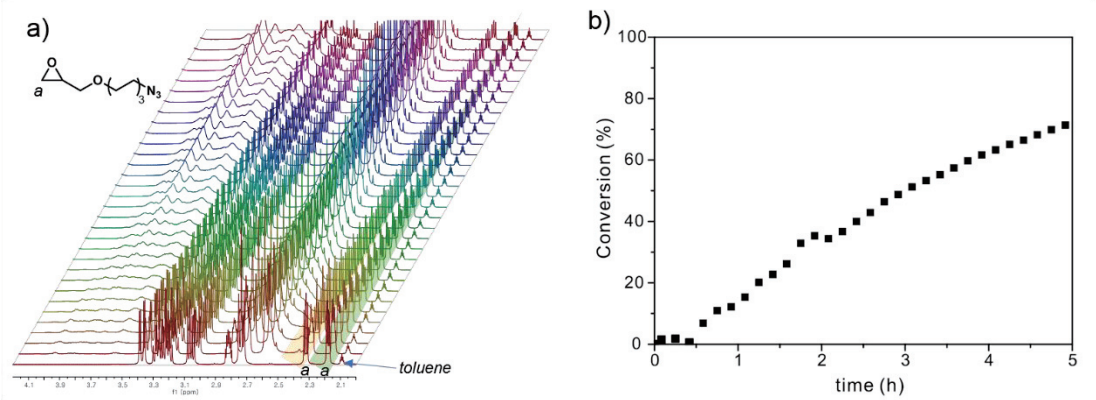

Figure 4.31. (a) *In situ* monitoring of the homopolymerization kinetics of AHGE. (b) Conversion versus time for the homopolymerization of AHGE.

ULSAN NATIONAL INSTITUTE OF SCIENCE AND TECHNOLOGY

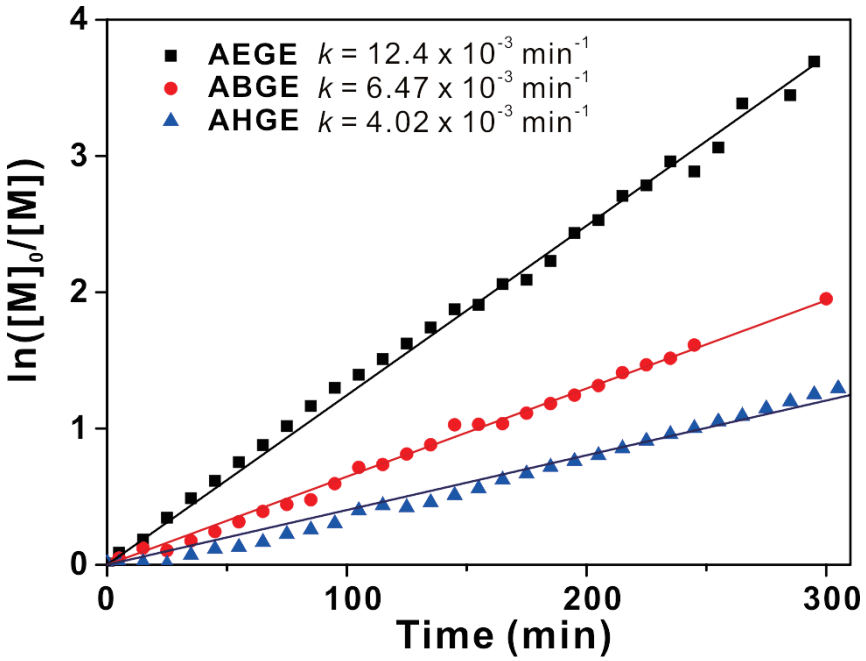

Figure 4.32. First-order kinetic plots of $\ln([M]_0/[M]_t)$ *vs* time for the polymerization of (black square) AEGE, (red circle) ABGE, and (blue triangle) AHGE monomers targeting degree of polymerization of 20.

ULSAN NATIONAL INSTITUTE OF SCIENCE AND TECHNOLOGY

Table 4.3. Calculated Log *P* Values and Polymerization Rate Data

Monomer	Log *P*	Polymerization rate (k, 10^{-3} min^{-1})
AEGE	1.19	12.4
ABGE	1.94	6.47
AHGE	2.60	4.02

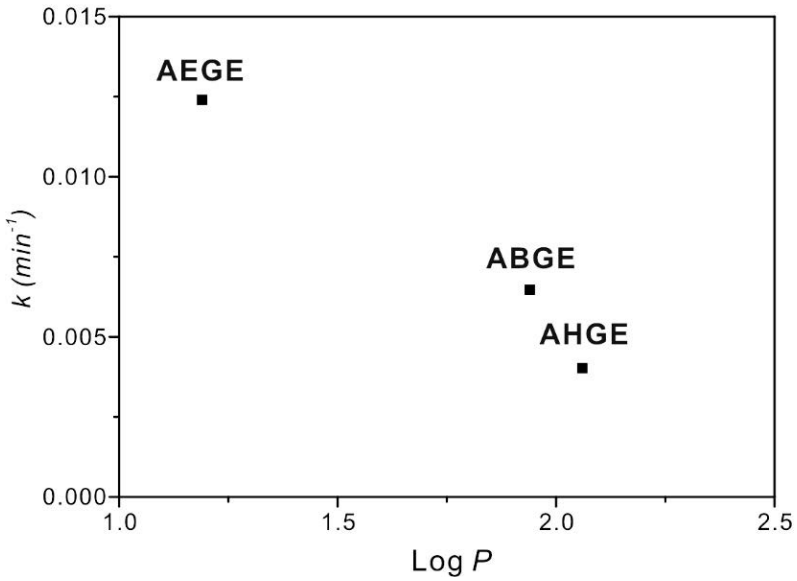

Figure 4.33. Correlation of calculated Log *P* and polymerization rate of monomers.

ULSAN NATIONAL INSTITUTE OF SCIENCE AND TECHNOLOGY

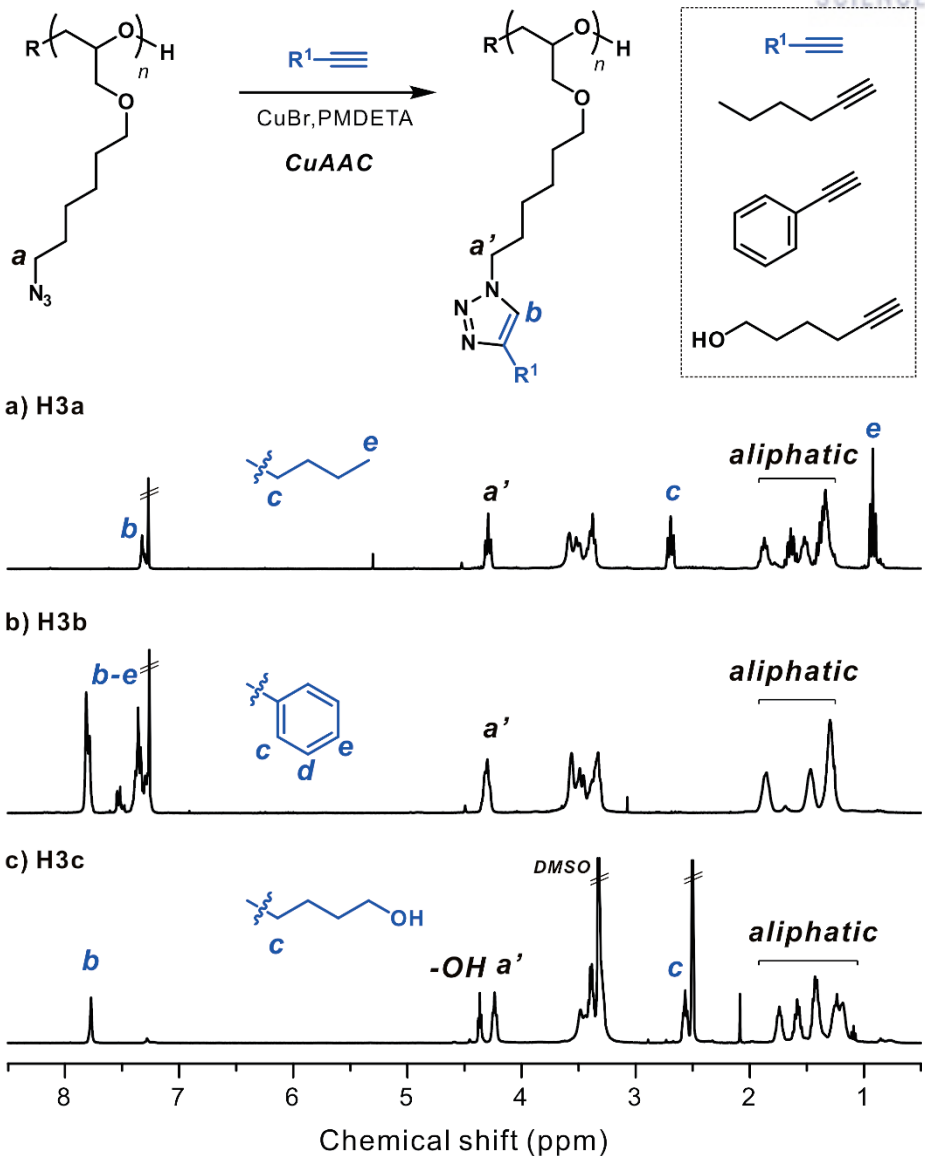

Figure 4.34. Post-polymerization modification of **H3** via CuAAC with various alkynes. (a – c) ^{1}H NMR spectra after CuAAC of **H3** with (a) 1-hexyne, (b) phenylacetylene and (c) 5-hexyn-1-ol.

ULSAN NATIONAL INSTITUTE OF SCIENCE AND TECHNOLOGY

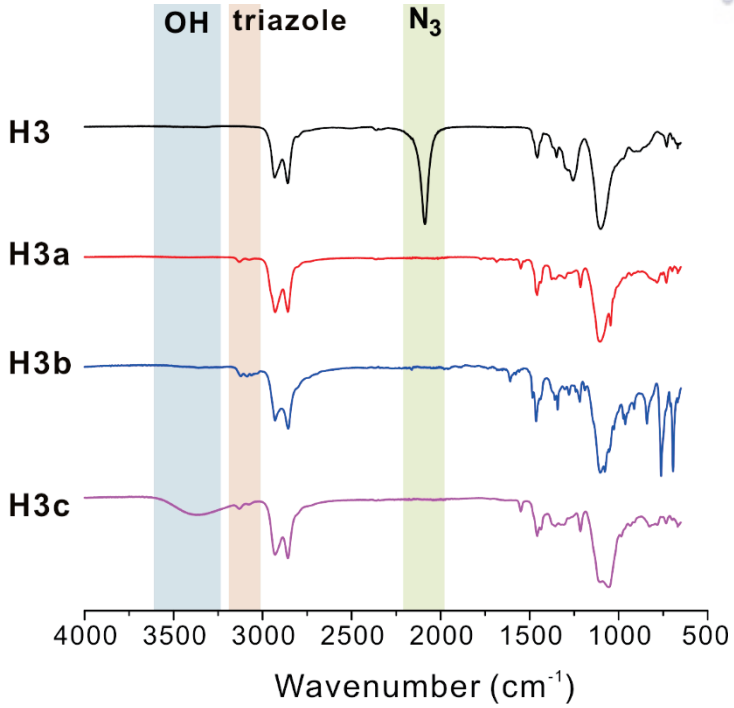

Figure 4.35. FT-IR spectra of **H3**, **H3a**, **H3b** and **H3c**.

ULSAN NATIONAL INSTITUTE OF SCIENCE AND TECHNOLOGY

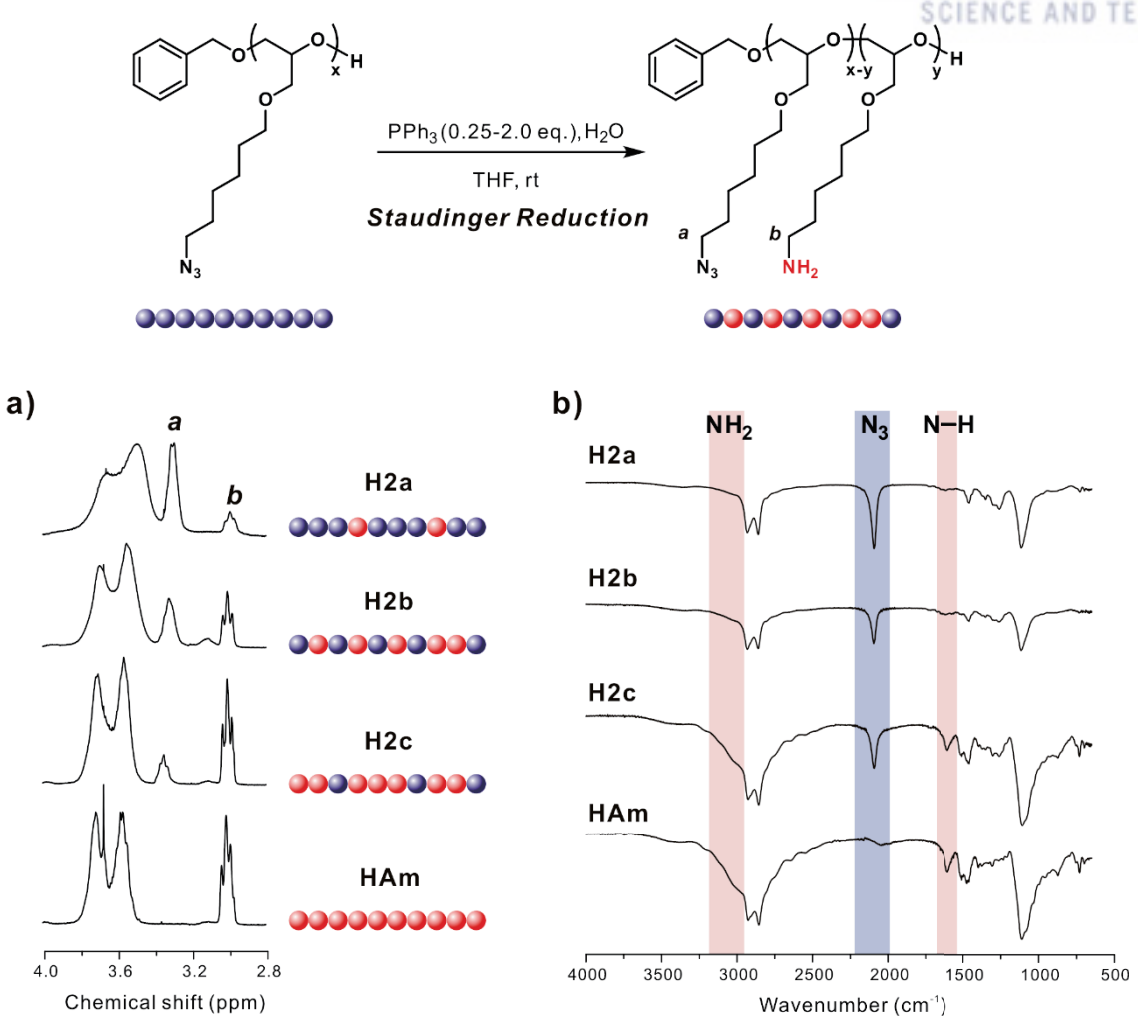

Figure 4.36. Staudinger reduction of **H2**. (a) ^{1}H NMR spectra of partially reduced polymers (**H2a** – **H2c**) and fully reduced polymer (**HAm**) in D_2O. (b) FT-IR spectra of **H2a – H2c** and **HAm**.

ULSAN NATIONAL INSTITUTE OF SCIENCE AND TECHNOLOGY

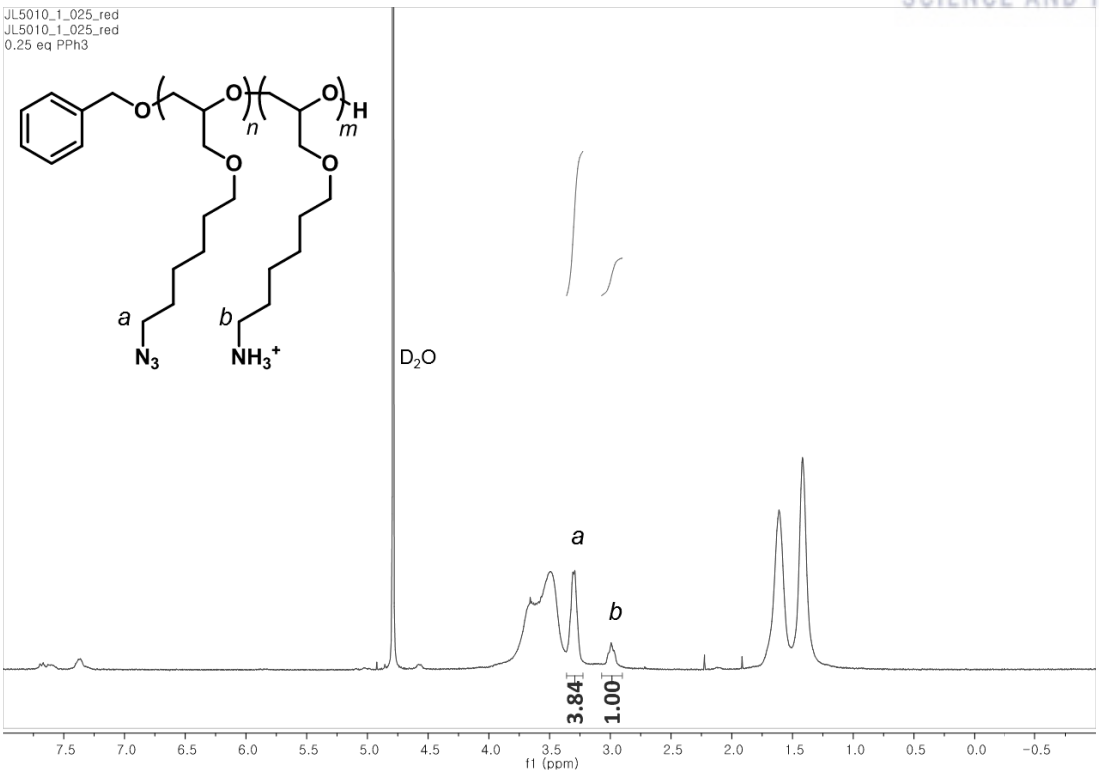

Figure 4.37. ^{1}H NMR spectrum of **H2a** in D_2O.

ULSAN NATIONAL INSTITUTE OF SCIENCE AND TECHNOLOGY

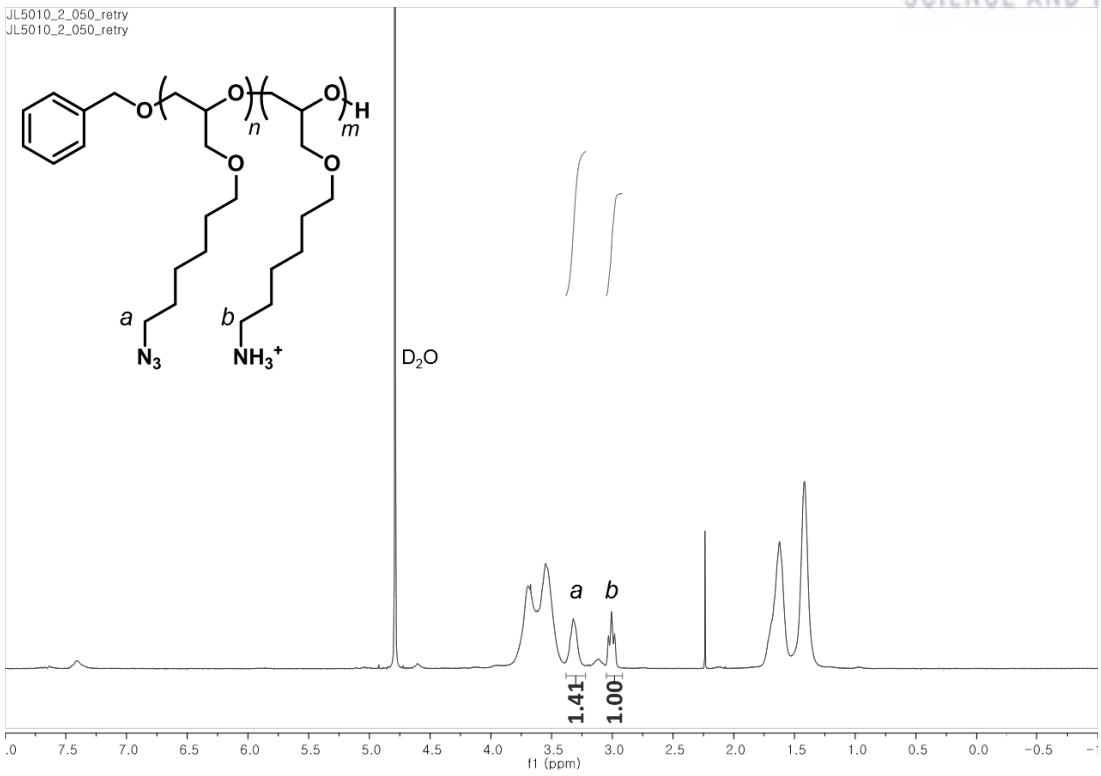

Figure 4.38. ^{1}H NMR spectrum of **H2b** in D_2O.

ULSAN NATIONAL INSTITUTE OF SCIENCE AND TECHNOLOGY

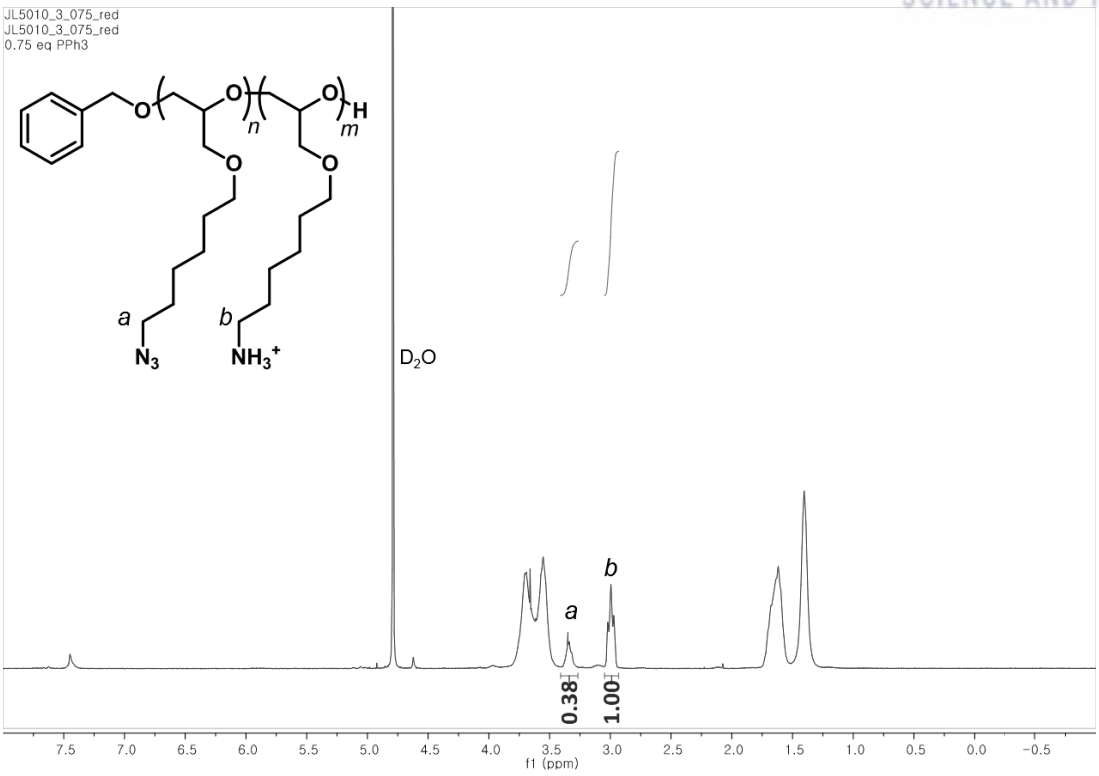

Figure 4.39. ^{1}H NMR spectrum of **H2c** in D_2O.

ULSAN NATIONAL INSTITUTE OF SCIENCE AND TECHNOLOGY

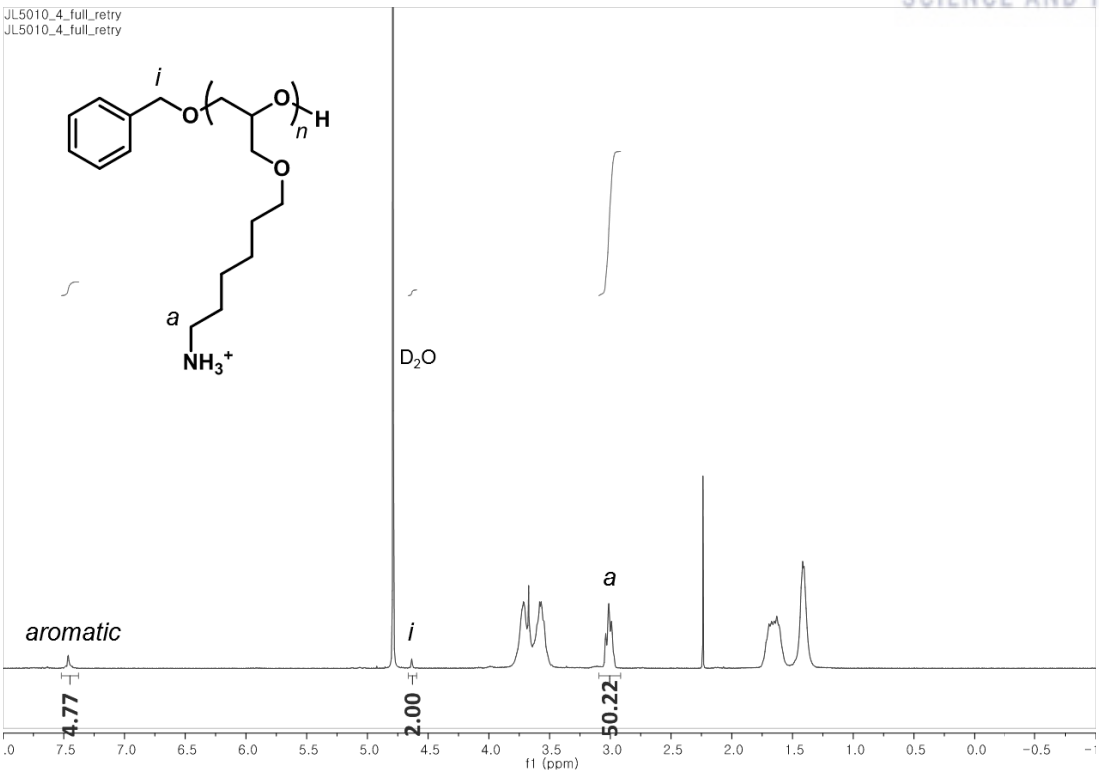

Figure 4.40. ^{1}H NMR spectrum of **HAm** in D_2O.

ULSAN NATIONAL INSTITUTE OF SCIENCE AND TECHNOLOGY

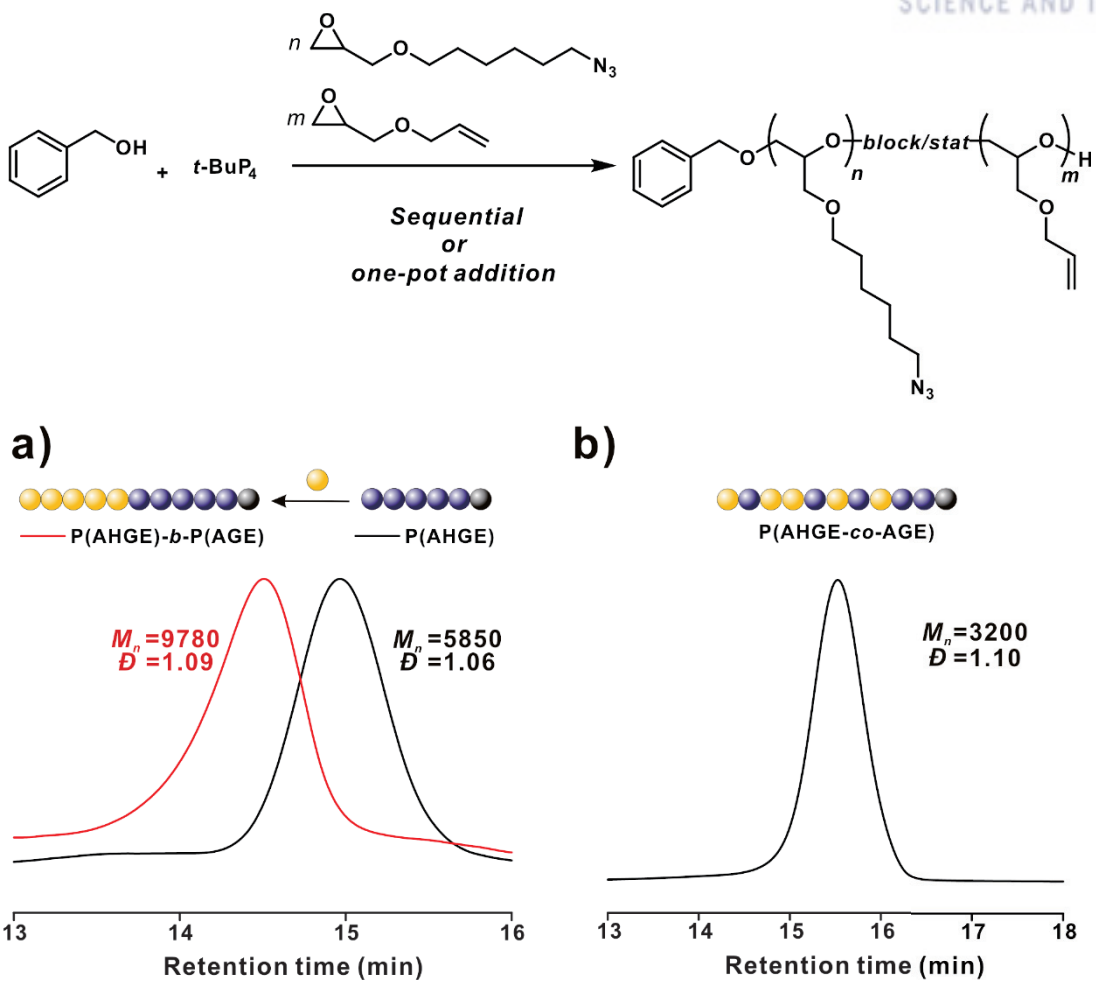

Figure 4.41. Synthesis of P(AHGE)-*b*-P(AGE) or P(AHGE-*co*-AGE) by sequential or one-pot monomer addition, respectively. SEC chromatograms of (a) P(AHGE) (black), P(AHGE)-*b*-P(AGE) (red) and (b) P(AHGE-*co*-AGE) measured in $CHCl_3$.

ULSAN NATIONAL INSTITUTE OF SCIENCE AND TECHNOLOGY

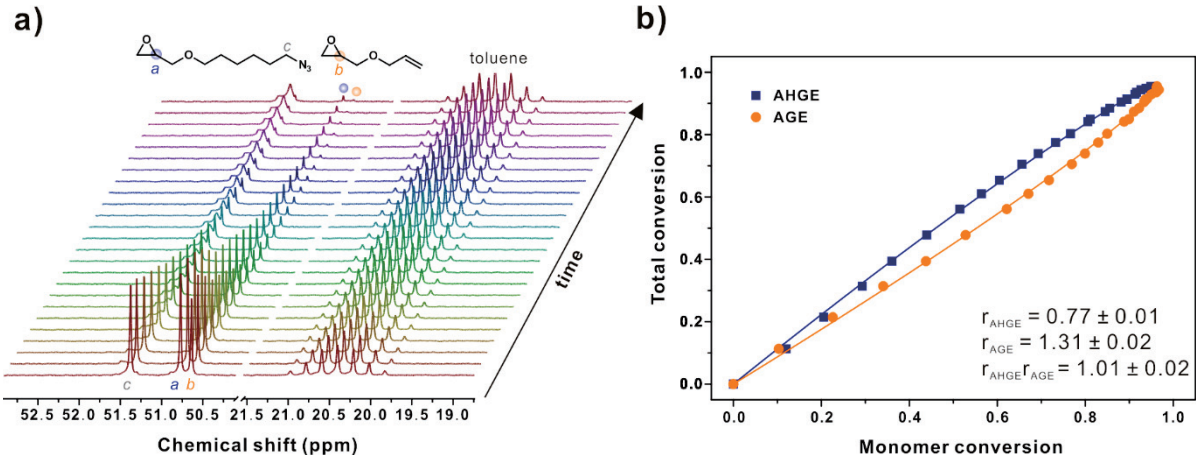

Figure 4.42. (a) Time-resolved ^{13}C NMR spectra of copolymerization of AHGE and AGE in toluene-d_8. (b) Total polymerization conversion versus monomer conversion for the copolymerization of AHGE (blue square) and AGE (orange square). The initial compositions: n_{AHGE} = 0.58 and n_{AGE} = 0.42.

ULSAN NATIONAL INSTITUTE OF SCIENCE AND TECHNOLOGY

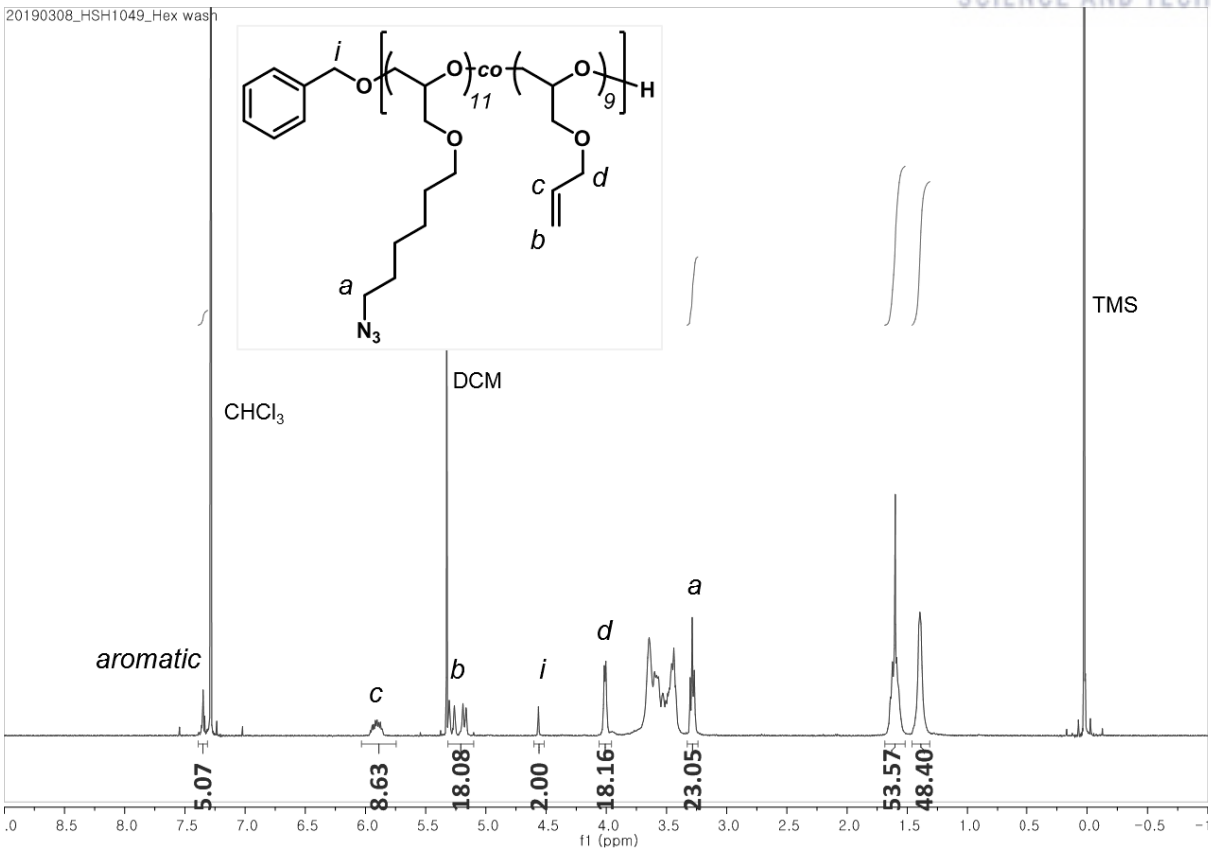

Figure 4.43. ^{1}H NMR spectrum of P(AHGE-*co*-AGE).

ULSAN NATIONAL INSTITUTE OF SCIENCE AND TECHNOLOGY

Table 4.4. Result of Copolymerizations Using AHGE and AGE

Polymer	Feed ratio ([AHGE]/[AGE])	Degree of Polymerization ([AHGE]/[AGE]) [a]
P(AHGE)-*b*-P(AGE)	30/30	32/34
P(AHGE-*co*-AGE)	10/10	11/9

[a]Determined from ^{1}H NMR spectra of resulting polymers

ULSAN NATIONAL INSTITUTE OF SCIENCE AND TECHNOLOGY

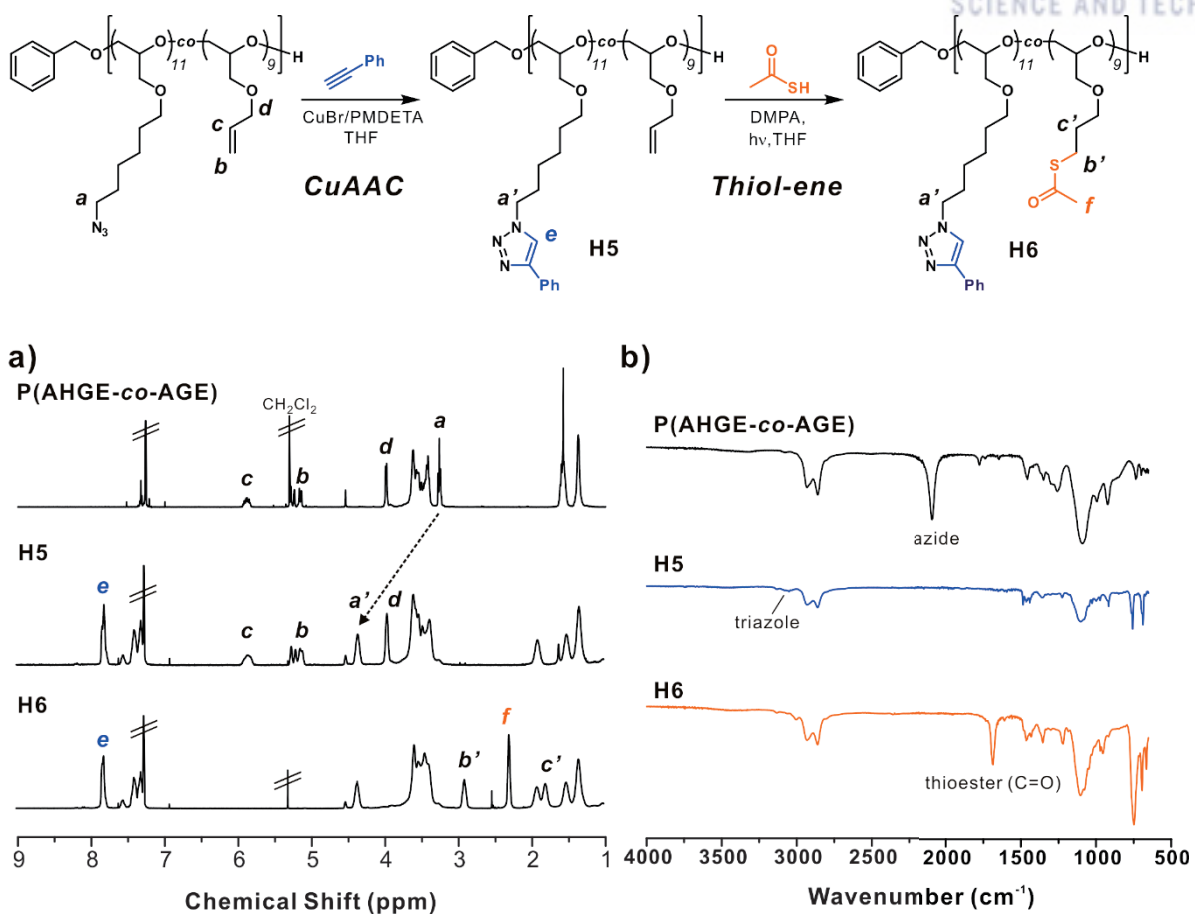

Figure 4.44. Orthogonal modification of P(AHGE-*co*-AGE) via sequential CuAAC and thiol-ene addition. (a) ^{1}H NMR and (b) FT-IR spectra of P(AHGE-*co*-AGE), **H5**, and **H6**.

ULSAN NATIONAL INSTITUTE OF
SCIENCE AND TECHNOLOGY

3.5 Conclusion

In conclusion, a series of azide-functionalized glycidyl monomers with different alkyl spacers have been introduced, including AEGE, ABGE, and AHGE. Interestingly, azide moieties of azidoalkyl glycidyl ethers were intact under highly basic AROP condition which were not in the case of glycidyl azide. The investigation on polymerization kinetics of the monomers revealed that the AEGE shows a much faster reaction rate than that of ABGE and AHGE. Using AHGE as a model monomer, versatile multi-functional polyethers were synthesized and primed for post-polymerization modification. Azide pendant groups appended to the polyether backbone enable diverse chemical modification to afford a variety of functionalities via CuAAC and Staudinger reduction. Copolymerization with other epoxide monomers, such as AGE, was used to access a variety of combinations of orthogonal functionalities. The introduction of the azide-functionalized epoxide monomer further diversifies the library of functional epoxide monomers increasing the potential to develop new multifunctional polyethers.

ULSAN NATIONAL INSTITUTE OF SCIENCE AND TECHNOLOGY

3.6 References

(1) Hill, M. R.; Carmean, R. N.; Sumerlin, B. S. Expanding the Scope of RAFT Polymerization: Recent Advances and New Horizons. *Macromolecules* **2015**, *48*, 5459–5469.

(2) Grubbs, R. B.; Grubbs, R. H. 50th Anniversary Perspective : Living Polymerization—Emphasizing the Molecule in Macromolecules. *Macromolecules* **2017**, *50*, 6979–6997.

(3) Perrier, S. 50th Anniversary Perspective: RAFT Polymerization—A User Guide. *Macromolecules* **2017**, *50*, 7433–7447.

(4) Blasco, E.; Sims, M. B.; Goldmann, A. S.; Sumerlin, B. S.; Barner-Kowollik, C. 50th Anniversary Perspective : Polymer Functionalization. *Macromolecules* **2017**, *50*, 5215–5252.

(5) Hawker, C. J. The Convergence of Synthetic Organic and Polymer Chemistries. *Science* **2005**, *309*, 1200–1205.

(6) Barner-Kowollik, C.; Du Prez, F. E.; Espeel, P.; Hawker, C. J.; Junkers, T.; Schlaad, H.; Van Camp, W. "Clicking" Polymers or Just Efficient Linking: What Is the Difference? *Angew. Chem. Int. Ed.* **2011**, *50*, 60–62.

(7) Kolb, H. C.; Finn, M. G.; Sharpless, K. B. Click Chemistry: Diverse Chemical Function from a Few Good Reactions. *Angew. Chem. Int. Ed.* **2001**, *40*, 2004–2021.

(8) Herzberger, J.; Leibig, D.; Langhanki, J.; Moers, C.; Opatz, T.; Frey, H. "Clickable PEG" via Anionic Copolymerization of Ethylene Oxide and Glycidyl Propargyl Ether. *Polym. Chem.* **2017**, *8*, 1882–1887.

(9) Doran, S.; Yilmaz, G.; Yagci, Y. Tandem Photoinduced Cationic Polymerization and CuAAC for Macromolecular Synthesis. *Macromolecules* **2015**, *48*, 7446–7452.

(10) Ito, D.; Ogura, Y.; Sawamoto, M.; Terashima, T. Acrylate-Selective Transesterification of Methacrylate/Acrylate Copolymers: Postfunctionalization with Common Acrylates and Alcohols. *ACS Macro Lett.* **2018**, *7*, 997–1002.

(11) Pelegri-O'Day, E. M.; Paluck, S. J.; Maynard, H. D. Substituted Polyesters by Thiol–Ene Modification: Rapid Diversification for Therapeutic Protein Stabilization. *J. Am. Chem. Soc.* **2017**, *139*, 1145–1154.

(12) Yuksekdag, Y. N.; Gevrek, T. N.; Sanyal, A. Diels-Alder "Clickable" Polymer Brushes: A Versatile Catalyst-Free Conjugation Platform. *ACS Macro Lett.* **2017**, *6*, 415–420.

(13) Howe, D. H.; McDaniel, R. M.; Magenau, A. J. D. From Click Chemistry to Cross-Coupling: Designer Polymers from One Efficient Reaction. *Macromolecules* **2017**, *50*, 8010–8018.

(14) Oakdale, J. S.; Kwisnek, L.; Fokin, V. V. Selective and Orthogonal Post-Polymerization Modification Using Sulfur(VI) Fluoride Exchange (SuFEx) and Copper-Catalyzed Azide–Alkyne Cycloaddition (CuAAC) Reactions. *Macromolecules* **2016**, *49*, 4473–4479.

(15) van de Wouw, H. L.; Lee, J. Y.; Awuyah, E. C.; Klausen, R. S. A BN Aromatic Ring Strategy for Tunable Hydroxy Content in Polystyrene. *Angew. Chem., Int. Ed.* **2018**, *57*, 1673–1677.

ULSAN NATIONAL INSTITUTE OF SCIENCE AND TECHNOLOGY

(16) Larsen, M. B.; Wang, S.-J.; Hillmyer, M. A. Poly(allyl alcohol) Homo- and Block Polymers by Postpolymerization Reduction of an Activated Polyacrylamide. *J. Am. Chem. Soc.* **2018**, *140*, 11911–11915.

(17) *Poly(ethylene glycol) Chemistry: Biotechnical and Biomedical Applications*; Harris, J. M., Ed.; Plenum Press: New York, **1992**.

(18) Knop, K.; Hoogenboom, R.; Fischer, D.; Schubert, U. S. Poly(ethylene glycol) in Drug Delivery: Pros and Cons as Well as Potential Alternatives. *Angew. Chem., Int. Ed.* **2010**, *49*, 6288–6308.

(19) Obermeier, B.; Wurm, F.; Mangold, C.; Frey, H. Multifunctional Poly(ethylene glycol)s. *Angew. Chem., Int. Ed.* **2011**, *50*, 7988–7997.

(20) Herzberger, J.; Niederer, K.; Pohlit, H.; Seiwert, J.; Worm, M.; Wurm, F. R.; Frey, H. Polymerization of Ethylene Oxide, Propylene Oxide, and Other Alkylene Oxides: Synthesis, Novel Polymer Architectures, and Bioconjugation. *Chem. Rev.* **2016**, *116*, 2170–2243.

(21) Carlotti, S.; Labbé, A.; Rejsek, V.; Doutaz, S.; Gervais, M.; Deffieux, A. Living/Controlled Anionic Polymerization and Copolymerization of Epichlorohydrin with Tetraoctylammonium Bromide-Triisobutylaluminum Initiating Systems. *Macromolecules* **2008**, *41*, 7058–7062.

(22) Meyer, J.; Keul, H.; Möller, M. Poly(glycidyl amine) and Copolymers with Glycidol and Glycidyl Amine Repeating Units: Synthesis and Characterization. *Macromolecules* **2011**, *44*, 4082–4091.

(23) Herzberger, J.; Frey, H. Epicyanohydrin: Polymerization by Monomer Activation Gives Access to Nitrile-, Amino-, and Carboxyl-Functional Poly(ethylene glycol). *Macromolecules* **2015**, *48*, 8144–8153.

(24) Obermeier, B.; Frey, H. Poly(ethylene glycol-co-allyl glycidyl ether)s: A PEG-Based Modular Synthetic Platform for Multiple Bioconjugation. *Bioconjugate Chem.* **2011**, *22*, 436–444.

(25) Le Devedec, F.; Won, A.; Oake, J.; Houdaihed, L.; Bohne, C.; Yip, C. M.; Allen, C. Postalkylation of a Common MPEG-*b*-PAGE Precursor to Produce Tunable Morphologies of Spheres, Filomicelles, Disks, and Polymersomes. *ACS Macro Lett.* **2016**, *5*, 128–133.

(26) Oleske, K. W.; Barteau, K. P.; Turker, M. Z.; Beaucage, P. A.; Estroff, L. A.; Wiesner, U. Block Copolymer Directed Nanostructured Surfaces as Templates for Confined Surface Reactions. *Macromolecules* **2017**, *50*, 542–549.

(27) Fleischmann, C.; Gopez, J.; Lundberg, P.; Ritter, H.; Killops, K. L.; Hawker, C. J.; Klinger, D. A Robust Platform for Functional Microgels via Thiol–ene Chemistry with Reactive Polyether-Based Nanoparticles. *Polym. Chem.* **2015**, *6*, 2029–2037.

(28) Lee, B. F.; Kade, M. J.; Chute, J. A.; Gupta, N.; Campos, L. M.; Fredrickson, G. H.; Kramer, E. J.; Lynd, N. A.; Hawker, C. J. Poly(allyl glycidyl ether)-A Versatile and Functional Polyether Platform. *J. Polym. Sci. Part A Polym. Chem.* **2011**, *49*, 4498–4504.

ULSAN NATIONAL INSTITUTE OF SCIENCE AND TECHNOLOGY

(29) Robb, M. J.; Connal, L. A.; Lee, B. F.; Lynd, N. A.; Hawker, C. J. Functional Block Copolymer Nanoparticles: Toward the next Generation of Delivery Vehicles. *Polym. Chem.* **2012**, *3*, 1618–1628.

(30) Lee, J.; McGrath, A. J.; Hawker, C. J.; Kim, B.-S. pH-Tunable Thermoresponsive PEO-Based Functional Polymers with Pendant Amine Groups. *ACS Macro Lett.* **2016**, *5*, 1391–1396.

(31) Murakami, T.; Schmidt, B. V. K. J.; Brown, H. R.; Hawker, C. J. One-Pot "Click" Fabrication of Slide-Ring Gels. *Macromolecules* **2015**, *48*, 7774–7781.

(32) Barteau, K. P.; Wolffs, M.; Lynd, N. A.; Fredrickson, G. H.; Kramer, E. J.; Hawker, C. J. Allyl Glycidyl Ether-Based Polymer Electrolytes for Room Temperature Lithium Batteries. *Macromolecules* **2013**, *46*, 8988–8994.

(33) Lee, B. F.; Wolffs, M.; Delaney, K. T.; Sprafke, J. K.; Leibfarth, F. A.; Hawker, C. J.; Lynd, N. A. Reactivity Ratios and Mechanistic Insight for Anionic Ring-Opening Copolymerization of Epoxides. *Macromolecules* **2012**, *45*, 3722–3731.

(34) Mattson, K. M.; Latimer, A. A.; McGrath, A. J.; Lynd, N. A.; Lundberg, P.; Hudson, Z. M.; Hawker, C. J. A Facile Synthesis of Catechol-Functionalized Poly(ethylene oxide) Block and Random Copolymers. *J. Polym. Sci. Part A Polym. Chem.* **2015**, *53*, 2685–2692.

(35) Tamesue, S.; Ohtani, M.; Yamada, K.; Ishida, Y.; Spruell, J. M.; Lynd, N. A.; Hawker, C. J.; Aida, T. Linear versus Dendritic Molecular Binders for Hydrogel Network Formation with Clay Nanosheets: Studies with ABA Triblock Copolyethers Carrying Guanidinium Ion Pendants. *J. Am. Chem. Soc.* **2013**, *135*, 15650–15655.

(36) Blankenburg, J.; Maciol, K.; Hahn, C.; Frey, H. Poly(ethylene glycol) with Multiple Aldehyde Functionalities Opens up a Rich and Versatile Post-Polymerization Chemistry. *Macromolecules* **2019**, *52*, 1785–1793.

(37) Song, J.; Palanikumar, L.; Choi, Y.; Kim, I.; Heo, T.; Ahn, E.; Choi, S.-H.; Lee, E.; Shibasaki, Y.; Ryu, J.-H.; et al. The Power of the Ring: A pH-Responsive Hydrophobic Epoxide Monomer for Superior Micelle Stability. *Polym. Chem.* **2017**, *8*, 7119–7132.

(38) Son, S.; Shin, E.; Kim, B.-S. Redox-Degradable Biocompatible Hyperbranched Polyglycerols: Synthesis, Copolymerization Kinetics, Degradation, and Biocompatibility. *Macromolecules* **2015**, *48*, 600–609.

(39) Ahn, G.; Kweon, S.; Yang, C.; Hwang, J. E.; Kim, K.; Kim, B.-S. One-Pot Synthesis of Hyperbranched Polyamines Based on Novel Amino Glycidyl Ether. *J. Polym. Sci. Part A: Polym. Chem.* **2017**, *55*, 4013–4019.

(40) Song, S.; Lee, J.; Kweon, S.; Song, J.; Kim, K.; Kim, B.-S. Hyperbranched Copolymers Based on Glycidol and Amino Glycidyl Ether: Highly Biocompatible Polyamines Sheathed in Polyglycerols. *Biomacromolecules* **2016**, *17*, 3632–3639.

ULSAN NATIONAL INSTITUTE OF SCIENCE AND TECHNOLOGY

(41) Hwang, E.; Kim, K.; Lee, C. G.; Kwon, T.-H.; Lee, S.-H.; Min, S. K.; Kim, B.-S. Tailorable Degradation of pH-Responsive All-Polyether Micelles: Unveiling the Role of Monomer Structure and Hydrophilic–Hydrophobic Balance. *Macromolecules* **2019**, *52*, 5884–5893.

(42) Song, J.; Hwang, E.; Lee, Y.; Palanikumar, L.; Choi, S. H.; Ryu, J. H.; Kim, B. S. Tailorable Degradation of pH-Responsive All Polyether Micelles: Via Copolymerisation with Varying Acetal Groups. *Polym. Chem.* **2019**, *10*, 582–592.

(43) Park, H.; Choi, Y.; Jeena, M. T.; Ahn, E.; Choi, Y.; Kang, M. G.; Lee, C. G.; Kwon, T. H.; Rhee, H. W.; Ryu, J. H.; et al. Reduction-Triggered Self-Cross-Linked Hyperbranched Polyglycerol Nanogels for Intracellular Delivery of Drugs and Proteins. *Macromol. Biosci.* **2018**, *18*, 1–9.

(44) Malkoch, M.; Schleicher, K.; Drockenmuller, E.; Hawker, C. J.; Russell, T. P.; Wu, P.; Fokin, V. V. Structurally Diverse Dendritic Libraries: A Highly Efficient Functionalization Approach Using Click Chemistry. *Macromolecules* **2005**, *38*, 3663–3678.

(45) Brun, M. A.; Tan, K.-T.; Griss, R.; Kielkowska, A.; Reymond, L.; Johnsson, K. A Semisynthetic Fluorescent Sensor Protein for Glutamate. *J. Am. Chem. Soc.* **2012**, *134*, 7676–7678.

(46) Niederer, K.; Schüll, C.; Leibig, D.; Johann, T.; Frey, H. Catechol Acetonide Glycidyl Ether (CAGE): A Functional Epoxide Monomer for Linear and Hyperbranched Multi-Catechol Functional Polyether Architectures. *Macromolecules* **2016**, *49*, 1655–1665.

(47) Boopathi, S. K.; Hadjichristidis, N.; Gnanou, Y.; Feng, X. Direct Access to Poly(glycidyl azide) and Its Copolymers through Anionic (co-)Polymerization of Glycidyl Azide. *Nat. Commun.* **2019**, *10*, 293.

(48) Boileau, S.; Illy, N. Activation in Anionic Polymerization: Why Phosphazene Bases Are Very Exciting Promoters. *Prog. Polym. Sci.* **2011**, *36*, 1132–1151.

(49) Hans, M.; Keul, H.; Moeller, M. Chain Transfer Reactions Limit the Molecular Weight of Polyglycidol Prepared via Alkali Metal Based Initiating Systems. *Polymer* **2009**, *50*, 1103–1108.

(50) Stolarzewicz, A. *Makromol. Chem.* **1986**, *187*, 745–752.

(51) Tetko, I. V.; Gasteiger, J.; Todeschini, R.; Mauri, A.; Livingstone, D.; Ertl, P.; Palyulin, V. A.; Radchenko, E. V.; Zefirov, N. S.; Makarenko, A. S.; Tanchuk, V. Y.; Prokopenko, V. V. Virtual Computational Chemistry Laboratory – Design and Description. *J. Comput.-Aided Mol. Des.* **2005**, *19*, 453-463.

(52) VCCLAB, Virtual Computational Chemistry Laboratory; http://www.vcclab.org, 2005.

(53) Creary, X.; Chormanski, K.; Peirats, G.; Renneburg, C. Electronic Properties of Triazoles. Experimental and Computational Determination of Carbocation and Radical-Stabilizing Properties. *J. Org. Chem.* **2017**, *82*, 5720–5730.

(54) Isono, T.; Asai, S.; Satoh, Y.; Takaoka, T.; Tajima, K.; Kakuchi, T.; Satoh, T. Controlled/Living Ring-Opening Polymerization of Glycidylamine Derivatives Using *t*-Bu-P_4/Alcohol Initiating

ULSAN NATIONAL INSTITUTE OF SCIENCE AND TECHNOLOGY

System Leading to Polyethers with Pendant Primary, Secondary, and Tertiary Amino Groups. *Macromolecules* **2015**, *48*, 3217–3229.

(54) Beckingham, B. S.; Sanoja, G. E.; Lynd, N. A. Simple and Accurate Determination of Reactivity Ratios Using a Nonterminal Model of Chain Copolymerization. *Macromolecules* **2015**, *48*, 6922–6930.

ULSAN NATIONAL INSTITUTE OF
SCIENCE AND TECHNOLOGY

Chapter 5

Summary

The invention and development of synthetic polymers triggered the increase in production of numerous industrial materials, thereby providing a great improvement to the quality of our life. However, there still remains room for development of new value-added products, and the synthetic polymer chemistry can play an important role to achieve advancement in the polymeric materials. Polyether, one of the synthetic polymers, has attracted significant interest in a broad range of areas, while it is still challenging to synthesize diverse functional polyethers. In this regard, this thesis describes our efforts towards preparing myriad functional polyethers through rational design and synthesis of functional epoxide monomers.

First, we introduced the synthesis and properties of pH-tunable thermoresponsive polyethers containing various pendant amine groups. Commercially available allyl glycidyl ether (AGE) was used to synthesize a platform polymer, aiming for the modular thiol-ene reaction with several aminothiols. Allyl groups in the platform polymer carried various functionalities, exploiting thiol-ene click chemistry. This work is the first systematic study on the effect of polyether copolymer side chains on cloud point, and it shows potential for development of new thermoresponsive polymers.

Second, a newly designed amine-functional epoxide monomer, BBAG, was introduced to demonstrate the anionic ring-opening multibranching polymerization to yield a series of amine-functional hyperbranched polyglycerol (hbPG). The superior biocompatibility of the polymer was achieved by the sheathed amines in the hyperbranched polyglycerols.

Lastly, a series of novel azide-functionalized epoxide monomers are presented as universal candidates for preparing platform polymers for post-polymerization modification. Newly designed three azide-functionalized glycidyl ether monomers containing different alkyl spacers were synthesized. Non-ionic organic superbase-catalyzed anionic ring-opening polymerization (AROP) was demonstrated to afford well-controlled azide-functional polyethers. The azide pendant groups were readily transformed into amine groups by Staudinger reduction. Copper-catalyzed azide-alkyne cycloaddition (CuAAC) was conducted to modify the azide groups to a variety of functional groups.

In conclusion, versatile functional polyethers were synthesized by using commercially available epoxide monomers and newly designed novel monomers. We anticipate that the work described in this thesis greatly expands the scope of functional epoxide monomers for the preparation of valuable polymeric materials.

ULSAN NATIONAL INSTITUTE OF SCIENCE AND TECHNOLOGY

List of Publications

Published works

(1) Song, S.†; **Lee, J.**†; Kweon, S.; Song, J.; Kim, K.; Kim, B.-S. Hyperbranched Copolymers Based on Glycidol and Amino Glycidyl Ether: Highly Biocompatible Polyamines Sheathed in Polyglycerols. *Biomacromolecules* **2016**, *17*, 3632–3639.

(2) **Lee, J.**; McGrath, A. J.; Hawker, C. J.; Kim, B.-S. pH-Tunable Thermoresponsive PEO-Based Functional Polymers with Pendant Amine Groups. *ACS Macro Lett.* **2016**, *5*, 1391–1396.

(3) **Lee, J.**; Han, S.; Kim, M.; Kim, B.-S. Anionic Polymerization of Azidoalkyl Glycidyl Ethers and Post-Polymerization Modification. *Macromolecules* **2019**, ASAP Article

Unpublished works

(4) Park, M.; **Lee, J.**; Kim, B.-S. Bifunctional Graphene Based Carbocatalysts to Reform Biomass from Glucose to 5-Hydroxymethylfurfural. *In preparation* **2019**

(5) Han, S.; **Lee, J.**; Kim, B.-S. Synthesis of Dynamic Imine-Based Polymeric Micelles for Efficient Drug Delivery. *In preparation*, **2020**

(6) **Lee, J.** †; Park, S. †; Kim, B. -S.; Kim, J. G. Post-Polymerization Modification of Ammonium Functionalized Polyethers by Mechanochemical Reaction. *In preparation*, **2020**

†These authors contributed equally to this work.

ULSAN NATIONAL INSTITUTE OF SCIENCE AND TECHNOLOGY

Acknowledgments

끝나지 않을 것 같았던 긴 여정이 이제 마무리가 되는 것 같아 기쁜 마음이지만, 떠날 때가 되었다고 생각하니 좀 더 잘 했으면 어떨까 하는 아쉬운 마음도 듭니다. 우선 석박사통합과정이라는 6 년의 긴 시간동안 아낌없는 지원으로 좋은 연구자가 될 수 있도록 지도해 주신 김병수 교수님께 감사하다는 말씀을 드립니다. 그리고 박사학위 심사를 위해서 자리해 주셨던 권태혁 교수님, 박영석 교수님, 이동욱 교수님께 감사드리고, 또 멀리서 와주신 김정곤 교수님께도 감사하다는 말씀을 전합니다. 신입생때 부터 함께 지냈던 선배님들이 많이 생각 납니다. 가장 처음 인턴으로 들어왔을 때 저를 잘 가르쳐주셨던 최유리 박사님, 항상 모범적이고 배울점이 많았던 이태민 박사님, 혼자였으면 더 힘들었을 미국생활에 정말 큰 도움이 되어주셨던 서은용 교수님께 고마웠던 마음을 전합니다. 그리고 저의 앞날을 위해 정말 좋은 조언 많이 해주시고 잘 챙겨주신 이상호 박사님께도 감사하다는 말씀을 드리고 싶습니다. 미국에서 outstanding 한 실력으로 박사학위중이신 기영이형과 필재형, 그리고 박사님들이지만 아직은 그 호칭이 어색할만큼 친근했던 응진이형, 민수, 이슬. 그동안 함께한 좋은 추억들이 많네요. 감사합니다. 긴 시간은 아니었지만 저의 부사수로서 많은 도움을 주었던 혜원, 지영, 금석, 윤경이도 생각이 많이 나고 고맙다는 말을 전하고 싶습니다. 윤경이는 남은 박사학위과정 지혜롭게 잘 헤쳐나가기를! 오랜시간 함께했던 그리고 아직 갈 길이 남은 민성, 태형 역시 긴 학위과정과 병역의 의무를 잘 수행하기를 바랍니다. 나를 선배라고 너무 잘 맞춰주는 동석이, 항상 밝은모습으로 무엇이든 척척 해내는 마지막 부사수 소희, 똑부러지는 수빈이, 이젠 카리스마까지 갖춘 영주, 그리고 운동하는 사나이들 일오, 기환, 주원이도 짧은시간이었지만 잘 따라줘서 고맙습니다. 마지막으로 가장 오랜시간 가까이서 또는 멀리서 함께한 나의 동기 민주와 병호에게도 고맙다는 말을 전합니다. 앞으로도 좋은 일만 있기를 바라며.

학교 밖에서 먼저 사회로 나가, 만날때마다 밥 사주는 고향친구들 홍렬, 재민, 진형, 재섭, 성민, 그리고 유부 도연이, 독일유학 준비중인 석진이, 패피 경원이에게 큰 고마움을 전합니다. 취업때문에 많이 힘들었지만 늘 연락해주고 또 이제는 잘 자리잡은 현빈이에게도 고맙고 수고했다는 말을 전합니다. 그리고 소중한 대학동기들, 그중 나에게 처음 졸업논문이라는 것을 받아보게 해준 윤선이를 비롯해 온유, 미나, 선우햄, 윤석이. 정말 안본지 오래됐는데 오랜만에 보고싶네요 다들. 그리고 하나크루! 서울오고 좀 더 자주볼 수 있어서 좋았던 수민, 하나, 창형, 민섭, 란희, 민령 그리고 리하누나 연아누나. 앞으로도 잘 지냅시다! 마지막으로, 저를 이렇게 잘 키워주시고 오랜 기간동안 든든한 지원으로 학위과정을 잘 마칠수 있도록 도와주신 어머니, 아버지, 그리고 동생에게 너무나도 고맙고 사랑한다는 말을 전하고 싶습니다. 저 혼자만이 이룰 수 있는 결과는 없었습니다. 다 언급하진 못했지만 6 년동안 지나갔던 많은 소중한 인연들에 감사합니다.